Fakultät für Medizin

Institut für Medizinische Mikrobiologie, Immunologie und Hygiene

Characterization of cell alterations caused by fluorescence activated cell sorting and development of new technical sorting approaches

Immanuel Anton Andrä

Vollständiger Abdruck der von der Fakultät für Medizin der Technischen Universität München zur Erlangung des akademischen Grades eines

Doktors der Naturwissenschaften (Dr. rer. nat.)

genehmigten Dissertation.

Vorsitzender:	Prof. Dr. Marc Schmidt-Supprian
Prüfer der Dissertation:	1. Prof. Dr. Dirk H. Busch 2. Prof. Angelika Schnieke, Ph.D.

Die Dissertation wurde am 06.05.2019 bei der Technischen Universität München eingereicht und durch die Fakultät für Medizin am 11.02.2020 angenommen.

Table of contents

List of figures

Table of abbreviations

CAR	Chimeric antigen receptor
MSC	Mesenchymal Stem Cell
CD	Cluster of Differentiation
RQI	RNA Quality Indicator
DNase	Desoxiribonuclease
ECL	Enhanced Chemiluminescence
HRP	Horseradish Peroxidase
BSA	Bovine Serum Albumin
o.N.	Over night
PenStrep	Penicillin and Streptomycin
SDS-PAGE	Sodium Dodecyl Sulfate PolyacrylAmide Gel Electrophoresis
GvHD	Graft versus Host Disease
CCR7	C-C chemokine receptor 7
INF	Interferon
IL	Interleukin
E:T ratio	Effector to Target ratio
SEM	structural equation modeling
Hz	Herz
EPS	Events per Second
MHC I	Major Histocompatibility Complex I
TC-beads	TrueCount-beads
WT1	Wilms Tumor antigen 1
HLA	Human Leucocyte Antigen
FluMP	Flu Membrane Protein
MLR	Mixed Lymphocyte Reaction
Th 1/17	T helper cell Typ 1/17
CMV	Cytomegalovirus
MART1	Melanoma antigen recognized by T cells 1
pp65	phosphoprotein molecular weight 65
GMP	Good Manufacturing Practice
MACS	Magnetically cell sorting
FACS	Fluorescence activated cell sorting
PMT	Photomultiplier Tube
DNA	deoxyribonucleic acid

GFP	Green fluorescence protein
PI	Propidium Iodide
e.g.	Lat.: Exempli gratia “for example”
POI	Point of interrogation
TCR	T cell receptor
FSC	Forward scatter
SSC	Sideward scatter
kHz	Kilo Herz
RPMI-1640	Roswell Park Memorial Institute-1640 (medium)
mRNA	Messenger ribonucleic acid
snRNA	Small nuclear ribonucleic acid
D-Biotin	Desthiobiotin
Fc	Fragment crystallizable
Fab	Fragment antigen binding
ITAMs	Immunoreceptor tyrosine-based activation motif
EDTA	Ethylenediaminetetraacetic acid
PBS	Phosphate Buffered Saline
MAPK	mitogen-activated protein kinase
psi	Pound force per square inch
mW	milli Watt
UV	UltraViolet
hPBMCs	Human peripheral blood mononuclear cell
ACT	Tris-Buffered Ammonium Chloride
FCS	Fetal calf serum
JNK (SAPK)	C-Jun-N-terminal kinase (stress activated protein kinase)
FITC	Fluorescein isothiocyanate
PE	Phycoerythrin
PETxR	Phycoerythrin TexasRed
PECy5/7	Phycoerythrin cyanin 5/7
BV421/650	Brilliant Violet 421/650
PB	Pacific Blue
eF450	eFluor
APC	Allophycocyanin
Erk	extracellular signal-regulated kinases
EGFR	Epidermal Growth Factor Receptor
PD-1	Programmed cell death protein 1
CTLA-4	cytotoxic T-lymphocyte-associated Protein 4
FasR	first apoptosis signal receptor

ZAP-70	Zeta-chain-associated protein kinase 70
LAT	Linker of Activated T cells
7AAD	Aminoactinomycin D
PS	Phosphatidyserine
EMA	Ethidium Monoazide
SE	*Speed Enrichment*
CREM	cAMP Responsive Element Modulator
TNFAIP3	TNF Alpha-Induced Protein 3
CML	X-C Motif Chemokine Ligand 1
AP-1	Activator protein 1
NF-AT	nuclear factor of activated T cells
Okt3	Muromonab- CD3 Orthoclone
NT5C3	5´-Nucleotidase, Cytosolic IIIA
C2	Complement component 2
RNVU1-3	RNA Variant U1 Small Nuclear 1, 2 and 3
cAMP	Cyclic adenosine monophosphate
TNF	Tumor necrosis factor
LPS	lipopolysacchrides

List of tables

Abstract

Cells evolved a signaling machinery constantly sensing their environment intra- and extracellular to react to certain stimuli and changes. Flow cytometry cell sorting relies on mechanical and physical forces to separate cells and needs in many cases elaborate sample prearrangements. In this thesis we evaluate cellular behavior to certain forces occurring in the course of flow cytometry cell sorting and highlight caveats in sample preparation processes. Further on we show opportunities to minimize potential cell alterations by new technological developments with reversible reagents. We developed a cell sorter under complete temperature control to assure constant cell hibernation during sorting when using reversible reagents.

From our results we conclude that primary cells like mononucleated cells from peripheral blood can be processed and FACS sorted minimally affected. More sensitive cell culture cells need short preparation times or higher temperature not to be damaged by cold stress responses. However cell stress signaling molecules like mitogen activated protein kinases (MAPK) sense flow cytometry cell sorting by phosphorylation, even at low temperatures. Especially the p38 MAPK pathway showed mechanical or physical FACS force susceptibility. We therefore evaluated the different forces one after the other to identify responsible inducers. The p38 activation was early on activated, not by pressure, but by shear stress and/or acceleration, as these forces are not discernable. Other forces did not stack appreciable.

We therefore surveyed p38 associated cell functions in PBMCs and CD8 positive T-cells after sorting. We found only little changes in mRNA, survival, proliferation, migration and organization of the cytoskeleton. The data indicate, that FACS sorting is sensed by the cellular machinery but the stimulus seem insufficient in promoting cellular stress responses.

These findings in mind we propagated a method to overcome time issues and cell number based drawbacks by flow cytometry cell sorting, to further improve this superior purification method. By triggering on fluorescence channels, which identify certain target populations, we adjusted threshold detection levels above intrinsic fluorescence to process only information of the target cell population calling this method "*Speed Enrichment*". This enabled us in enriching very small cell populations ($1:10^6$) by flow cytometry and processing incredibly high sample numbers ($>10^9$) with high flowrates ($>10^6$ eps) in short time (1 hour). We used this method to enrich naïve antigen specific T cells, NK cells, plasmacitoidic dentritic cells (pDCs) and haematopoietic stem cells.

Kurzzusammenfassung

Zellen entwickelten evolutionär komplexe Signalkaskaden, welche stetig die Umwelt überprüfen auf sowohl intra- wie auch extrazelluläre Änderungen, um schnell und angemessen reagieren zu können. Die Durchflusszytometrische Zellsortierung benötigt aufwendige Probenvorbereitungen und ist abhängig von mechanischen und physikalischen Kräften um Zellen aufreinigen zu können. Deshalb wenden wir uns in dieser Arbeit der Frage zu ob sich Zellen aufgrund dieser Kräfte verändern und ob durch Vorsichtsmassnahmen in der Probenvorbereitung und Zellsortierung Veränderungen abgewendet werden können, sowie neue alternative Technologien, wie die reversiblen Reagenzien, die Zellveränderungen minimieren können. Da niedrige Temperaturen die Zellen in eine Art Winterschlaf versetzen können sind so minimalveränderte Färbungen mit reversiblen Reagenzien beispielsweise möglich. Dies animierte uns auch ein temperaturkonstantes Zellsortiergerät zu entwickeln, welches diesen Winterschlaf während des gesamten Sortierprozesses aufrecht erhält. Wir fanden, dass eine Sortierung primärer einkerniger Zellen aus dem pripheren Blut (PBMC) minimal Zellveränderungen auslöste, jedoch sensitive Zellkulturlinien Kältestressreaktionen zeigten, wenn die Verarbeitungszeit zu lange war oder die Arbeitstemperaturen zu niedrig gewählt wurden. Ungeachtet unserer Temperatureinflüsse zeigten MAP Kinase Wege eine Aktivierung durch Zellsortierung allein. Speziell die p38 MAPK zeigte eine Phosphorylierung durch mechanische und physikalische Zellsortierungskräfte. Um die verantwortlichen Kräfte zu identifizieren, nahmen wir eine Kraft nach der anderen aus der Gleichung. Am Ende konnten Scherkräfte und die Beschleunigung als erste Kräfte dieser Aktivierung ausgemacht werden, welche jedoch für die Zellsortierung unerlässlich und unvermeidbar sind. Einflüsse anderer Kräfte konnten die p38 Aktivierung nicht maßgeblich verstärken. Als wir herausfinden wollten ob Zellen durch diese Aktivierung verändert werden nutzen wir reine $CD8^+$ Zellen oder PBMC Proben, da diese mit Methoden angereichert wurden die die Zellen initial nicht veränderten für die nachfolgenden Untersuchungen. In diesen Proben fanden wir nur geringe Veränderungen im Migrationsverhalten, Zellüberleben, Proliferation, Organisation des Zytoskeletts oder Ihrer mRNA Expression. Was darauf hindeutete, dass Zellen die Sortierung zwar durch die zellulären Signalkaskaden bemerken, der Stimulus jedoch nicht stark genug scheint um Zellveränderungen dauerhaft auszulösen. Mit diesem Befund, dass Durchflusszytometrische Zellsortierung eine sehr valide und schonende Methode der Zellaufreinigung ist, versuchten wir beständige Probleme in der FACS basierten Zellaufreinigung wie Probenmenge und zeitraubende langzeit Analysen zu addressieren. Dies erreichten wir indem die Signalerkennung in den Geräten auf einen Fluoreszenzkanal gelegt wurde, welcher die Zielpopulation genau definierte, und durch

Adjustierung eines Grenzwertes in der Signalerkennung der überhalb der intrinsischen Zellfluoreszenz lag konnten unmarkierte Zellen ausgeblendet werden. Diese Methode wurde "*Speed Enrichment*" genannt und ermöglichte es uns sehr seltene ($1:10^6$) und kleine Zellpopulationen, aus sehr grossem Ausgangsmaterial (10^9) mit hohen Flussraten ($>10^6$ eps), anzureichern. Damit wurden unterschiedliche Zellpopulationen wie naïve T Zellen, NK Zellen, Plasmacytiode dentitische Zellen und Hämatopetische Zellen angreichert für nachfolgende Anwendungen und Experimente.

1. Introduction

1.1. Cell separation methods

Cell separation for life science applications is a common tool in basic research (e.g. single cell or rare event analysis), as well as a fundamental pillar in clinical cell-based therapies (e.g. stem cell transplantations, cell-based cancer therapies, infectious or autoimmune diseases). The separation of heterogeneous samples into defined subpopulations helps to evaluate the function of individual cell types in *in vitro* and in *in vivo* studies [1-3]. For clinical applications, cell purification entails the potential for more predictable therapeutic efficacy, as well as the reduction or elimination of side effects of treatment [4]. Nowadays, different options and technologies to purify homogeneous cell material for users' exist. These technologies can be best distinguished by different methodological principles: adherence, density, microfluidics and/or antibody binding [5].

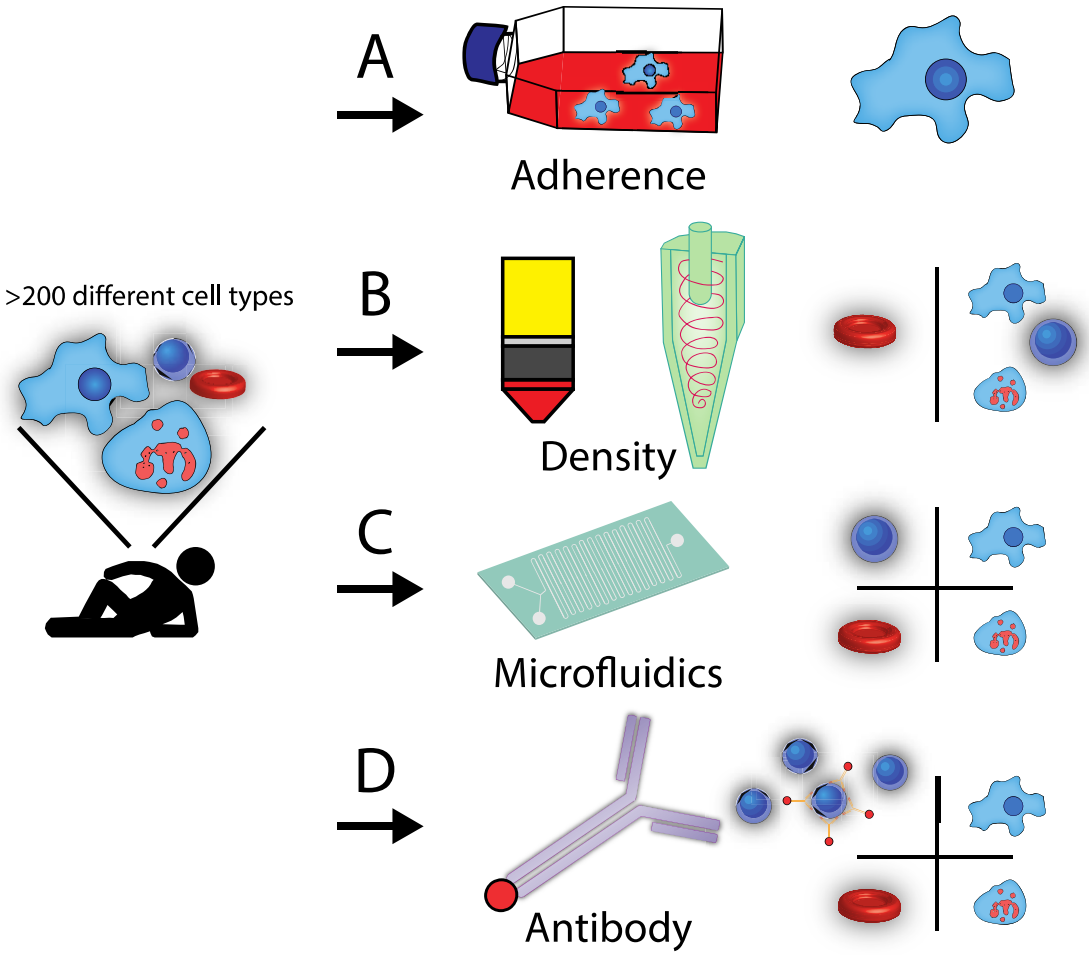

Figure 1: Overview of currently available cell separation technologies.
The human body consists of more than 200 different cell types fulfilling different roles to facilitate a higher order of functions by synergic effects. To evaluate its function, a defined cell type must be isolated and purified. This is mainly done by cell separation methods like adherence, density, physiological and physical properties, or affinity. (A) Cell separation via adherence is a relatively cheap cell culture-based method with a high demand of time. Only a separation of soluble and adherent cell types is achievable. (B) Density-based purification methods like gradient centrifugation or apheresis are widely used and have numerous applications across different cell types (primary and immortalized), as well as organisms like bacteria and even viruses. This method is often used especially for a fast and efficient separation of blood cells. (C) Microfluidic chip-based systems enable a defined separation based on physical properties often with cheap disposable systems and are very precise and pure for their target population. However, these systems have been very time consuming. (D) Antibodies labeled with utilities for cell separation (e.g. fluorochromes and magnetic beads) guarantee the purification of the most defined subpopulations. Precise enrichment methods like FACS and MACS are a fast way to process large amounts of sample material. However, when it comes to cost, they show some drawbacks. All four methods generate different yield and purity values of separated materials; nevertheless due to cost, workflow and needed equipment, each purification method has its use and application.

The first two methods illustrated (Fig. 1A and B) represent quite unspecific approaches to the enrichment of defined subpopulations. Adherence utilizes cell culture characteristics to distinguish and purify adherent from suspended cells like dendritic cells[6], monocytes or mesenchymal stem cells (MSC)[7] isolated from tissue or blood. Density-based approaches utilize density differences of subsequent layers of media to disperse the cell mixture. Enrichment in different layers can be achieved by centrifugation in a gradient separation medium. Ficoll[8] or Percoll[9] solutions, which may be applied to peripheral blood, virus or organelle separation, are well known. These are well-suited and widely used separation methods, although for the Ficoll-Hypaque solution a loss of certain cell types[10] compared to whole blood and a downregulation of CD34[11] have been described. Another prominent density-centrifugation-based purification method with a pivotal role in clinical applications to yield material from human blood under good manufacturing practice (GMP) conditions is apheresis. Overall, adherence and density-based methods are more suitable for pre-enrichment steps. These pre-enrichments can be of great use for the following cell separation methods, namely microfluidics and antibody staining-based technologies. Those methods, which in some cases are used simultaneously, are more specific concerning defined subpopulations and usually are accompanied by high purity. Microfluidic systems are an upcoming field for cell purification approaches (Fig. 1C). Their principles of “particle sorting” differ tremendously from established methods. Their use of microfluidic systems in chip-based technologies or lab on a chip molecular sorting switches[12] are unique. Systems like filters[13,14] or filter-like structures, dielectrophoretic field flow fractionation[15] and acoustoforesis[16,17] that separate by the deformability of the cells, their size or their polarization are used. These methods are a promising candidate for future applications, still mainly acquisition speed and upscaling are an issue. So MACS and FACS still remain the gold standard in particle/cell separation.

1.1.1. Antibody-based cell purification and separation

Antibody binding offers the highest purity, specificity and speed compared to all other methods (Fig. 1D). Key technologies in the field of antibody-based cell separation are magnetically activated cell sorting (MACS) or fluorescence activated cell sorting (FACS). In the following, these techniques will be highlighted separately. Although MACS is used as a brand name, magnetic separation methods include comparable operating modes from various companies, e.g. Dynal[18,19] and Miltenyi[20,21].

1.1.2. Magnetically Activated Cell Sorting

In principle, MACS uses monoclonal antibodies covalently coupled with magnetic particles (MACSbeads) of a size around 50nm, which were first described in 1977[22]. These MACSbead-coupled antibodies, with paramagnetic particles, are either directed against cellular surface proteins or the Fc-part of other antibodies already bound to their structures (Fig. 2A). By using a strong magnetic field surrounding a column composed of ferromagnetic material such as iron-particle spheres, labeled cells can be retained in this field and separated from unlabeled cells[20] (Fig. 2B).

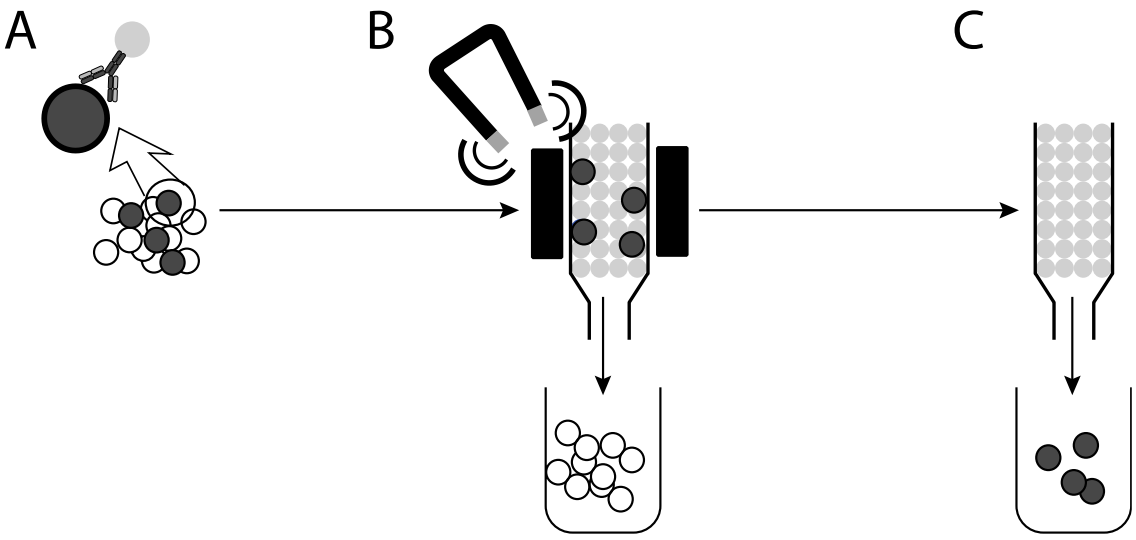

Figure 2: Scheme of magnetic cell separation (MACS).
(A) Antibody-based magnetically-labeled (dark) and unlabeled (white) cells are added to a paramagnetic iron-particle column. (B) Labeled cells are retained in a magnetic field and unlabeled cells can freely pass through the column. (C) After removal of the magnetic field, stained target cells can be washed und eluted from the column matrix (figure adapted from master's thesis of Hanna Ulrich).

After removing the column from the magnetic field, retained cells can be washed from the column matrix (Fig. 2C). This method allows positive or negative selection. Positive selection is achieved by using an antibody against a cellular marker that is expressed by the cell. In contrast, negative selection stains unwanted cells with multiple antibodies directed against surface markers not shared with the target population, thus increasing the target cell frequency. By using first negative and then positive selection in sequential steps, it is possible to separate different subpopulations which share certain surface markers[23]. Overall MACS is known for its potential to separate large cell populations with high purity, yield and recovery, as well as its ability to be easily combined with other purification methods[24]. For example, $2x10^{10}$ cells can be applied to a column, of which up to $1x10^{9}$ cells can be held back onto the column matrix. Another advantage for MACS is a fast workflow, which takes about 1h. Especially for sample multiplexing, time is nearly

constant whether 1 or 10 samples have to be processed. MACS and other magnetic bead-based purification methods have already been used for various clinical applications[25-27]. Although mostly used for the depletion of certain cell types by negative selection approaches, positive selection is also possible even under GMP conditions with the CliniMACS system. However, MACS has some drawbacks when isolating cell populations defined by multiple surface markers. Here another technology offers multi-parameter single cell resolution and purification.

1.1.3. Fluorescence Activated Cell Sorting

The commonly used abbreviation FACS for fluorescence activated cell sorting, generally accepted in the field to describe a separation of cells by a deflected fluid stream, is a trademark of one specific company. The term FACS is used hereafter independently of a specific company, although it is worth mentioning that the correct nomenclature is flow cytometry cell sorting.

FACS evolved from the technology of ink-printing, the deflection of a charged fluid stream developed at Stanford University[28], and the Coulter counter[29], which counted single aligned cells in a fluid stream generating electronic signals by their size. The development of fluorescence-based microscopy and particle counting[30] also had some influence. Various people helped develop this technology, directing it to life science purposes. In 1969, a group of immunologists at Stanford University under the leadership of Leonard Herzenberg started to combine the counting of cells and deflection of droplets in an electromagnetic field (Coulter Counter) with a mercury lamp as light source to gain additional cell information for discrimination via photomultiplier tube (PMT) detectors[31-33]. In the following decades there was a continued evolution of FACS instruments, so that by the 1990s the basic methods of fluidic systems and optical layout remained largely unchanged, while the electronic and software was steadily improved, which led to faster and higher cell acquisition rates. Nowadays instruments continue to advance, changing and improving the traditional systems of fluidics as well as optics. Examples are the Attune™, with its acoustic focusing and the spectral analyzer SP6800[34], which uses a novel optical approach. These upcoming technologies are still under development. Today it is still necessary to use hydrodynamic focusing and up to 7 laser offsets, in different stages with up to 6 PMTs per laser to attain signals of up to 18 different fluorophores in modern multicolor panels[35]. FACS allows the determination and characterization of cells by their size, granularity, surface proteins and intracellular components like DNA or cytoplasmic proteins[36]. In most cases, this determination is based on fluorescent dyes which can be expressed by the cell itself in the form of fluorescent proteins[37] (e.g. GFP by transduction with viral vectors), covalently bound or

integrated into cellular structures[38-40] (e.g. DNA binding dyes Hoechst and propidium iodide), or dyes covalently bound to monoclonal or polyclonal antibodies[41] which then recognize specific antigen targets. FACS can be used for sorting bacteria, cells and cellular compartments (e.g. mitochondria), even particles or viruses[42] – limited only to the solubility in aqueous buffers, their size and the physical detectability by laser light (fluorescence or scattering). As a rule of thumb, 20% of the nozzle size diameter is achievable in FACS sorting, which limits particles to a size of around max. 80 µm using a 400 µm nozzle. This type of cell separation is based on the following basic principles:

I. Hydrodynamic focusing
II. Gathering the particle's information at the "Point of Interrogation" (POI) by light, optics and electronics
III. Droplet generation and deflection

Hydrodynamic focusing is the alignment and focusing of cells in the center of a fluidic stream generated by an outer laminar flow of sheath fluid[43]. The cells are stably transported in the stream and stay aligned in the center when the Reynolds number is below 2300; above that, a transition from laminar to turbulent flow is generated. The Reynolds number is defined by the density (ρ) of the fluid, the velocity (ν) and diameter (d) of the stream in respect to the viscosity (η) of the fluid.

$$Re = \frac{\rho * \upsilon * d}{\eta}$$

For FACS, density and viscosity are mainly unchanged, while diameter and velocity change dependent on the nozzle. This way, when the Reynolds number is kept within laminar limits, cells pass one after another down the POI like pearls on a string (Fig. 3A).

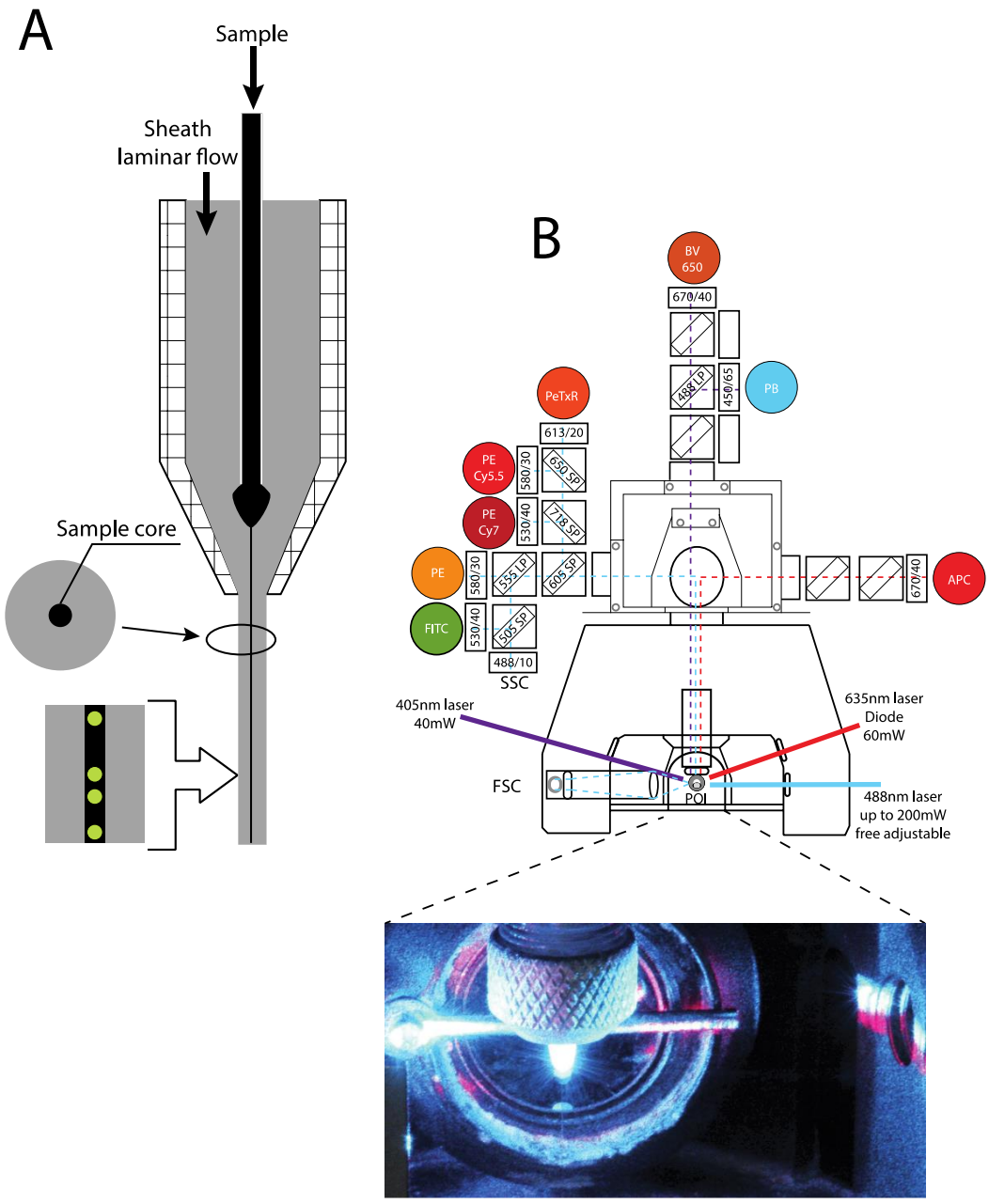

Figure 3: Sketch of the basic principles of fluorescence activated cell sorting (FACS).
(A) Adapted draft[44] of a cell sorter nozzle assembly and hydrodynamic focusing by laminar flow. Under pressure, sheath fluid engulfs the sample fluid in a center stream. The stream leaves the nozzle assembly into the air, keeping the cells of a sample fluid loose, centered and aligned. (B) Laser interrogation point and optical design of a MoFlo™ Legacy cell sorter. In the photograph two laser beams (488nm and 635nm) hit the fluidic stream after leaving the nozzle assembly and get diffracted in a horizontal line. The draft of the optical system visualizes lasers lines at the point of interrogation (POI), generating scattered light and fluorescence. Light signals are detected in PMTs in different blocks for each laser line.

At the POI, laser light hits the center of the stream and is diffracted horizontally by the fluid (Fig. 3B, photograph). This diffraction ring is blocked by bars and is neither detected as scattered light nor as fluorescence, as it would increase background signals strongly. Only light scattered or emitted in a certain angle is detected. For forward scatter (FSC), light is detected in a straight line to the laser with an angle of roughly 4 to 9%, as a measurement of cell size (Fig. 3B, Graphics). Fluorescence and side scattered (SSC) light are collected by a lens in a 90° angle to the laser beam, which is seen as the round object behind the nozzle and stream in the photograph (Fig. 3B). To enable separation of signals from each laser specifically in their optical blocks, the beams of different lasers are slightly offset, which can be seen by the different height of diffraction rings of the 488 nm (blue) laser and the 635 nm (red) laser (Fig. 3B, photography). In the optical block, spectra from different dyes segregate by dichroic filters to specific channels with bandpass filters, which provide a dye-specific wavelength window (Fig. 3B, graphic). In these channels, the transformation and amplification of the light signal into electronic information takes place via photomultiplier tubes (PMT) by photoelectric effect. The electronic information of the particle is processed, temporarily saved in the cache, and visually displayed in a software program while the particle continues its way downstream for sorting. While the sheath fluid stream vibrates constantly at a frequency of about 100 kHz through a piezo element, this leads to droplet formation of the stream with $1x10^5$ drops/sec equal to the adjusted frequency of the piezo element. At a specific time point, which is kept constant by adjusting the amplitude of the frequency, the droplet disconnects from the stream; this is generally called “drop delay”. When a particle of interest is enclosed in that last attached droplet the whole stream is charged. A charged droplet disconnects from the stream, keeping its charge, while instantly after that the stream itself is de-charged. The charged, particle-containing droplet is deflected in an electro-magnetic field between two electrical plates[45]. Depending on its charge, the droplet is deflected right or left and collected in a vessel. Overall, cells are separated and purified at single cell resolution by physical and mechanical effects and forces.

1.2. Cell propagation by sorting

Some of the forces underlying FACS sorting, as well as the sample preparation prior to sorting, may affect cell phenotypes and cell functionality. The biological status of cells, their viability, vitality and functionality after a sort are crucial for the value and outcome of subsequent experiments. So far, few attempts have been made to systematically evaluate sorting parameters and their influences on the quality of sorted cells[46-48].

1.2.1. Mechanical forces during FACS sorting

Mechanical, physical and chemical forces (Fig. 4) are needed for FACS. In fact, one force often brings about another, as for example the pressurized sorting system generates decompression, shearing and acceleration. The pressurized system is needed to produce the sheath fluid stream and laminar flow, with pressures ranging from 10 to 100 pounds force per square inch (psi), depending on the nozzle size, which equals 0,7 to 6,9 bar. A 70 µm nozzle with a pressure of 60 psi (4,1 bar) is mainly used, especially for sorting primary cells isolated from blood. Due to this pressure, sorted particles accelerate and leave the tip of the nozzle at around 90 km/h, where they are instantaneously depressurized to atmospheric pressure. In the sample line, particles flow through narrow tubing with a diameter of 150 µm, potentially generating shearing forces. In line with this, other groups reported a cellular hyperpolarization of pressure-dependent ion channels in the inner cells of blood vessels (vascular endothelial cells) due to shear stress[49].

Also crucial for FACS sorting is laser light. High energy laser light is known to harm and potentially kill cells[50], but laser powers in the range of 200 mW which only last split-seconds during sorting are unlikely to have such effects. UV laser light has already been in the scientific focus for potential DNA strand ruptures due to sorting, but no damage[51] or little alterations[46] have been observed. As UV laser light has the greatest potential to cell damage due to its high energy, this effect seems negligible.

Further down the sorting process, cells of interest are charged, which potentially leads to activation of voltage-gated ion channels, expressed by all cell types, or a depolarization of the cell membrane[52].

Finally, after the sorting process, the cell in the droplet ends up colliding into a vessel at 90 km/h. Buffer added to the collection tubes before sorting dampens this impact, providing a cushion. This precaution minimizes the effects of the impact, but involves potential cell alterations by buffers hereafter explained.

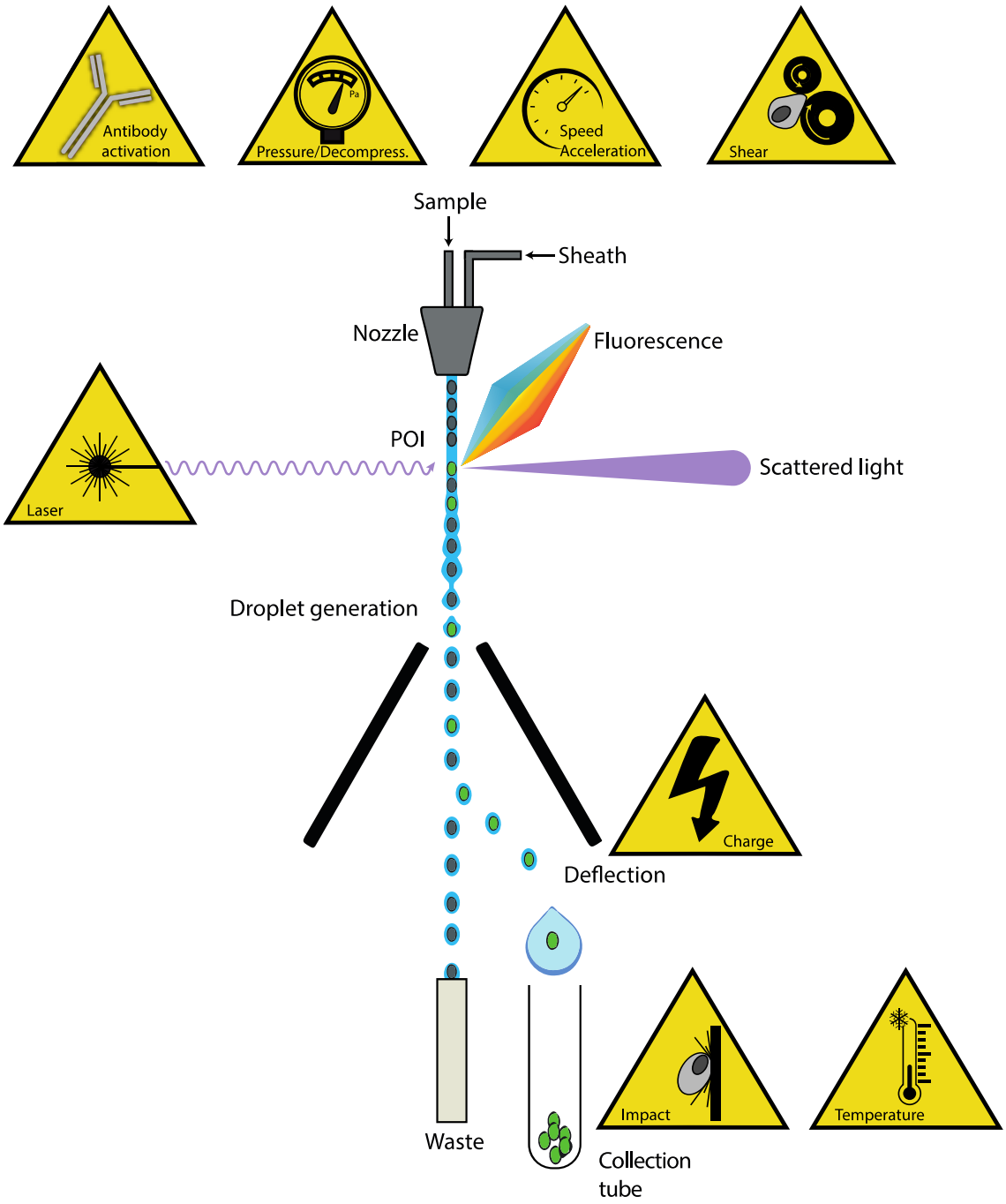

Figure 4: Mechanical and physical forces during FACS.
Listed are different forces and cell alterations by sample preparation for sorting. Some sorting parameters have an effect over the whole sorting process like temperature or antibody activation. Most sorting parameters interact with the cells only for a short time and only on certain locations within the sorter, e.g. mechanical forces.

1.2.2. Potential alterations due to sample preparation

Three main causes can alter cells in the course of cell preparation. First, as already mentioned, there are potential buffer alterations due to osmosis[53-55], pH or mitogens[56]. Second, staining with antibodies is known to alter cell physiology and function[57], although this can be minimized by low temperatures. In line with that the temperature is of importance during preparation, as it can change protein synthesis[58] via eIF2α and induce cell stress signaling[59] via MAPK. A temperature influence concerning membrane fluidity is also described[60]. Finally, the process of sample preparation bears pitfalls for cell alteration due to e.g. homogenization[61] of donor material or collagenase digestion[48] and anticoagulants like heparin[62].

1.2.2.1. Buffer alteration

Phosphate-buffered saline (PBS) solutions, which are also the basis for sheath fluid, are most commonly used for FACS sorting. This solution is nontoxic for cells, isotonic and buffered in a pH range comparable to physiological conditions. Ethylenediaminetetraacetic acid (EDTA) is often added to FACS buffers to prevent cells from clumping and as a metallic ion catcher (chelating agent). Often 0.5% (m/v) bovine serum albumin (BSA) is added, reducing cell attachment to surrounding surfaces and improving viability[63]. This buffer lacks all sorts of nutrition needed for primary cells of animal origin, potentially starving cells over longer sort times, which are known to downregulate and abort protein synthesis[64] via the phosphorylation of eIF2α in response to this stress type[65,66]. Therefore, fetal calf serum (FCS), the cell-free blood serum of unborn calves, is often added to apply “optimal” buffer conditions. However, FCS can induce side effects in cells due to its high content of growth factors. Cells react to these mitogens especially in their cytokine responses and intracellular MAPK pathways[67], e.g. Erk1/2[68].

1.2.2.2. Staining alteration

The usage of antibodies presents an especially potent factor for cell alteration in three different ways. First, the “immunological sensing” of antibodies via Fc-receptors on cell surfaces can lead to immune responses in cells[69]. Second, some surface receptors can be blocked for their ligand via antibody binding like CD25[70,71] (clinically relevant with Daclizumab) or EGFR[72]. Third, surface molecules can be activated by crosslinking due to antibody binding, e.g. CD3, CD28, 4-1BB[73]. Cells may also become exhausted or driven into cell death. For example surface molecules PD-1[74], CTLA-4, 4-1BB or FasR are known to induce those outcomes by crosslinking. Hereafter examples of antibody-induced alteration and an alternative to minimize these are discussed.

1.2.3. TCR signaling due to CD3 staining

Initial antigen-specific activation of T cells is driven by a multimerization of the T cell receptor complex with MHC molecules in an immunological synapse of APC and T cell. There are multiple pathways for the activation of T cell receptor signaling involving also co-receptor molecules CD4 or CD8. Multimerization of T cell receptor complex molecules induce transmembrane signaling effects, which lead to a phosphorylation of immunoreceptor tyrosine-based activation motifs (ITAMs) in the intracellular domains of the CD3 ζ chain via Src family kinases. This classical TCR signaling activation is also inducible by certain antibody clones directed against CD3. A good activator of TCR signaling is the CD3 clone Okt3®, which binds to the CD3 ε chain, historically known as surface molecule T3, and is able to induce TCR signaling in the presence of accessory cells[75], presented by feeder cells or in PBMC mixture. As a monoclonal IgG2a antibody, this clone crosslinks two or more CD3 molecules, leading to phosphorylation of the TCR signaling cascade (shown in Figure 5). The ITAM phosphorylation signals further downstream via tyrosine kinases. One of the first protein-tyrosine kinases to be involved is zeta-chain-associated protein kinase 70 (ZAP-70), which binds to phosphorylated ITAMs, indicating the earliest time point of TCR signaling processes (Suppl. Fig. 1).
By the phosphorylation of the linker for the activation of T cells (LAT), phosphorylated ZAP-70 addresses two discrete TCR signaling pathways via a tyrosine-protein kinase complex composed of multiple kinases, the so-called proximal signaling complex, a signalosome for TCR signal transduction[76,77].
This signaling bifurcation separates the signal into two cascades, leading to an activation of mitogen-activated protein kinases (MAPK) and the release of intracellularly stored Ca^{2+} from the endoplasmic reticulum. The MAPK pathway initiates the transition from the intracellular phospho-signaling to the translocation of transcription factors to the nucleus via the MAPK p44/42, also known as extracellular signal-regulated kinases 1 and 2 (ERK1/2) (Suppl. Fig. 1). ERK1/2 has a certain historical checkpoint function for the activation of the TCR as it induces the expression of cFos and the dimerization of Fos and Jun to AP-1 via Elk phosphorylation. The intracellular Ca^{2+}-release triggers the influx of extracellular calcium-ions into the cell via membrane-bound ion channels, amplifying this signal. The inhibition of the calcineurin/calmodulin complex due to Ca^{2+} triggers the de-phosphorylation of the nuclear factor of activated T cells (NF-AT), which leads to the translocation of NF-AT from the cytoplasm to the nucleus. Artificially induced TCR signaling effects, like CD3 antibody binding, potentially change T cell functionality by an initial activation step leading to cytokine secretion and proliferation. A CD3 multimerized TCR complex can be internalized by the cell if the antibody is soluble, which leads to the termination of the signal. However, if surface bound CD3 is used, for example in cell

culture plates, a lasting and sustained TCR signal is induced, leading ultimately to T cell anergy and cell death. Especially the clinical relevance of Okt3® as the clinical antibody Muromonab relies on T cell toxic properties.

In many cases, with antibody based purification methods, a CD3 marker staining is crucial for population differentiation. Nevertheless, after purification, TCR signaling should preferably be avoided for subsequent experiments.

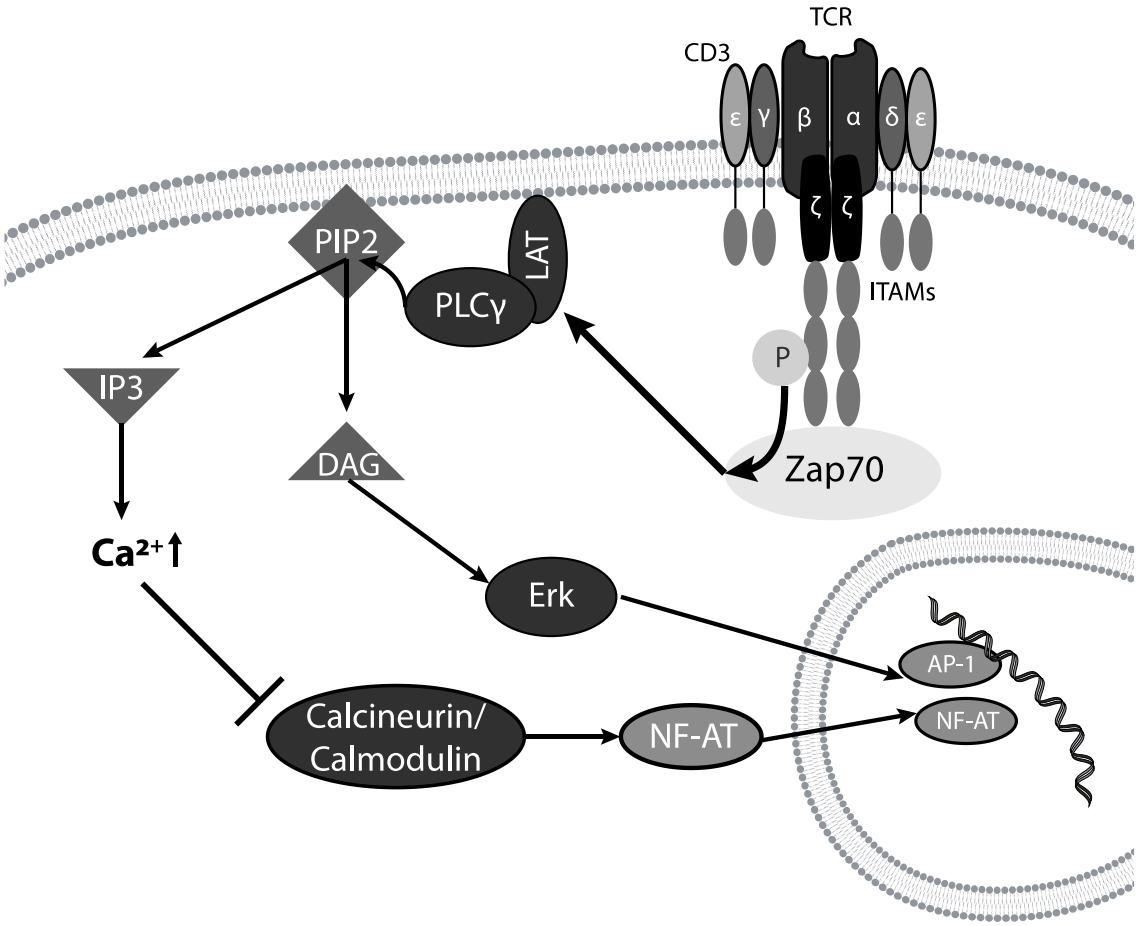

Figure 5: Simplified signaling pathway of the T cell receptor (TCR) after activation.
Certain checkpoints are highlighted, which in the following thesis were measured with different assays, or play a pivotal role in signaling procession and signal bifurcation.

There are first efforts to avoid these changes by using reversible antibodies[78], but changes induced by crosslinking can only be avoided by handling cells at low temperatures around 4°C. This is shown to work properly in the example of multimer staining[79] as the origin of Fab technology. But unpublished data also show a complete removal of surface Fabs at 4 °C (Fig. 6E) and no downstream TCR signaling at low temperatures.

1.2.3.1. Antibody-based reversible staining reagents

For a better understanding of the reversible reagent technology, it is important to elucidate the antibody structure first. Antibody structure can be divided into two major parts. When antibodies are digested with the enzyme papain, certain fragments remain (Fig. 6A). The cleavage of papain takes place in the hinge region of the antibody, generating two antigen-binding fragments (Fab) and one fragment crystallizable region (Fc). The Fab fragment has a light and heavy chain, each consisting of a domain of their variable and constant region. Fab fragments have the property to bind their antigen specifically at their antigen binding site, a 15 to 22 amino acid long sequence composed of both heavy and light variable chains. A certain binding strength to their antigen is necessary. The binding strength of an antibody, also referred to as binding affinity (K_D), is increased by the linking of two Fab fragments via the Fc part. Without the Fc part, Fabs as monomers have a different affinity, potentially enabling dissociation from their antigen.

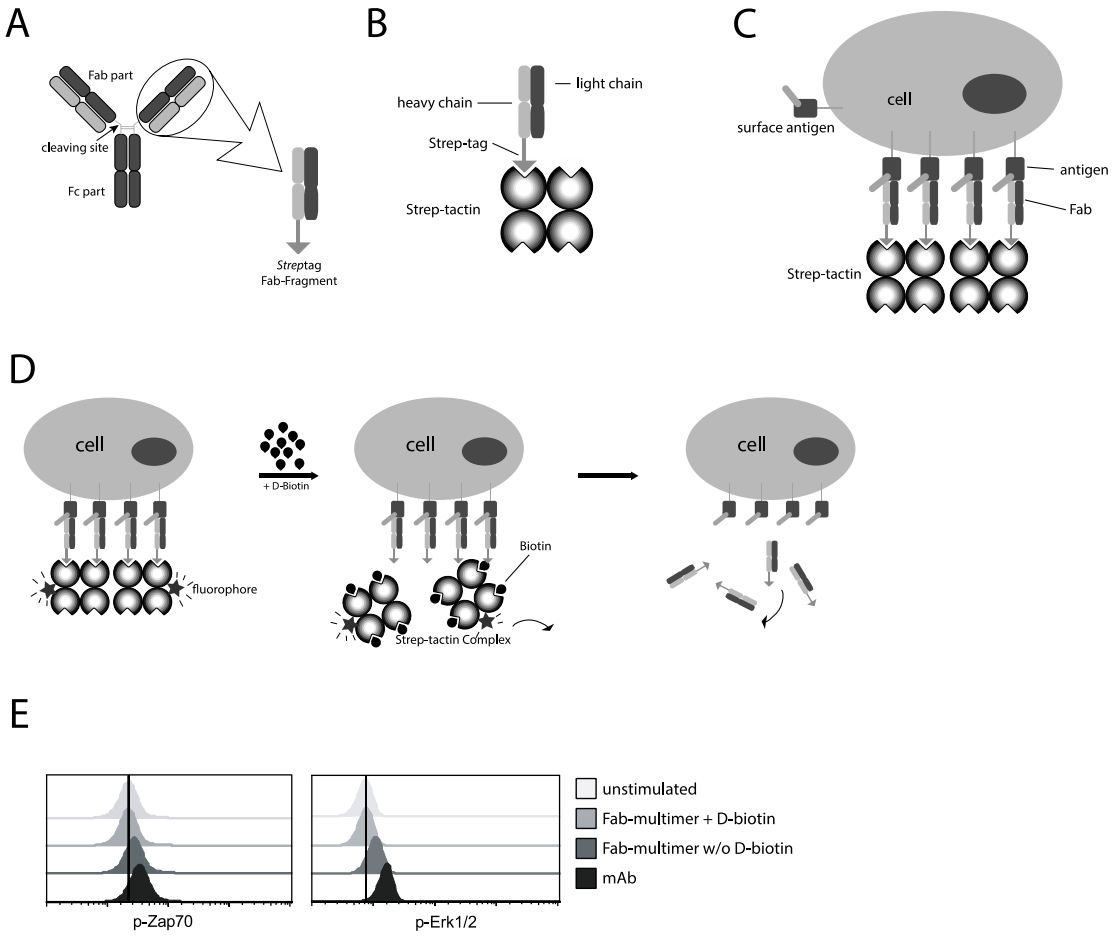

Figure 6: Scheme of reversible staining with Fab fragments.
(A-D) The principles of the reversible staining with *Strep*tag Fab fragments adapted from the original publication[78]. (A) Fab fragments originate from antibody structures; thus they are specific against certain antigens. They are designed without the Fc part, and are often mutated in their amino acid sequence for weaker binding (B) *Strep*tag Fab fragments can be multimerized via Strep-tactin, thus generating sufficient binding of monomers which otherwise would dissociate from their antigen. (C) Fab-multimers recognize their antigen and enable stable binding to surface expressed cell molecules. (D) Fluorescence-labeled Strep-tactin can be used for specific staining in flow cytometry. After the enrichment for specific markers, e.g. by FACS sorting, labels can be removed by the addition of D-Biotin. Due to low binding affinity, Fab-monomers do dissociate from their antigen after removal of the Strep-tactin backbone.
(E) Flow cytometry analysis of cellular phosphorylation states in CD8 T cells (pre-gated on living, single, and CD8 positive lymphocytes) for Zap70 and Erk1/2. Cells were stimulated or not with Orthoclone (mAb) or stained with a reversible CD3 Fab-multimer. Dissociation of CD3 *Strep*tag Fab-monomers after addition of D-Biotin results in a cell minimally altered by surface staining (data kindly provided by Stefan Dreher).

The idea is to use Fab fragments, which have a low avidity against their antigen, thus binding stably to their recognized antigen only in a multimerized[78] state (Fig. 6 C). In some cases, monomeric Fab fragments already show a low avidity and do not stably bind their antigen. In other cases, the Fab avidity is reduced by an amino acid mutation in the antigen binding site. This way, Fab fragment monomers are generated which dissociate with a fast K_{off} rate. Additionally a *Strep*-tag[80] is genetically fused to the heavy chain of these Fab fragments, enabling purification and multimerization of these monomers by a backbone (Fig. 6 B). The Streptamer technology offers a Streptactin backbone, which is reversible by the addition of Desthiobiotin (D-Biotin) as a competing ligand for backbone binding (Fig. 6 D). With this technology nearly all concerns for cell alteration due to antibody binding are addressed. As no Fc part is present, it prevents activation of the complement system, as well as cell-mediated killing of labeled cells. The dissociation of the Fab monomers assures no blocking of surface receptors for their ligands. The concerns for an antibody-induced alteration of surface TCR activation during staining and purification process are avoidable (Fig. 6 E).

1.2.3.1.1. Streptamer technology has the potential to dampen antibody-caused alterations

Hereinafter the binding of conventional Okt3® antibody, as well as Okt3-derived Fab-multimer and their cell activation due to staining were measured by flow cytometry. Intracellular staining with phosphorylation detecting antibodies against Zap70 and Erk1 and 2 was performed. Remarkably, hPBMCs stained with Fab-Streptamer which were treated with D-Biotin after staining and before flow cytometric acquisition, fit precisely into the Gaussian distribution of unstimulated cells, showing neither activation of Zap70 nor Erk1 and 2 after CD3 binding. In contrast, if the backbone of the Streptamer was not removed by D-Biotin, crosslinking of the TCRs led to a Zap70 phosphorylation and downstream signaling to the Erk1/2 MAPK. The Okt3 antibody alone was an even better activator of the TCR signaling cascade.

This indicates the potency of the reversible Fab-Streptamer technology to purify minimally altered, so-called unaffected cells. In combination with an antibody-based purification method at 4°C, cell alterations induced by this staining can be avoided. After purification under temperature control and addition of D-Biotin, all staining reagents can be washed off the cells, leaving unlabeled cells for further experimentation. So far complete temperature control can easily be provided for “low tech” column-based purification methods in a cold room. However, FACS, which requires a computer and other sensitive electrical and optical apparatus, is not well-suited for cold room storage. Nevertheless, we were aiming in an approach to be able to exclude staining induced cell

alteration by fully temperature-controlled FACS sorting, so far to our knowledge unreported.

2. Aim of this work

Fluorescence activated cell sorting (FACS) is a commonly used technique for detection and purification of specific cell types due to marker-based staining and morphological properties. The biological status of cells, their viability, vitality and functionality after a sort are crucial for the value and outcome of subsequent experiments. So far few attempts have been made to systematically evaluate sorting parameters and their influences on the quality of sorted cells. The physical mechanisms of FACS sorting mean that some sorting parameters like temperature, pressure, electric charge and shearing effects during the sort, as well as antibody staining and buffer composition, potentially affect cell phenotypes and cell functionality. We hypothesize that in varying, controlling, and monitoring certain sort conditions, we can minimize cell alterations and cell activation.

With Fab-TACS® Traceless Affinity Cell Selection and reversible Fab-Streptamers we hold important tools in our hands to evaluate cell alteration in minimally altered primary cell populations due to isolation processes. In previous publications of changes in cellular physiology due to FACS sorting, isolation processes of primary cells or artificial activation in cultured cells proofed to hold the greatest effects.

Special emphasis of this thesis project was to put on the importance of optimal control of sort temperatures. This has not yet been systematically analyzed due to the lack of machines allowing to strictly control this parameter. Since there is no commercially available cell sorter for variable temperature control at low temperatures, we had to develop a prototype for performing such experiments. Examining FACS in detail revealed certain obstacles, such as when large amounts of sample material or small target populations were purified, work time and sort purities were negatively affected. Because of that, we established a fast FACS-based pre-enrichment method, built on fluorescence triggering and developed optimized staining panels for certain applications.

Therefore, following aims should be achieved in the present thesis:

1. Construction of a modified cell sorter with strict temperature control assessing stable temperature sorting.

2. Investigation of the influence of current cell sorting procedures on the functionality and physiology of sorted cell types.

3. Development of a new technical sorting procedure to overcome FACS obstacles with respect to high cell count and rare event sorting.

.

3. Results

Until today, there is no commercially available cell sorter that controls low temperature over the entire instrument's sort lines. Only the sample holder and receptacle holder can be cooled, and no chilling of sheath fluid or the sample line is available. Therefore, we started to modify a sorter to get complete temperature monitoring and control, in order to test if cell activation due to antibody staining can be reduced or prevented (Suppl. Fig. 1 A). Since antibody binding can activate T cell receptor signaling after CD3 staining within 30 sec at room temperature, a time frame fitting the expected duration of cells passing sample lines in FACS instruments, even the short time cells spend in the un-chilled sample line should be considered (Suppl. Fig. 1 B). As already described, the survival of cells at low temperature is critical and has to be evaluated for each cell type individually, as low temperature storage can severely affect cells after restoration to normal conditions[81].

3.1. Temperature-controlled FACS

Condensation in cold rooms, unavoidable without expensive air conditions, can potentially harm the electronics and reduce light signals on the optical mirrors and filters. To avoid damages on our equipment we chose to use an approach that provides complete temperature control just for the fluidics system, instead of the whole instrument. This way, one instrument is capable of sorting cells at any temperature applied to the fluidics systems. The compartmentation, especially for FACS sorters based on the technology of DakoCytomation, enables a division into three separate major areas: first the optical system with mirrors and lasers, second side electronics and data displaying and processing tools, and finally the sorting module containing the fluidics system and deflection. Hereafter, the basic principle of the fluidics system of a MoFlo XDP is shown, highlighting the modifications enabling temperature-controlled cell sorting.

3.1.1. Temperature-controlled cell sorting modifications

The pressure control provides freely adjustable compressed air for two different fluidic lines (Fig. 7). One of these pressurized fluidic lines is the sheath stream, generating the baseline pressure of the system, depending on the nozzle size. The other pressurized fluidic line is commonly referred to as the sample line, which is also freely adjustable and pressurizes either a sample tube or a cylinder containing sample material. The differential pressure of sheath pressure and sample pressure is a direct measure of the

sample flowrate and within certain boundaries linearly dependent, giving the user the ability to adjust EPS (events per second) rates suitable for the experimental settings. The sheath system and sample line come together in the nozzle just before the sort stream is generated. After leaving the nozzle assembly, the fluidic system is depressurized. The mixture of sheath buffer and sample line fluid forms droplets which end up either in the waste stream or deflected to the sides of the stream are collected in tubes. FACS sorters in most facilities are standardly mounted with a cooling system for the sample tube holder at the beginning of the sample line, and the receptacle holder at the end containing the tubes for deflected droplets, hereinafter termed conventional sorting. This way the cooling system assures a constant temperature for the cells over the whole sorting process, ensuring for example no antibody internalization. As already shown (Suppl. Fig. 1), CD3 activates PBMCs and Jurkats after 2 min at room temperature with a downstream signaling of Erk1/2 and even earlier at ZAP70. With differential pressures of lower than 1 psi, cells travel through the sample line with a speed of around 0,001 to 0,01 m/s, taking 2 to 3 minutes to pass through entirely. During this time frame, measurements within the tube showed rewarming of the sample fluid to surrounding temperatures, shown in previous work done by Martin Schatte. Thus, the usage of reversible staining would not exclude cell activation due to surface receptor activation in conventional sorting. To ensure absolute temperature control over the sorted sample, the entire sample line must be cooled. Furthermore, the sheath fluid has to be adjusted to the low temperature, as both mix in the nozzle assembly. For this purpose, we created the following changes (Fig. 7). A first pre-cooling of the sheath fluid to 4°C at the filter reservoir ensures subsequent lower sheath temperature, which is possible to maintain even with nozzle sizes larger than 70 µm. The sheath filter tubing is completely insulated, preventing rewarming of the sheath fluid and condensation formation after this pre-cooling. Before the valve control of the manual sample station, the sheath lines vermiculate through an aluminum block chilled down to 4°C, maintaining the adjusted temperature for the sheath fluid. Still carefully insulated, the tubing of sample line and sheath lines join after the manual station to be actively chilled by a surrounding cooling fluid adjusted to 4°C until entering the nozzle assembly. Hereafter, during sheath stream and droplet formation, neither insulation nor cooling was possible until the deflected droplets collected in the receptacle holder. Temperature measurements showed a rewarming of the fluids to 5 – 12°C during system passage (Table 1), a temperature shown to be sufficient to avoid activation processes in PBMCs with Okt3 staining (Suppl. Fig. 1 A). To evaluate system temperatures at different access points, we chose a fiber optical measurement (Fig. 7 B and C). Due to the small diameter and flexibility of the sensors, we could provide temperature surveillance at the indicated eight red access points (Figure 7 A). During cell acquisition and sorting, a four-channel

opSense instrument (model: TMS-G4-20-100ST-L) was used (Fig. 7 B) and the temperature was monitored at the access points 4, 5, 6 and 8.

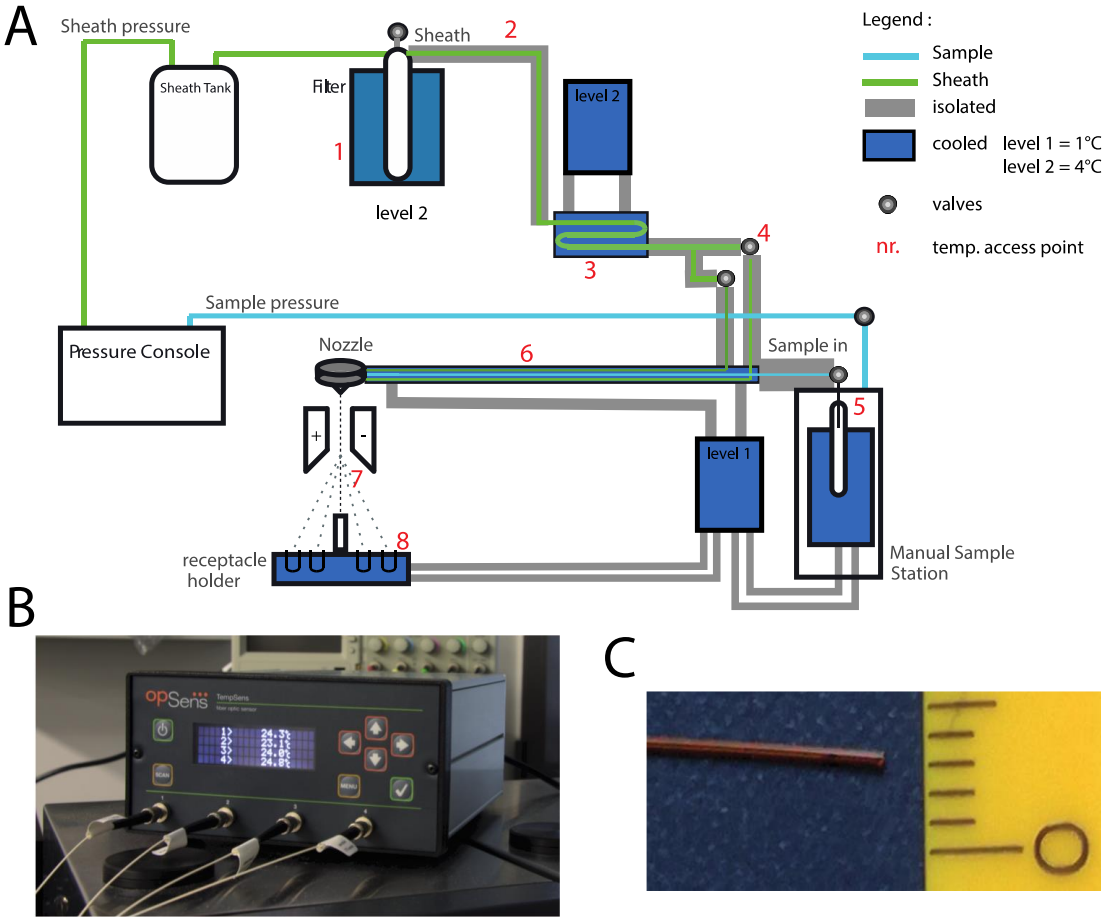

Figure 7: (A) Schematic drawing of the fluidic system of a MoFlo™ XDP.
Three different coolers and strict fluidic line insulation enable complete temperature control. Sheath buffer and sample line temperatures are freely adjustable, contrasting commercially available FACS instruments. (B) Temperature measurement under constant control during sample acquisition by a fiber optical four-channel instrument (opSense). (C) Photography of the fiber optic tip. Changes of the refraction index in the tip by temperature can be measured. For size comparison ruler shows 1 mm point to point distances.

Hereafter, a measurement series for sorting under complete temperature control at 4°C with surrounding room temperature at 23°C is shown for all access points:

Measurement access point (Nr.)	Temperature (°C)
1	4
2	14
3	4
4	7,9
5	5,6
6	8,1
7	11.4
8	7,2

Table 1: Temperature screening of the sheath fluid in a fully controlled system.
Values of the measured temperatures at the different access points from Figure 7A under the described cooler conditions (Level 2: 4°C/Level 1: 1°C).

After pre-cooling of the sheath filter to 4°C, the sheath fluid leaving the filter rewarms to 14°C, but after entering the aluminum block, the second sheath cooling stage at 4°C, the final sheath temperature measured at the valves of the manual sample station is 7,9°C. Manual sample station, sample line tubing and receptacle holder are temperature-controlled by a cooler operating at 1°C, which allows a temperature of 5,6°C in the sample tube and a temperature of 7,2°C in the collection tube during sorting. The sheath fluid lines and sample line joining together after the valves of the sample station are kept at 8,1°C. After leaving the un-cooled nozzle assembly, sheath fluid stream rewarms to 11,4°C, thereby indicating the highest temperature sample material is exposed to during system passage. Hereafter differences between conventional, un-cooled and temperature-controlled sorting concerning cell activation via Okt3 are elucidated.

3.1.2. Antibody-induced cell alterations in temperature-controlled cell sorting

The Calcio-metric dye Indo-1 was used for the measurement of intracellular Ca^{2+} levels after TCR stimulation. The emission fluorescence intensity of this dye shifts due to calcium concentration in the media, indicated by the different lines (Fig. 8 A). Unbound Indo-1 emits light on a green wavelength, whereas bound to calcium, the fluorescence shifts to the violet spectrum. This shift, based on the binding of Ca^{2+}, is measurable by the quotient of the two emission spectra. Dye excitation by the 355 nm laser generates fluorescence signals detected by two channels with bandpass filters at 405/30 and 530/40 (optical layout Fig. 8 B). The ratio of the two fluorescence channels, determined by light signals from the channel UV1 (405/30) divided by the light signals from UV2 (530/40), is displayed over a time course in FACS plots (Fig. 8 C). Rising of the signal shows binding of free Calcium ions inside the cells.

For measurements, the CD3 crosslinking clone Okt3 (trade name Orthoclone) was added in real-time to Jurkat cells during acquisition. At indicated time points, marked with an arrow (Nr. 1), TCR stimulating agent was added to the Jurkat cells. At the second indicated time point, accessible Ca^{2+} was removed by complex formation from the storage buffer by the addition of EGTA (8mM). With the change of the Indo-1 fluorescence spectrum, a direct measurement of the intracellular calcium level by the activation of the TCR was measured, indicated by the increased fluorescence signal from the UV1/UV2 ratio (Fig. 8 C).

By cooling the entire instrument, even the un-physiologically strong stimulus of ionomycin causes less TCR stimulation, as compared to conventional sorting.

While a CD3 stimulus is sufficient to activate Jurkat cells at sheath temperatures of 21°C, but chilled sample holders (conventional sorting), activation does not occur at completely controlled 4°C conditions (Fig. 8 C). Completely temperature-controlled cell sorting started at a higher fluorescence baseline ratio, as alignment issues caused this effect. Completely cooled sheath fluid required a realignment of the laser to sheath fluid for optimal alignment. For Orthoclone stimulation of Jurkat cells, only small differences between fully cooled and conventional were observable, as the calcium flux to this stimulation was significant smaller. Hence completely temperature-controlled sorting showed lower activation compared to an un-cooled sample line. To evaluate this, we tested for intracellular MAPK phosphorylation after TCR stimulation.

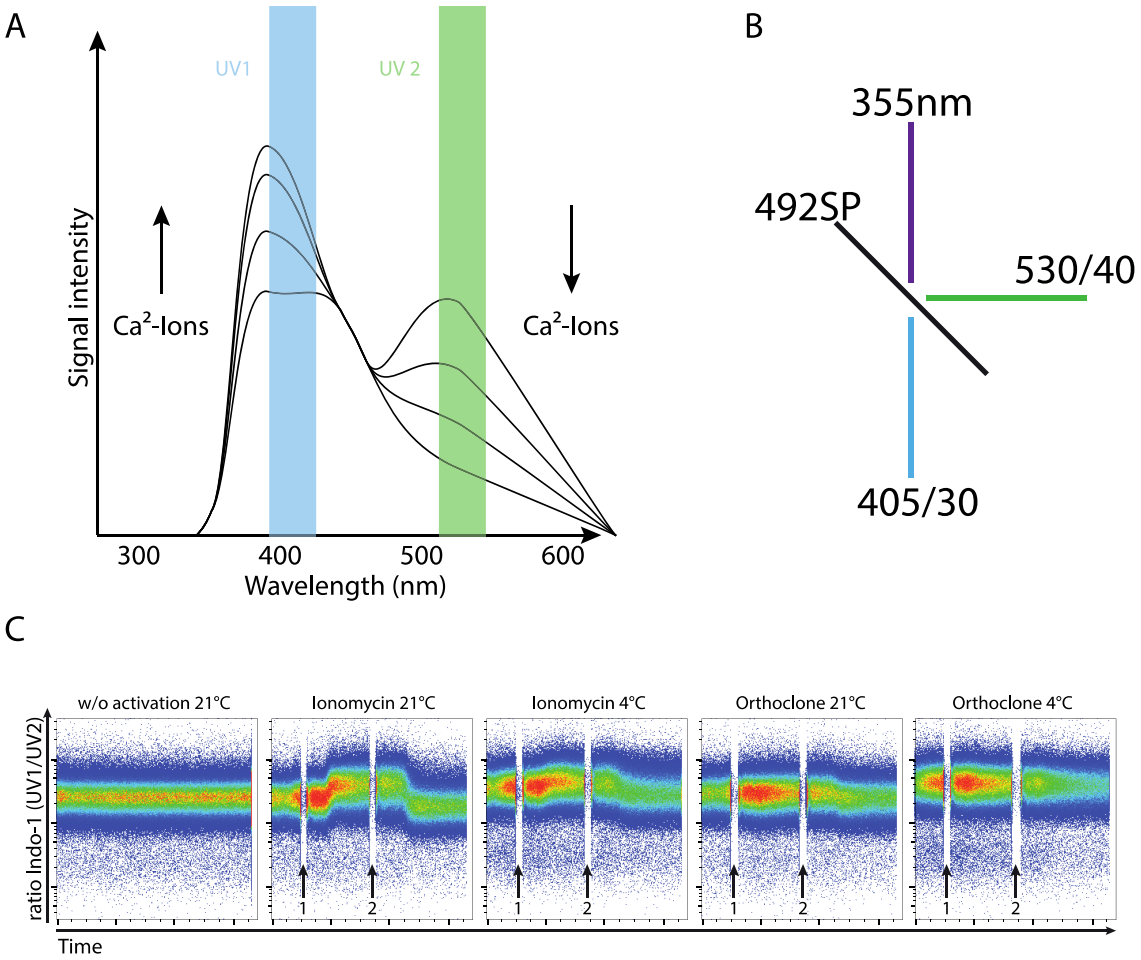

Figure 8: Calcium flux measurements in a temperature-controlled sorter.
(A) The fluorescence spectrum of Indo-1 shifts by the binding of calcium ions. Here artificial emission spectra for 340nm excitation are shown. Fluorescence intensities of Indo-1 increase or decrease for different wavelength areas depending on the Ca^{2+} concentration; measurement of these intensities in two different channels UV1 and UV2 makes differences in Ca^{2+} levels visible. (B) Optical setup for the detection of changes in the Indo-1 spectrum on the MoFlo™ XDP. 355nm laser excitation generates fluorescence signals for detection in UV1 channel 405/30 and UV2 channel 530/40nm. Signals are split by 492nm short pass dichroic filter. (C) Flow cytometric analysis of intracellular Ca^{2+}-Ion concentrations in Jurkat cells stained with the Ca^{2+} sensitive dye Indo-1. At indicated time points cells were stimulated (1) by addition of Ionomycin or Orthoclone. At indicated time points (2) extracellularly accessible Calcium was removed by addition of EGTA (8mM).

After calcium flux, the TCR signaling molecules Zap70 and Erk1/2 were examined. For this, 10^6 Jurkat cells were lysed after sorting with or without CD3 stimulus. Their phosphorylation status was determined by Immunoblot (Fig. 9 A). Sorting decisions were based only on FSC/SSC properties, excluding cell debris, henceforth referred to as “mock sorting” (Fig. 9 B). Unsorted Jurkat cells stored at 4°C served as a negative control (Fig. 9 A). Unsorted cells incubated with Okt3 displayed only Zap70 phosphorylation, merely indicating surface activation of stimulated cells, without downstream signaling to Erk1/2 at 4°C. Similar to the negative control, in every case of sorted and CD3 stimulated cells Zap70 was activated. Phosphorylation of Erk1/2 was slightly induced in sorted samples, regardless of CD3 stimulation. Un-cooled sorting at 21°C room temperature led to downstream signaling Erk1/2 phosphorylation of the TCR surface complex. Chilling of the sample in conventional sorting, as well as cooling of sample and receptacle holders, already inhibited ZAP70 downstream signaling. This phosphorylation pattern also appeared in the 4°C completely temperature-controlled sorting approach. The housekeeper protein beta actin was used as a loading control for protein content within different conditions.

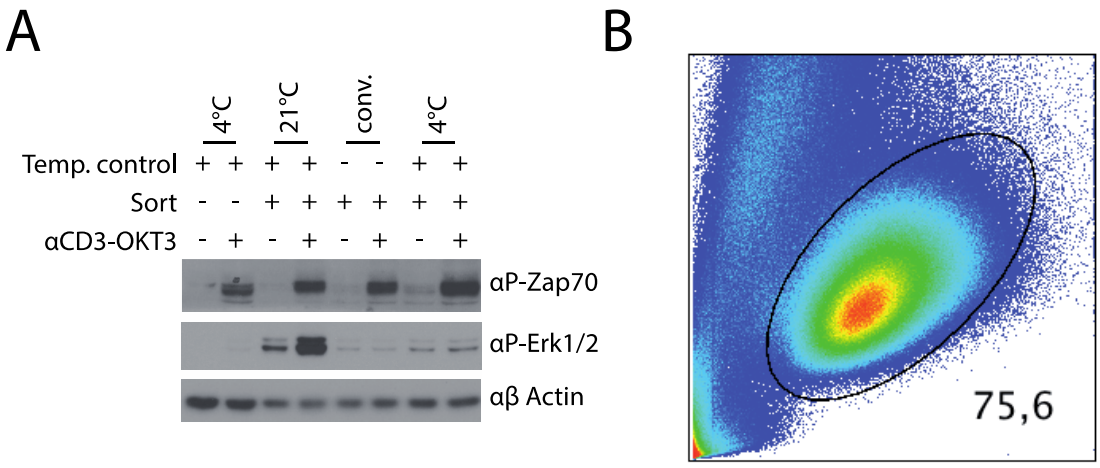

Figure 9: TCR activation of Jurkat cells due to CD3 activation in a temperature-controlled sorter. (A) Immunoblot of Jurkat ACC282 lysates. Orthoclone (CD3 clone Okt3) was used for TCR stimulation. Sorting or no sorting of ACC282 cells on a MoFlo™ XDP, where temperatures for sheath buffer and sample line and sample storage were fully controlled and monitored. Anti-phospho Zap70 and anti-phospho Erk1/2 antibodies were used, as loading control anti-beta actin. (B) “Mock” sorting of Jurkat cells with exclusion gates only on FSC/SSC properties excludes cell debris only. Enabling closest accordance between sorted and unsorted.

Overall, in the case of Ca^{2+}-flux, temperature-controlled cell sorting did slightly exceed conventional sorting approaches, while for MAPK signaling both approaches seem sufficient to avoid activation compared to uncontrolled temperature conditions. The rewarming of cell material in the sample line itself in conventional sorting is not capable of triggering downstream signaling to MAPK Erk1/2. However, the activation of ZAP70 under 4°C chilled sample storage conditions still allows for downstream signaling after rewarming. We cannot exclude that we missed the TCR signal between ZAP70 and Erk1/2 in conventional sorting approaches at the time point we checked. Our temperature-controlled system supports, by excluding any possible cell alteration during reversible staining protocols and sorting, minimally altered cell phenotypes post-purification.

However, despite the benefits the danger of hypothermic conditions in all chilled sorting approaches of induced cell death is commonly agreed upon[58,60,81,82]. Therefore we evaluated cell survival under storage conditions of different cell types and temperatures.

3.1.3. Temperature effects on cells - Viability

We used optimal buffer conditions (cell culture medium RPMI, 10% FCS; murine culture medium was supplemented with β-mercaptoethanol) for different cell types. Two primary cell types, human PBMCs and murine splenocytes, were used. PBMCs were generated from buffy coat material via Ficoll gradient centrifugation. Splenocytes were generated from sacrificed C57BL/6 donor mice. Spleens were homogenized with a 100 µm cell strainer and subsequently red blood cells were depleted by Tris-buffered ammonium chloride (ACT) lysis. For immortalized cell cultures, either K562 cells, a human derived lymphoblast suspension cell line, or Jurkat cells ACC282 were used. Survival under three different temperature conditions for each cell line was evaluated by PI staining over a time frame of 3 h (Fig. 10 A). Cells were kept under indicated temperature conditions, harvested at certain time points (0, 60, 180 min), and after live/dead staining analyzed by flow cytometry. Human PBMCs did not show any effect concerning their viability even after 3 h storage at 4°C, proving resistance against temperature-induced apoptosis for a time frame reasonable in FACS sorting. Murine splenocytes did not differ from human primary cells during long term ice storage, as no additional apoptosis occurred after 60 minutes. The main factor for cell death for this cell type was the homogenization and lysis process, since post-isolation this cell type already displays the lowest survival counts of all cell types. The cultured cells K562 did not show any effect at physiological or room temperature storage conditions. Yet at 4°C, survival drastically drops when stored for longer than 1 h. Since cultured cells are often used for cell sorting approaches in basic research, we evaluated whether hypothermic stress can be avoided while still

minimizing potential antibody alterations at low temperatures. For this we applied different hypothermic conditions 4°C, 8°C and 12°C as well as 21°C and evaluated induced cell death by Caspase 1 activity (Fig. 10 B). The dye Flica, which is sensitive for cleaved Caspase 1, indicates early apoptotic processes mediated by a mitochondrial pathway.

After storage for the indicated time (0, 60, 120 and 360 minutes), Jurkat cells were harvested, stained and analyzed by flow cytometry. Similar to the K562 cells, Jurkats did not survive well at 4°C conditions for longer storage times, whereas a warmer storage condition of 8°C already drastically increased cell survival even after 6h of incubation. Surprisingly, 12°C conditions were already sufficient for Jurkat cells to survive as well as under room temperature conditions. A temperature adjustment to 12°C for longer FACS sorting times with cultured cells in cooled systems would be preferable.

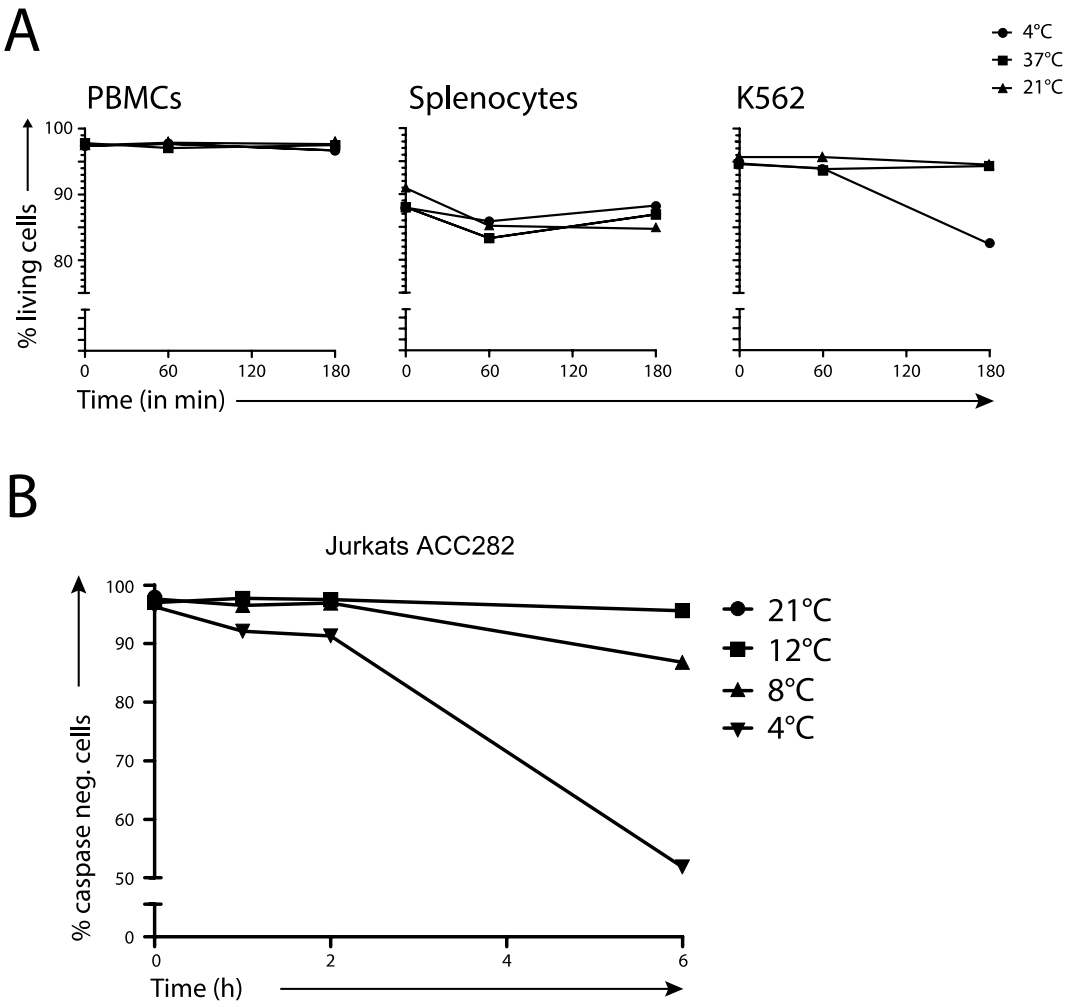

Figure 10: Survival of different cell types under hypothermal conditions.
(A) Time course of cell survival after storage under different temperature conditions. Primary cells from human material (PBMCs), murine material (Splenocytes) and cultured cells (K562) were pre-gated on FSC/SSC properties. Staining with propidium iodide (PI) and flow cytometric analysis at 0, 60 and 180 min showed the overall survival of cells under the different temperature conditions. (B) The Jurkat cell culture line ACC282 was stained for cleavage and activation of intracellular Caspase 1 by FLICA. Different temperature gradients from room temperatures of 21°C to 12 and 8°C, down to 4°C were analyzed for the time points 0, 60, 120 and 360 min.

3.2. Screening for possible cell alterations by FACS

Besides cell alterations caused by sample storage and preparation, temperature or antibodies, FACS sorting may also harm cells by its mechanic or physical properties. We intended to clarify sorting-induced cell alterations by the FACS instrument itself with the following approaches.

3.2.1. Viability of cells after cell sorting

As already described, certain physical and mechanical forces are needed to allow fluorescence activated cell sorting (Fig. 4). The most obvious force is the high system

pressure defined by the nozzle size. Although most instruments, especially the more sophisticated cell sorters, allow freely adjustable nozzle sizes, some do not. In our facility we are fortunate to have three different cell sorting instruments in one room, which gives us the opportunity to use them simultaneously with the same sample material operated by the same person. The sorters were operated with comparable system pressures by consistently using a 100 µm nozzle. Some sorters generate a stream, which is hit by the laser in the air, commonly referred to as the "Jet in Air" system. Others acquire light signals first in a cuvette and generate the stream for droplet generation and sorting after data acquisition. Hereafter we compared two "Jet in Air" systems, a MoFlo Legacy (Beckman Coulter) and an Avalon cell sorter (PropelLabs), as well as one cuvette-based system, the Aria III (Becton Dickinson). As with the experimental setting for temperature influences, the evaluation of induced cell death and apoptosis was in focus. For this, three different early and late apoptotic markers were applied. 7-Aminoactinomycin D (7AAD) intercalates in the DNA between cytosine and guanine, entering the cell when membrane integrity is lost, thus indicating a late stage in the apoptotic process. Earlier markers of programmed cell death are the activation of caspase 1 and the accumulation of phosphatidylserine (PS)-based phospholipids at the outer membrane layer. Except for erythrocytes, cells actively keep PS located at the cytoplasmic side of their cell membrane by an enzyme called Flippase. In contrast, the enzyme scramblase is responsible for an active transport of PS to the outer membrane, activated by high intracellular Ca^{2+} levels. AnnexinV, the third marker used for apoptotic processes in this panel, can bind surface-exposed PS. Both early apoptotic markers, Flica and AnnexinV, can potentially be activated by pathways not related to programmed cell death, like the inflammasome, which can activate caspase 1 and cellular responses like cell activation by Wnt signaling or IP3, which release Ca^{2+} from intracellular endoplasmic storage. Yet the combination of both markers can be used to visualize early apoptotic processes in the cell. A staining of murine splenocytes after ACT lysis, FACS-sorted on three different instruments in parallel, with these three apoptotic markers was carried out (Fig. 11 A). Splenocytes were sorted for living single lymphocytes by PI staining and scatter properties for the exclusion of dead cells after cell preparation. Nevertheless, after sorting and re-staining, still 8 to 11% of splenocytes were dead cells according to 7AAD exclusion, even though analyzed sorting purities were PI negative. This indicates occurring cell death after sorting. The Aria III and Avalon performed similarly, while the MoFlo had the lowest 7AAD numbers, with overall 92,4% living cells. The 7AAD negative population was further gated for Flica and AnnexinV staining. The double positive population for those two early apoptotic markers was below 1% for all instruments, with the highest proportion of 0,87% resulting from the Avalon. This indicates that, despite the 8 to 11% of 7AAD dead cells, a low number of cells undergo an apoptotic process

after sorting. For the Aria III, higher AnnexinV single positive numbers were detected compared to the other instruments. Gating of 7AAD positive cells emphasizes the correlation of all three apoptotic markers, since more than 90% of 7AAD positive cells are also double positive for Flica and AnnexinV. The instruments showed no clear effects between different sorters when compared head to head in parallel. We further evaluated the instrument comparison of different sorters by the transfer of the apoptotic panel on PBMCs (Suppl. Fig. 2). In addition to FACS sorting, MACS-sorted and unsorted cells were included. For a direct comparison between the conditions we could not exclude dead cells prior to sorting, which led to the use of freshly isolated PBMCs. These would be least affected by purification steps before sorting, since this primary cell type proved most resistant to harsh external conditions in previous experiments. Taken together PBMCs also show similar performance between different FACS sorter. When compared to a MACS purification, in which cells only passed the column and were collected afterwards, FACS sorting did not show any drawbacks. All purification methods led to more dead cells compared to unsorted counterparts immediately after purification. However, over a time course of two days all conditions show similar patterns of apoptotic and dead cells. The initially higher count of dead cells after sorting (MACS as FACS), compared to unsorted cells, indicated an accelerated induction of apoptosis, also seen in the FLICA and AnnexinV stainings. But cells from the unsorted control died rapidly later on, detected by AnnexinV and FLICA after 24 hours, while counts for apoptotic cells in FACS-sorted controls stayed constant low even at later time points. These data indicate that sorting accelerates the dying of cells, while no to little additional apoptosis is induced due to sorting.

As the induction of early apoptotic markers was only minimally detectable after sorting, we evaluated the viability of cells post-sort in multiple experiments (Fig. 11 B) via the late apoptosis marker membrane integrity. Murine splenocytes were gated on living single lymphocytes for $CD4^+$ and $CD8^+$ during the sort. The frequencies of PI negative cells post-sort were between 95,55% and 96,7%. After sorting, cells rested for two hours at room temperature to assure the apoptotic cells' loss of membrane integrity. Subsequently, sorted samples were split and analyzed via trypan blue staining on a ViCell automated cell counter or via PI staining with flow cytometry. All data for all experiments were pooled (Fig. 11 B). Altogether ViCell analysis generated very homogeneous data sets for each instrument, while analysis by flow cytometry produced higher survival for the "Jet in Air" systems when compared to the Aria III by students t-test (p value of 0,0053). Nevertheless, the majority of experiments with the Aria III showed comparable survival values to "Jet in Air" systems. Mostly the Aria III sorted above 80% living cells, except one outlier.

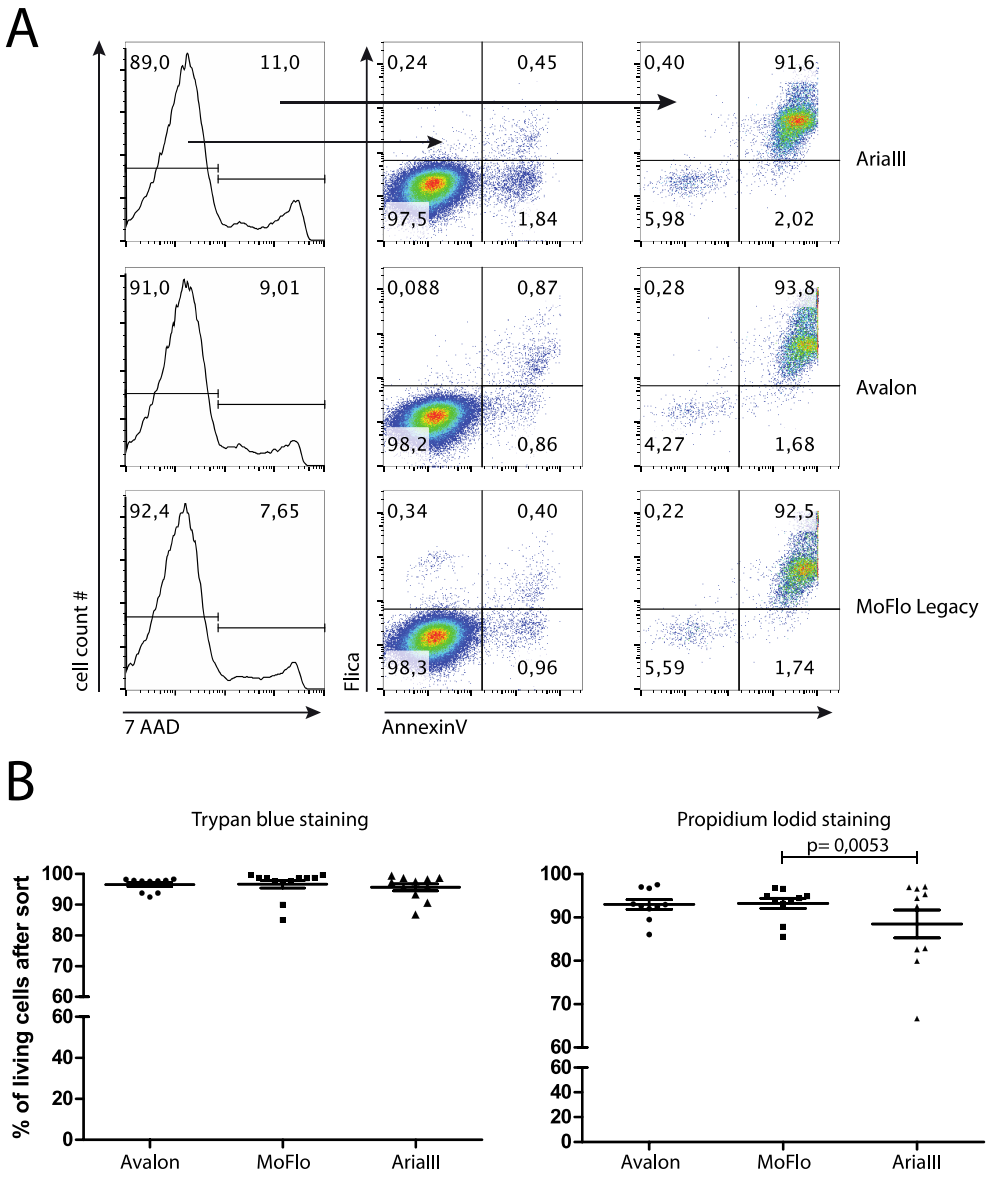

Figure 11: Survival of murine splenocytes after flow cytometry cell sorting.
(A) Murine Splenocytes (pregated for all cells FSC/SSC, singlets and PI exclusion) stained with early and late apoptotic markers, 7AAD, AnnexinV and Flica, after sort on three different FACS instruments. (B) Murine splenocytes were sorted on three different FACS instruments, all operated with a 100 µm Nozzle. Splenocytes were stained and sorted for CD4 and CD8 populations (pre-gated on lymphocytes, singlets and living cells) und subsequently analyzed via two readout systems: trypan blue staining on a ViCell instrument and PI staining by flow cytometry. Data of different sort experiments from CD4 and CD8 cells were pooled.

Overall, data indicated good performance of the cell sorters in keeping primary cells viable after sorting.

Since we found AnnexinV single positive cells within the 7AAD negative population, we went deeper into cellular signaling pathways to evaluate cell activation due to sorting.

3.2.2. Intracellular signaling pathways after sorting

Increased activation of cells by external factors is a conserved mechanism of many different species as plants, fungi and mammals, and is mostly mediated by the mitogen-activated protein kinase (MAPK) pathways[83]. Four major MAPK nodes are described which can be activated separately from each other depending on the stimuli (Fig. 12). First, Erk1 and 2 have already been described as part of this machinery, where they react very sensitively to extracellular stimulus. Second, extracellular-signaling-regulated kinase 5 (Erk5) is known for being activated by stress signals like oxidative stress, hyperosmolarity or mitogens[84]. Third, there is the c-Jun-amino-terminal kinase (JNK), also known as stress-activated phospho-kinase (SNPK). One of its main functions is a reaction to osmotic shock, ultraviolet irradiation or heat shock. Finally, the p38 family which in mammals activates in response to environmental factors and inflammation; it consists of four different members α, β, γ and δ, with the α-p38 ubiquitously expressed in nearly all tissues.

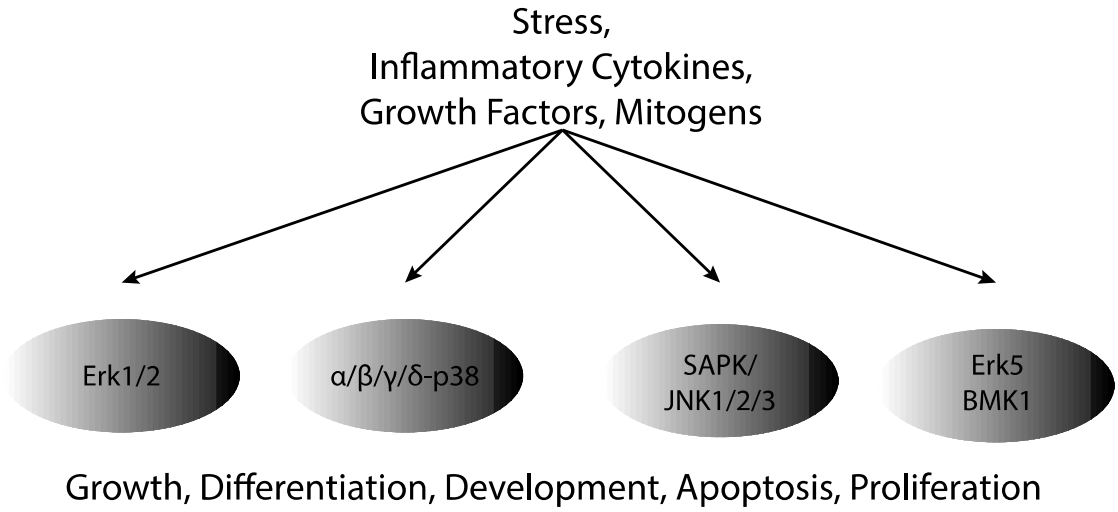

Figure 12: Schematic drawing of extra cellular stress factors in MAPK pathways.
Most species evolved a complex cellular machinery for sensing extracellular stress signaling by the MAPK pathway. In mammalian cells multiple different signaling pathways mediated by a broad spectrum of stimuli coalesce at four molecular signaling nodes Erk1/2, p38, JNK and Erk5. An activation of these MAPKs by phosphorylation to these stimuli mediates gene regulation via transcription factors and cellular responses.

3.2.2.1. Screening of MAPK pathways

For the purpose of cell activation screening, we dispensed with the use of antibodies and performed sorting based on scatter properties only. This type of mock sorting requires a pre-purification method to determine responses in a specific primary cell population, which ensures the greatest possible comparison between unsorted and sorted populations and well-defined cell type dependent responses. Two purification methods of choice were used on human blood-derived material, as certain cell types can be easily purified from it: either PBMC samples from buffy coat after Ficoll gradient density centrifugation, or CD8 positive cells enriched by the Fab-TACS® method. Fab-TACS® relies on reversible reagents and is explained later on in detail. Cells isolated with both purification methods were rested in starving medium overnight to reduce artifacts generated by the pre-purification method and to synchronize the cells. hPBMCs were either rested or mock-sorted on a MoFlo XDP using a 488 nm 200 mW and a 355 nm 100 mW laser, and then processed immediately and after 30 min with a subsequent staining. Samples were live/dead discriminated with ethidium monoazide (EMA), permeabilized and stained with phospho-specific antibodies directed against JNK, Erk1/2 and p38. Afterwards, flow cytometric analysis for living single lymphocytes displayed the following phosphorylation pattern (Fig. 13 A). No activation of JNK could be detected, although 355nm laser light was used during sorting, which hints that UV irradiation is not strong enough or lasts too briefly to activate this pathway. In comparison, a high number of cells were phosphorylated for the MAPK Erk1/2 and p38 after mock sorting conditions. During a sort, cells come in contact with various buffers and fluids, indicating a potential activation of MAPK by osmolality changes or mitogens like FCS. To differentiate whether sorting buffers or the FACS instrument induced the occurring phosphorylation, hPBMCs were stored in buffers composed similarly to the ones used for mock sorting. Cells of the same origin as used for mock sorting were stored in cell culture medium, sheath fluid or high amounts of FCS, to examine the p38 and Erk1/2 phosphorylation (Fig. 13 B) by mimicking different sorting fluids and buffer. The ratio of phosphorylated and endogenous p38 after storage in these media was calculated with ImageJ, where p38 did not show a buffer dependent phosphorylation pattern. The numbers of this ratio made clear that different sorting buffers do not explain the strong activation after sort.

In contrast, buffers induced an activation of Erk1/2. A high content of FCS, 20% FCS in FACS buffer (FF), drastically increased the overall amount of phosphorylated p44/42 over the time course of up to 30 minutes (Fig. 13 B). No other buffer condition induced activation that strongly, hinting at a potential activation by mitogens from the FCS.

Finally, the activation of the fourth MAPK pathway Erk5 by mock sorting was evaluated by Immunoblot, as no commercial flow cytometric antibodies for detecting this

phosphorylation were available (Fig. 13 C). An aliquot of hPBMCs pre-sort, pressurized by the sorter with 4 bar and afterwards depressurized, served as control. On the other hand, hPBMCs were mock-sorted on a MoFlo XDP. Sorting did not alter Erk5 phosphorylation patterns. Protein content of β-actin was used as loading controls.

The activation of another stress signaling pathway was evaluated in addition to the MAPK screening (Suppl. Fig. 3 A). Immunoblots for the phosphorylation of eIF2α due to sorting were performed with hPBMCs, but indicated no clear role in a FACS-induced activation (Suppl. Fig. 3 B).

All in all, only p38 and Erk1/2 showed pronounced activation due to sorting. Yet sorted cells did sense different stimuli in the consequence of their MAPK activation. Erk1/2 is in part activated by buffer conditions; in contrast sorting alone activates p38 due to mechanical or physical forces. In subsequent experiments we evaluated potential mechanical FACS forces responsible for this activation.

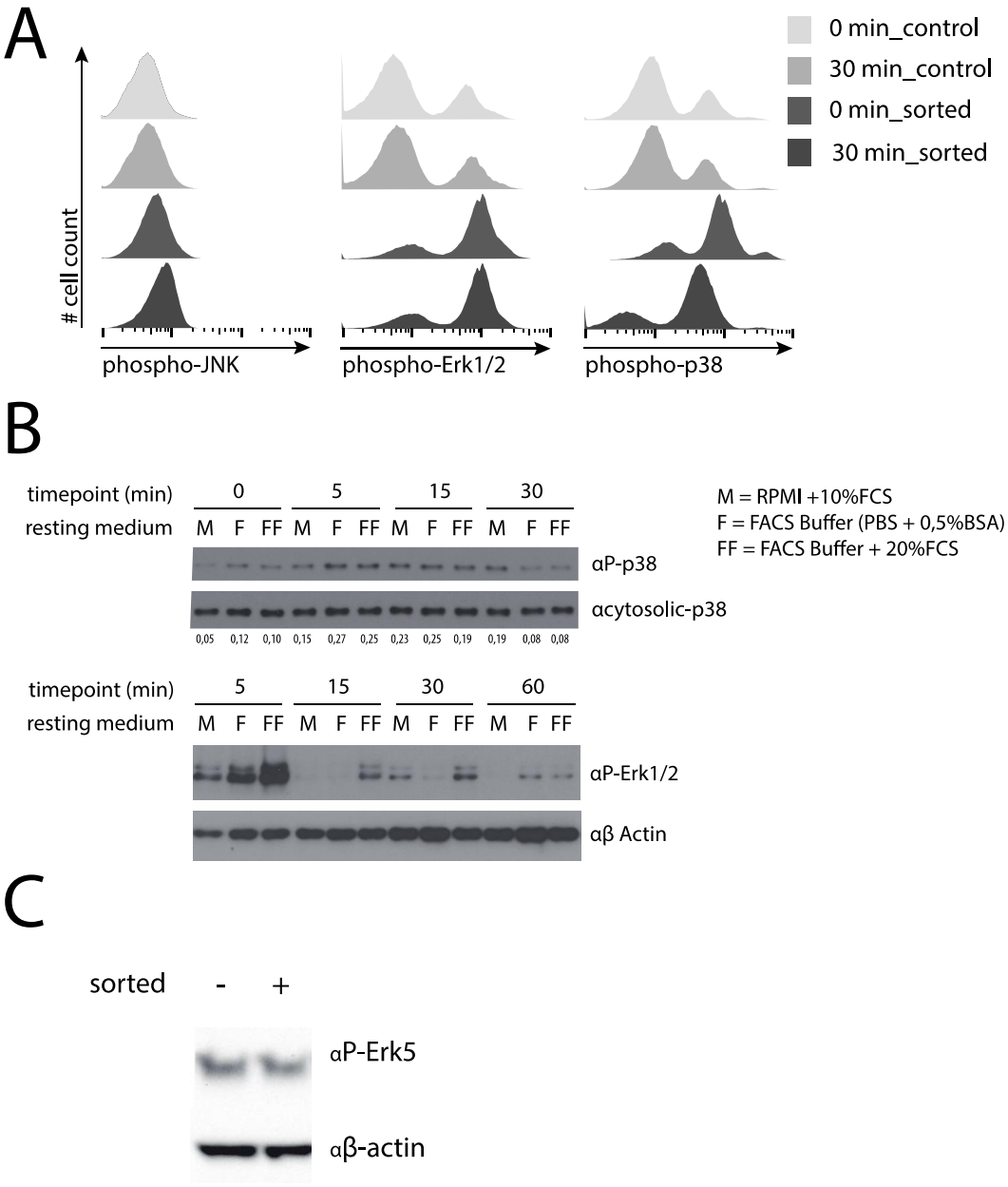

Figure 13: Checkpoint molecules of the MAPK pathway and their phosphorylation status after sorting.
(A) Phospho-flow for Erk1/2, p38 and JNK of living, single human PBMCs and comparison after mock sorting to unsorted controls. (B) Immunoblot of cell lysates from hPBMCs stored in different buffers over a time course. Detection of phosphorylation patterns for the MAPK p38 and Erk1/2. Commonly used buffers for cell sorting were used as controls (M) cell culture medium, (F) PBS-based FACS buffer and (FF) FACS buffer containing high amounts of FCS. (C) Immunoblot of the Erk5 phosphorylation in cytoplasmic PBMC lysates before and after mock sorting. Anti-β-actin was used for overall protein measurement.

The FACS-induced p38 phosphorylation was measured considering both endogenous and cytoplasmic p38. Human PBMCs after Ficoll and cultivation in RPMI medium containing 10% FCS (Fig. 14 A) were minimally activated by cell culture conditions. A comparable activation status was seen after pressurizing and depressurizing with 4 bar. In contrast, PBMCs sorted by FACS did show an increased phosphorylation status of their p38 levels, quantified by ImageJ with a ratio of phosphorylated to endogenous p38 (Fig. 14 A). We demonstrated no specific p38 activation by the preparation processes for cell sorting, e.g. Ficoll and buffer conditions, and PBMCs were even unaffected by the overall pressure conditions of FACS instruments. We assumed that a force other than pressure triggers the activation of p38 during FACS sorting.

To find out if the FACS-induced p38 activation can be avoided by cell hibernation during sorting, the fully temperature-controlled sorting approach was tested (Fig. 14 B). PBMCs stored in culture medium were pressurized or not and sorted under different temperature conditions to check which combined condition led to p38 activation. In summary, FACS sorting at any given temperature condition induces and increases p38 phosphorylation patterns. Constant hibernation of PBMCs before and during sorting enhances the tendency for increased phosphorylation, with an unphysiologically rapid loss of signal after rewarming. We tested the phosphorylation activation for 4°C conditions, with PBMCs stored and sorted with or without deflection and charging (Fig. 14 C). However, the Immunoblot shows that 4°C alone did not induce the p38 signal. Although collected cells sorted at 4°C were not deflected by the plates nor charged in the stream, the phosphorylation status of p38 was visible. Endogenous p38 levels showed comparable amounts of protein within the samples. In summary, cell hibernation during sorting at 4°C in a completely temperature-controlled system did not prevent p38 activation.

While potential alterations by preparation or buffers were excluded, another approach was chosen to unravel a specific FACS force responsible for the phosphorylation. We started to switch on one force after another during FACS sorting to evaluate different FACS forces, either mechanical or physical. By the basic principle of FACS, pressurizing and depressurizing occur first, which do not induce p38 phosphorylation (Fig. 14 D). However, passing cells through the narrow tubing of a cell sorter fluidic system does activate PBMCs by shear forces in a strong manner, so that subsequent FACS forces do not stack to the overall p38 phosphorylation. Droplet generation, charging and deflection in the electromagnetic field did not show any additional effect on the activation of p38 by FACS. All cell lysates were generated by mock sorting, gating on the scatter parameter only, enabling direct comparison of sorted to unsorted. No antibody labeling was used. Buffer conditions were ruled out by using sheath buffer only. As we were testing the sheath fluid of the sorters by adding it to the negative controls for MAPK signaling, we already ruled out the activation of p38 after sorting by LPS contaminations.

Nevertheless we verified that endotoxins were not responsible for p38 activation in separate test.

Endotoxins like Lipopolysacchrides (LPS) from gramnegative bacteria are known to phosphorylate p38 MAPK. A contamination of sorters is often described, so we tested for this effect by LAL (limulus amebocyte lysate) test. We found two of the MoFlo^{TM} sorter contaminated with LPS (ranging from 2.3 to 2.7 EU/ml), and the FACSAria III system nearly free (0,25 EU/ml) of endotoxins (Fig. 14 E). Endotoxin levels were measured in EU (endotoxin units) to keep the proteolytic activity of different types of endotoxins comparable. U.S. food and drug administration (FDA) requirements for medical products are less than 0.5 EU/ml, which equals roughly a concentration of 1ng/ml LPS. We compared the p38 signal between the MoFlo XDP system and the FACSAria III after sorting in PBMCs (Fig. 14 F) with anti CD3 as loading control. Here despite the differences within sorters concerning endotoxin levels disparities in the activation of p38 were not detectable. Which limits an impact of endotoxins at this low concentration levels to a non-detectable influence on p38, so that the FACS forces alone account for the phosphorylation.

Shearing and impact of the sort stream are forces, which cannot be evaluated in the system individually and are additionally indispensable for sorting, leading to the conclusion that an activation of the p38 MAPK by FACS sorting is inevitable.

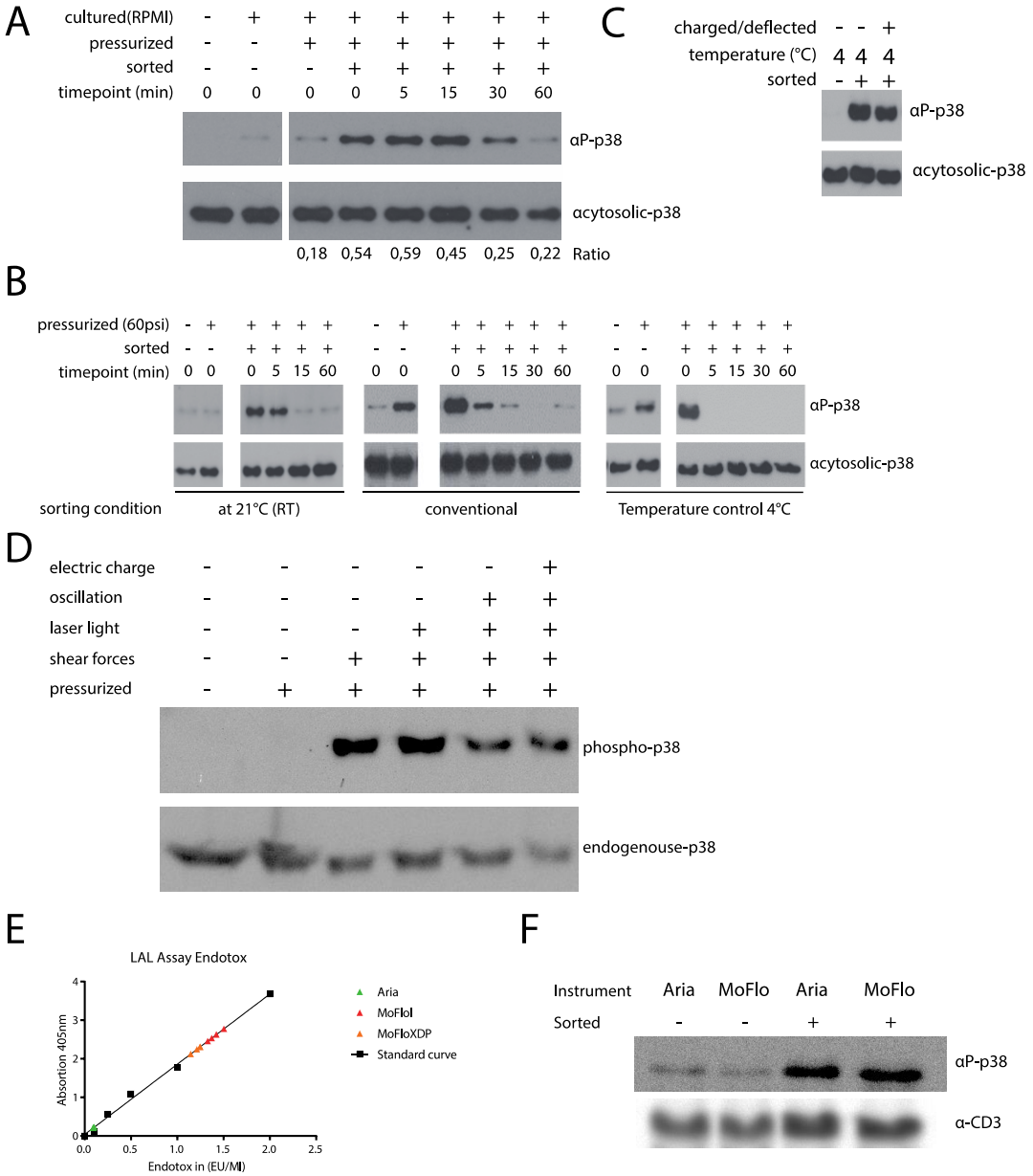

Figure 14: Sorter influences on the p38 MAPK pathway.
(A) Immunoblot of cell lysates of hPBMCs unsorted and mock-sorted. Phosphorylation and endogenous levels of p38 are detected. The ratio of phosphorylated to cytosolic p38 was determined with ImageJ. (B) For three different sorting temperatures (21°C, 4°C and conventional, sample and receptacle holder only chilled) FACS-induced activation of MAPK p38 was verified. Phosphorylated and endogenous p38 levels were determined. (C) PBMC lysates stored or sorted at 4°C. Sorting was done with or without deflection and charging. Phosphorylation status of cells was detected for p38 and compared to endogenous levels. (D) Evaluation of different mechanical and physical FACS parameters on the phosphorylation of p38 during sorting. (E) Endotoxin (LAL) test for the sheath fluid of different cell sorter (FACSAria III, and MoFlo™ Legacy and MoFlo™ XDP). (F) Immunoblot of unsorted and “mock” sorted human PBMCs on different sorter (FACSAria III and MoFlo XDP). Signal detection of phosphorylated p38 for the different conditions and endogenous CD3 of the T cells within the sample as loading control.

Since no technical variation of our sorter instruments could suppress MAPK signaling due to sorting, we started to evaluate which cell responses and alterations are measurable after p38 activation.

3.2.2.1.1. MAPK p38 connected cell responses

The extracellular sensing of signals for different stimuli is strongly connected to the MAPK pathways. MAPKs are a very conserved signaling pathway, nearly unchanged in all mammals, and with similar protein functions even in eukaryotes like yeast. These cell sensors link protein expression and responses to environmental conditions. Due to our previous findings, we further on will only highlight cell alterations induced by and connected to the phosphorylation pathway of p38.

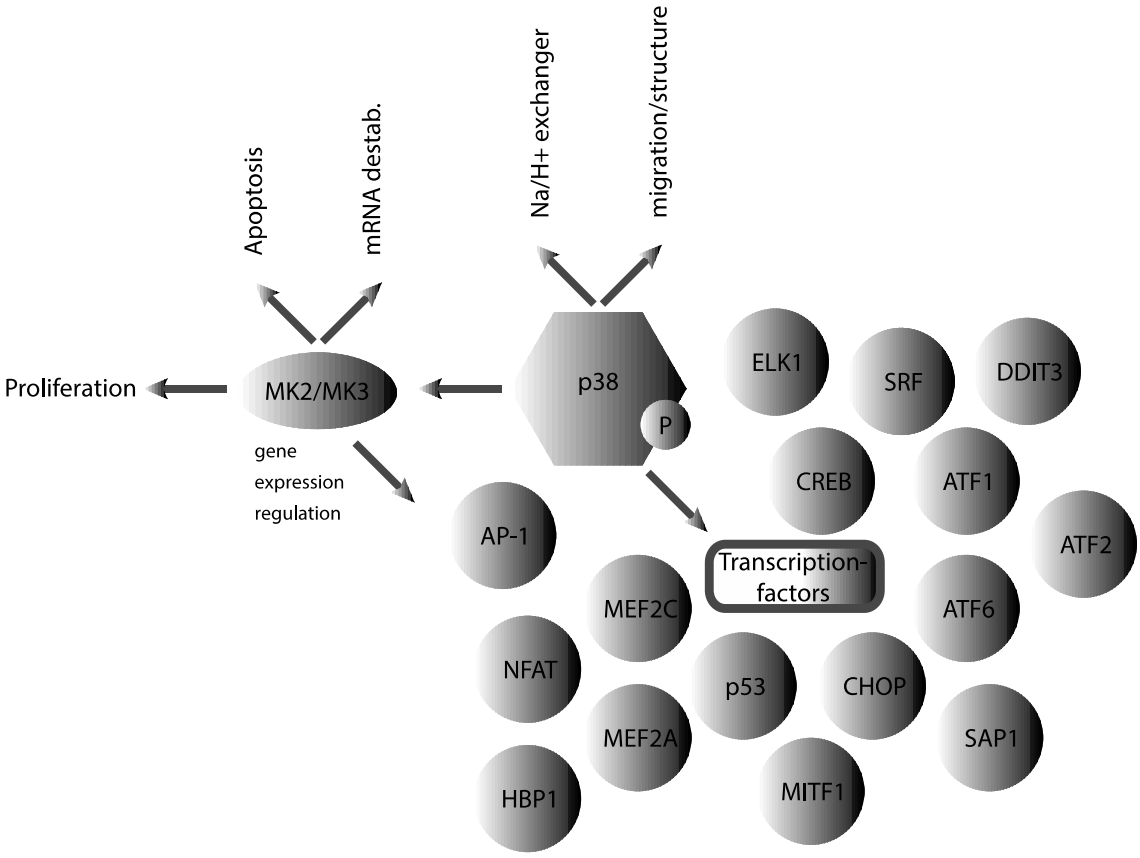

Figure 15: Draft of possible signaling targets of p38 after activation.
p38 is a master regulator for many signaling pathways known for activating a plethora of different transcription factors. Physiological cell changes are also reported, e.g. for proliferation (cell cycle regulation), cell migration, cellular structure organization and influences on cell survival.

The p38 phosphorylation concerning cell survival after sorting was already addressed (Fig. 11) for murine splenocytes and PBMCs (Suppl. Fig. 2). Splenocytes and PBMCs on different instruments showed accelerated dying but only little to no additional induction of apoptosis. To link survival and p38 phosphorylation of hPBMCs (Fig. 11, 13 and 14) to a more defined T cell subpopulation (CD8 positive cytotoxic T cells), in which we further could measure defined cellular function, we chose two new purification technologies, Fab-TACS® and *Speed Enrichment*. We used freshly drawn human

venous blood to enrich $CD8^+$ cells via Fab-TACS® column with the reversible CD8 Streptamer (Fig. 16 A). Before enrichment of CD8 cells, the blood material was composed of more than 99% CD235 positive erythrocytes. The remaining 1% of cell material was around 4% $CD3^+$ and $CD8^+$ T cells and 1,8% only single positive $CD8^+$ cells (in other experiments this cell population was identified as CD8 positive dendritic cells). After T-catch passage, sample material was tested for the depletion of $CD8^+$ cells. Only 0,2% of CD3, CD8 double positive and around 1% CD8 single positive cells remained in the depleted blood material. In contrast, purified T-catch material showed only 9,1% erythrocyte contamination and the CD235 negative population was composed of 99,8% $CD8^+$ cells. Of those 79,4% were cytotoxic T cells (CD3, CD8 double positive). An aliquot of the purified sample material was lysed immediately, the remaining material was mock sorted. Tip purification had no effect on p38, while the sorted $CD8^+$ sample material showed a comparable phosphorylation pattern (Fig. 16 B) as ficolled lymphocytes in previous experiments. This proved the robustness of the p38 sorting-induced phenotype for $CD8^+$ T cells and/or dendritic cells, in addition to PBMC and Jurkat material.

In another approach, we generated pure $CD8^+$ T cells also from freshly drawn peripheral venous blood by FACS with *Speed Enrichment* (Fig. 16 C). For this, we stained human whole blood with CD8-PE and CD3-APC and FACS enriched with the trigger on PE for CD8 and additional CD3 positivity, a method described in detail latter on. A subsequent purity sort on FSC trigger yielded a 91,5% pure $CD8^+$ and $CD3^+$ cell population, with erythrocyte impurities only. The depletion of contaminating erythrocytes is macroscopically visible to the naked eye as a decreasing red color of the sample material in each progress step. Double-sorted T cells were incubated over two days under cell culture conditions and a live/dead analysis was done at different time points via PI staining (Fig. 16 D). From the beginning, more than 80% of isolated CD8+ cells were alive, in line with previous findings with PBMCs, also was this number constant over the time course of two days. PI analysis at later time points of the whole blood starting material, gated for $CD235^-$ and $CD8^+$, also showed 79% PI negative cells. Since no additional cell death occurred over two days, the p38 phosphorylation in purified CD8 T cell populations seemed unrelated to an induction of programmed cell death. These data in addition to murine splenocytes (Fig. 11) and hPBMCs (Suppl. Fig. 2) exclude the p38 activation responsible for apoptotic cell processes after sorting.

Next we evaluated the migration behavior of $CD8^+$ cells after sorting in the context of the p38 activation.

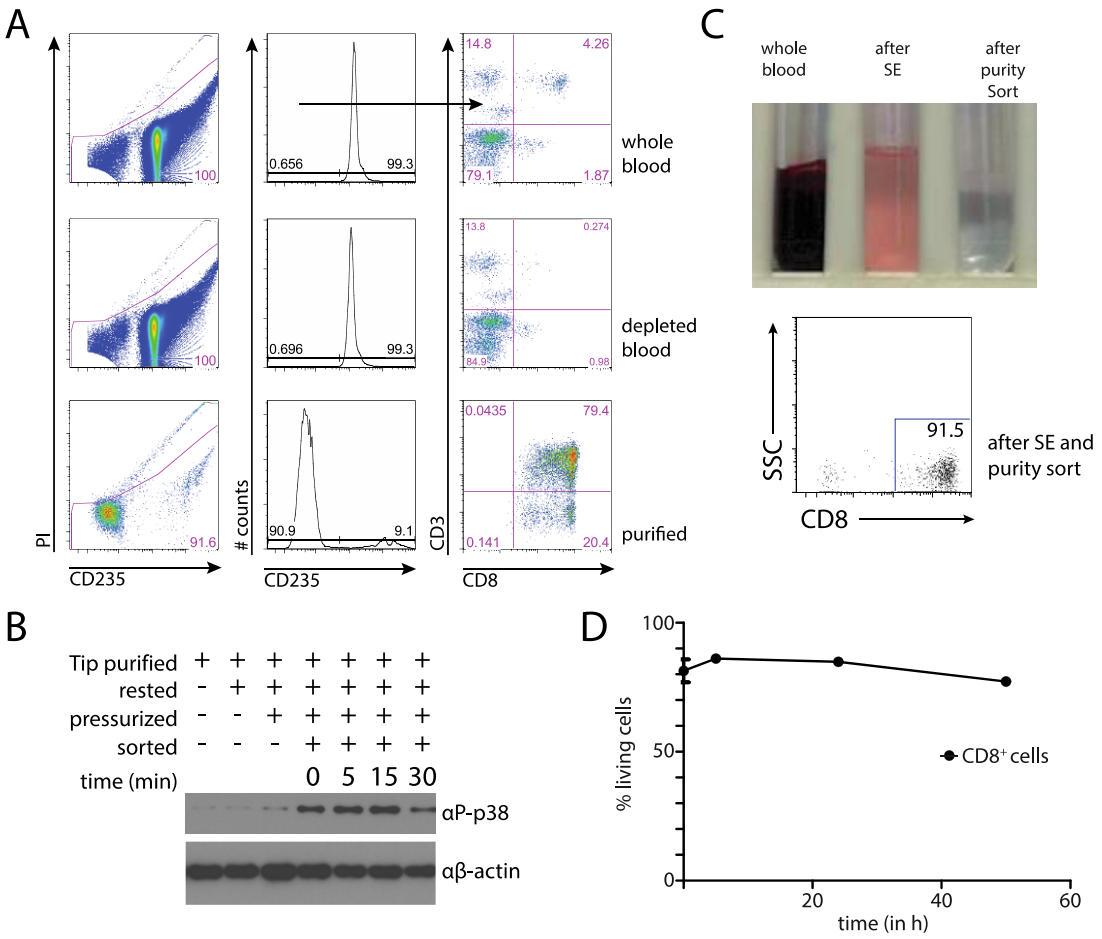

Figure 16: Evaluation of FACS influences in a pure CD8 T cell population.
(A) Fab-TACS® purification with reversible Fab CD8 streptamer from fresh donor whole blood. (B) Immunoblot of Fab-TACS® purified CD8 cells for phospho-p38 and β actin after FACS sorting. (C) *Speed Enrichment* of CD8+ cells from fresh donor whole blood and a second FACS purity sort. (D) Survival (measured by PI) of CD8+ double FACS-sorted cells (*Speed Enrichment* and purity sort) under cell culture conditions over 2 days.

We stained freshly isolated Ficolled human blood with two different dyes against CD8. For a long-time measurement under cell culture conditions, the dyes phycoerythrin (PE) and pacific blue (PB) proved best. Staining with two different antibodies for CD8 was necessary as a control for fluorochrome mediated alteration in migration or incubation effects. Additionally, we used antibodies directed against CD4, CD14, CD16 and CD19 to exclude different cell types like T helper cells, B cells, monocytes and phagocytes in our assay. However, CD8 positive dendritic cells may still be present and account for some migration. Cell frequencies after labeling for unsorted and mock-sorted in two different staining conditions are shown (Fig. 17 A). For each condition, starting frequencies were comparable, e.g. labeling with the same fluorochrome with different sorting conditions (PE 23.1% for mock-sorted and 25.2% for unsorted and for PB 20.5% for mock-sorted and 20.9% for unsorted). Migration was induced by a 1% FCS gradient in a 24 well 5 µm pore migration plate. Cells were harvested after 4 h and 9 h migration and frequencies for transmigrated CD8 cells, pre-gated for scatter properties and live/dead multilabeling dump channel were determined by flow cytometry (Fig. 17 B).

Results of the transmigration assay differed between wells and staining properties. Nevertheless, consistent data were achieved by measuring the migration in six different wells under different labeling conditions of PB and PE vice versa. After 9 h of incubation, higher frequencies of cells labeled with PE in comparison to PB, unrelated to sample preparation conditions, indicated a better detectability of this dye after incubation under cell culture conditions (Fig. 17 C). Later time points were not measurable with this method since tested dyes like PB (9 h) or APC (4 h) were no longer detectable. The signal for ECD dump staining also weakened drastically after 20 h.

Therefore, migration with this setup was measured up to 9h after establishment of the FCS gradient. Analyzed data over all time points and staining conditions did not show any impairment in the migratory behavior of CD8 cells due to sorting. Two-way ANOVA comparison of sorted and unsorted conditions gave a p value of 0.2714, for observing sorting effects. Mainly labeling color and time affected the percentage of migrated CD8 cells with a p value of <0.0001. These data indicate no measurable influence of the p38 phosphorylation on cells in their migratory behavior after sorting.

Also actin and cytoskeleton rearrangements are involved in cell migration, so that structural disruption, perturbance or reorganization of actin filaments after sorting would indicate impairment. To further emphasize the lack of migratory alteration due to p38 activation, cell structure proteins tubulin and actin were stained with confocal microscopy in the human bladder non-malignant epithelial cell line HCV-29[85] (Suppl. Fig. 4), as cytoskeleton analysis of primary PBMCs (Suppl. Fig. 5) or cultured Jurkat cells did not work to our satisfaction. Despite slight differences concerning tubulin and actin, no deformation or structure rupture was visible. Out of many image sections, four are shown (Fig. 16 D). Two single cell format sections (cropped from a 40 times magnification) and two complete sections are displayed. Despite slight differences between some pictures (beakoning of cells), which were not unique for one or the other condition, observers were not able to identify sorted versus unsorted samples reliably. A blind study with 6 people viewing 9 sections for each condition produced no reliable discernment between sorted and unsorted pictures.

Our conclusion was made that no differences in migration or cell structure can be visualized between FACS-sorted and unsorted cells. Thus, an influence of p38 concerning these cell functions is negligible.

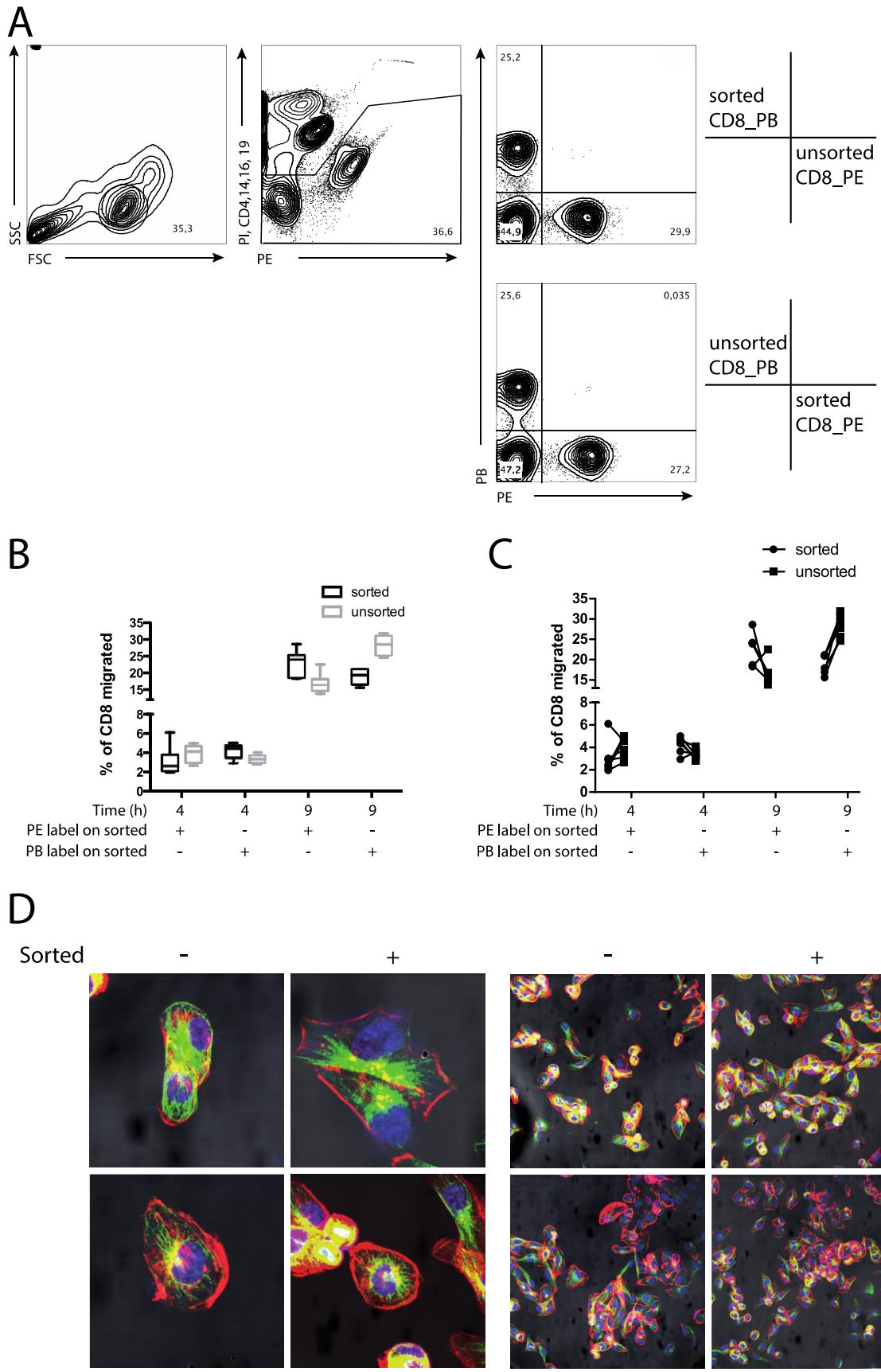

Figure 17: Migratory behavior of T cells and cytoskeleton structure after FACS sorting.
(A) FACS analysis of starting material for transmigration assay. Dump channel exclusion with CD4, CD14, CD16, CD19 ECD and PI. Differential (vice versa) staining of dump negative cells with CD8 phycoerythrin (PE) and pacific blue (PB) for cells, which were sorted or not. Labeling for the fluorochromes PE and PB is comparable between the different sorting conditions.

(B) Transmigration of CD8+ T cells through a 5nm pore membrane against a 1% FCS gradient after 4h in cell culture. (C) Percentage of transmigrated $CD8^+$ cells on a per well comparison. (D) Confocal microscopy of cell structure proteins tubulin (green) and actin (red) and the cell nucleus (blue) of mock-sorted and unsorted HCV-29 cells in an overlay. Single stains were measured for each channel also individually (Suppl. Fig. 4).

We also wanted to identify via MicroArray analysis if certain modulations of gene clusters are related with sorting induced p38 activation. Since phosphorylated p38 activates a plethora of transcription factors, this screening method appeared most promising to identify possible gene clusters. In addition to transcription factors, a translation stop of mRNA to protein is also supposed to increase overall mRNA levels. Especially mRNA with a long half-life before cytoplasmic degradation is supposed to accumulate. In this way the MicroArray also would addressed a possible effect of an eIF2α phosphorylation (Suppl. Fig. 3 A).

We tested whether sorting altered mRNA profiles with two MicroArrays performed with $CD8^+$ cells purified with Fab-TACS® technology (Fig. 18 A). These cells were isolated from fresh human donor blood, yielding more than 96% living cells with very good purities above 99% $CD8^+$. $CD8^+$ cells were rested overnight in starving medium for synchronization and at the next day mock-sorted or not, and then mRNA isolated for MicroArrays immediately or after 4 h at cell culture conditions. A cluster dendrogram analysis of the overall mRNA profiles within these conditions graphically displays the differences through a hierarchical tree (Fig. 18 B). The incubation time accounted for the biggest differences in mRNA profiles. Followed by the two assays, either by donor or isolation processes. Of all conditions, the fewest differences in mRNA changes were observed for sorted or not. The differences in the mRNA expression between mock-sorted $CD8^+$ cells and unsorted controls after 4 h incubation are visualized in a heatmap (Fig. 18 C). The threshold for significantly differentially expressed mRNA changes was set for more than 2-fold in the different groups. Out of 18.710 mRNA datasets, after normalization two mRNA profiles remained differentially expressed. In sorted cells, complement component 2 (C2) was overexpressed and 5´-Nucleotidase, Cytosolic IIIA (NT5C3) was downregulated. Both C2 and NT5C3 are described in literature as protein coding mRNA with specific function. Interestingly, C2 was also differentially expressed when comparing sorted and mock-sorted cells at time point zero (Suppl. Fig. 5 A). Here C2 in contrast was downregulated in mock-sorted cells, indicating a drastic increase of this mRNA in sorted cells after the resting phase. However, C2 functions as a part of the classical and lectin pathway in complement activation[86] and is essential to activate C3, the main opsonin in the complement pathway[87]. As a plasma protein physiologically produced in the liver, it is not likely to be specifically regulated by the p38 activation of cytotoxic T cells by sorting. More likely, the enrichment of also CD8 positive DCs after Tip purification is the cause for this finding. Previous work already showed increased

mRNA levels of C2 for different macrophages under stress and inflammatory conditions[88].

For a downregulation of NT5C3 after 4 h incubation we account another cell impurity in the samples. NT5C3 is a 5´nucleotidase and active especially in erythrocytes during their maturation. Erythrocytes still account for 5-10% impurity after Fab-TACS® purification. A mock sorting approach with certain FSC threshold settings may have led to a loss of this small cell type in sorted samples, accounting for the downregulation of this mRNA. We therefore did not see specific clusters of p38 signaling activated between sorted and unsorted samples.

After small differences comparing mock and unsorted after 4h, we compared changes in mRNA levels between incubation time effects. Heatmaps show data of all differentially expressed genes between the resting phase in both unsorted and mock-sorted samples (Suppl. Fig. 5 B and C). To exclude changes induced by the resting period, we generated an artificial heatmap adjusted for differentially expressed genes compared to the unsorted group (Fig. 18 D). This showed 8 differentially expressed mRNAs, of which 6 were upregulated and 2 downregulated. Seven of these regulated mRNAs were protein-coding, with the exception for the RNA Variant U1 Small Nuclear 1, 2 and 3 (RNVU1-3), which code for snRNA. The regulation of these protein coding genes is not closely related to the p38 activation, however some genes can be involved die this MAPK pathway. The X-C Motif Chemokine Ligand 1 (CML), TNF Alpha-Induced Protein 3 (TNFAIP3) and the S100 Calcium Binding Protein A8 can be regulated by transcription factors associated with p38 signaling. One gene could also be related an affected by a eIF2α phosphorylation like CAMP Responsive Element Modulator (CREM), however Immunoblots not clearly proofed an activation of this pathway (Suppl. Fig. 3 B). To summarize, seven differentially expressed genes were too small to identify enrichments, i.e. to identify sets of related genes, which are overrepresented and would identify a functional network. By that, a specific p38 MAPK signaling pathway was not identified.

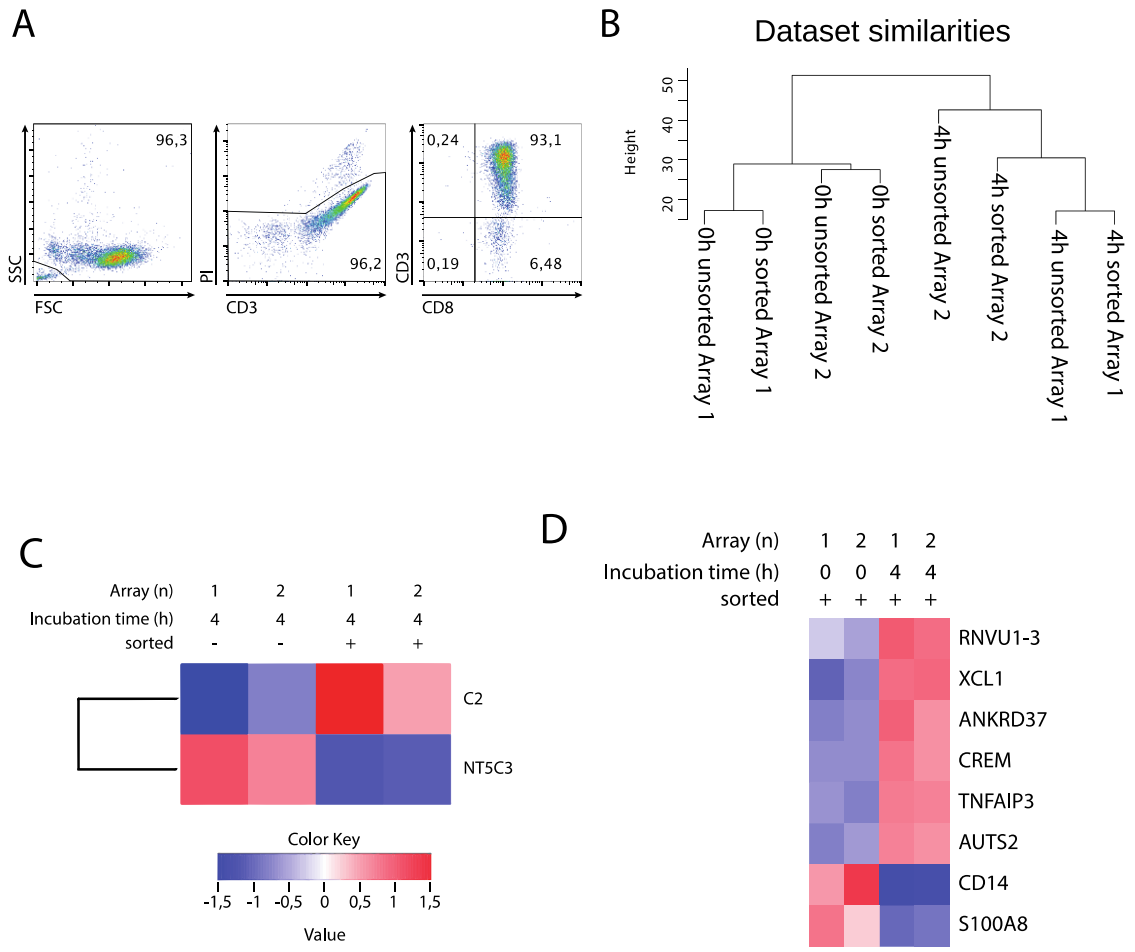

Figure 18: Transcriptional analysis of sorted CD8 T cells.
(A) Cell quality and purity of Fab-TACS®-purified CD8 cells before MicroArray analysis (PI live/dead stain, CD3 and CD8). (B) Cluster dendrogram giving the similarities within mRNA expression profiles of two MicroArrays comparing sorted to unsorted CD8⁺ Fab-TACS® purified human cells immediately after the sort and after 4 h of resting. (C) Heatmap of up- and downregulated mRNA of mock-sorted Fab-TACS® CD8 cells compared to unsorted Fab-TACS®-purified cells after a 4 hours incubation. (D) Heatmap of differential regulated mRNA from mock-sorted sample material before and after 4 hours of incubation under cell culture conditions. Expulsion of incubation effects were considered by deletion of mRNA also upregulated in unsorted controls incubated for 4 hours (Suppl. Fig. 5).

As an additional function p38 is described as a regulator for cell cycle progression[89-91]. Therefore, we tested for an impairment of FACS-sorted cells in a proliferation assay. A beta decay scintillator measured the uptake of ^{3}H-labeled thymidine into newly synthesized DNA during proliferation. PBMCs, purified from human peripheral blood, were stimulated by foreign HLA in a mixed lymphocyte reaction, leading to a proliferation of T cells. The proliferation of T cells for different time points, with or without allogenic stimulus, can be measured (Suppl. Fig. 7 A) and is highly significant ($p<0.0001$). The proliferation of PBMCs purified by different methods was measured at an early time point after 72 h of allogenic stimulation between FACS, MACS and their unpurified counterparts (Fig. 19 A). While additional stimulation of the effector cells with CD3 and CD28 led to more proliferation, irradiated stimulator cells showed no thymidine uptake. At this early time point three days after stimulus data sets correlated closely to each other

and showed no major spreading (Fig. 19 B) with no significant differences between purified und unpurified samples. However, sorted cells were prone to show a faster response to the allogeneic stimulus, which yielded a significantly better proliferation of mock-sorted T cells compared to unsorted ($p=0.0012$) at the peak of expansion of around day 6 (144 hours), implicating no cell cycle arrest due to p38 phosphorylation after FACS sorting. The longer the allogenic stimulation persisted (Fig. 19 C), the greater the differences within one condition varied and data points within conditions spreaded; thus, the early time points with no difference in the proliferative capacity of sorted cells are more reliable. The expansion of T cells in an MLR was not affected or dampened by FACS cell sorting as no drawback in their proliferative capacity was detected. In contrast, the p38 may give cells a stronger stimulus to proliferate. This strongly argues against a cell cycle arrest by p38 in S-phase (after DNA damage) or G2-phase (after osmostress)[89]. However a possible reason for this faster response to stimulation can be grounded on a pre-activation by danger signals (via PAMPs) associated with LPS in sorting buffers, as PBS based buffers were used for MACS and unsorted controls.

Like proliferation the effector function is a hallmark of CD8 positive cells. So we tested robust CD8-TCR associated cellular cytotoxicity. However this function is only partially related to the classical p38 activation. TCR stimulation can, however, be associated with p38 phosphorylation by $p56^{lck}$ and ZAP70. We tested this possibility although this phosphorylation of p38 takes place on a tyrosine on position 323 (Tyr^{323}) of p38, which our antibody in Immunoblots did not detect.

Human CD8 T cells were retrovirally transduced with a MART1-specific TCR (kindly provided by Manuel Effenberger). This resulted in chimeric T cells with their endogenous TCR and the expression of the MART-TCR. The transduced cells were enriched by a FACS sort, kept in cell culture under stimulating IL2 conditions, with peptide-specific presentation by feeder cells. Transgenic cells were used in four impedance-based kill assays. The adherent cell line A-375 was pulsed with the MART1 peptide and antigen-specific T cells were added in different effector-to-target ratios. One representative kill assay is shown with normalized curves for target-specific lysis (Figure 19 D). At high E:T ratios like 4:1, no difference between control and mock-sorted transgenic T cells was visible. At lower E:T ratios, curves between unsorted controls and sorted cells diverge, but with a lower specific killing for the controls which underwent a medium exchange. This medium exchange mimics the different buffer compositions during sorting, so that this impairment in cytotoxicity only due to FACS forces could be excluded. The performed kill assays were done with highly pure $CD8^+$ cell material, of which many cells were antigen-specific > 70% (Figure 19 E).

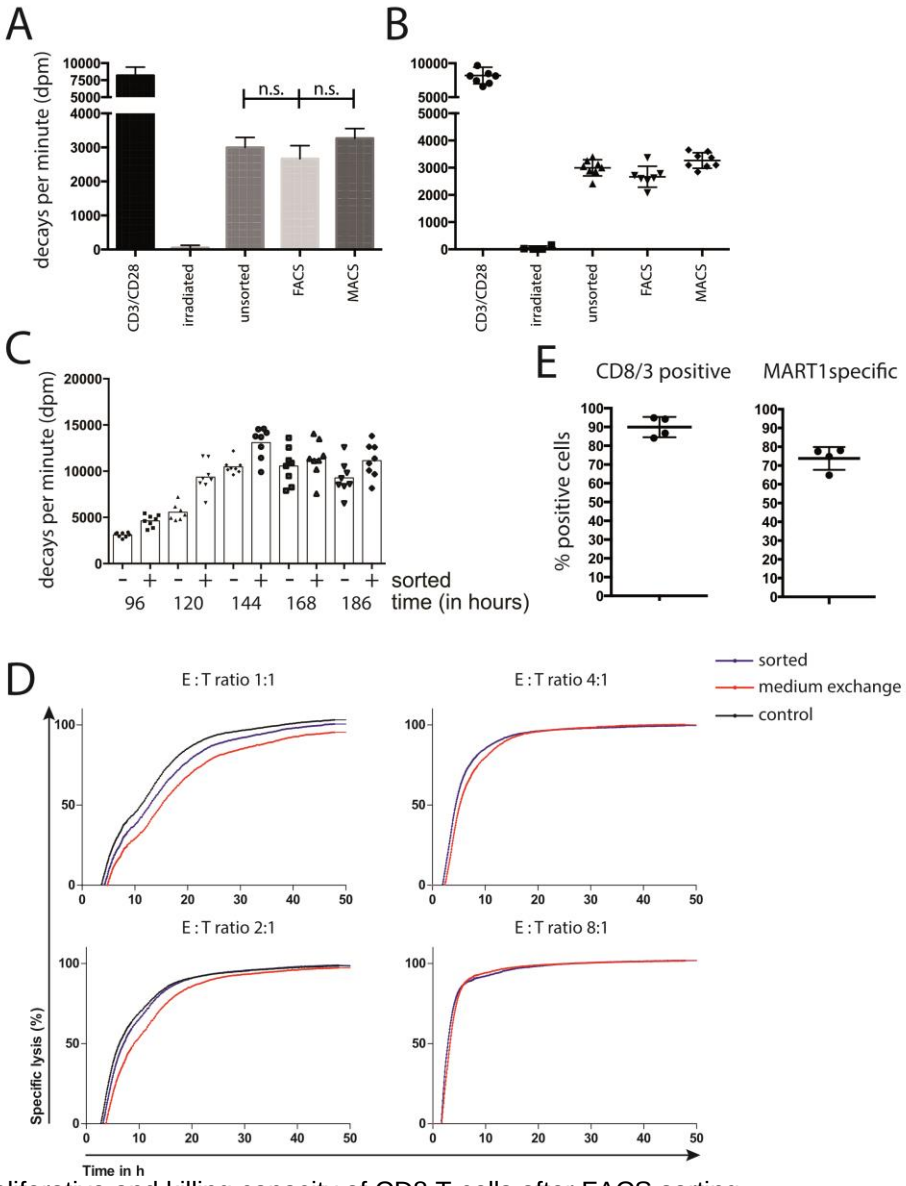

Figure 19: Proliferative and killing capacity of CD8 T cells after FACS sorting.
(A-C) Bar graphs for the beta-decay of radioactive H3-labeled thymidine in proliferated CD8 cells, due to foreign HLA stimulus of a mixed lymphocyte reaction (MLR). (D) Antigen-specific kill assay with MART1 transgenic T cells. Adherent cell lines A375 were peptide pulsed with MART1 antigen. Killing in different effector:target ratios (E:T) was measured with the XCellLigence impedance system. (E) Cell composition for CD8 positivity and antigen MART1-specificity of the effector cells used in killing assays. MART1-specific transgenic T cells were kindly provided by Manuel Effenberger.

In summary, we could visualize instrument-based effects of FACS sorting in cellular signaling cascades, especial the MAPK p38. Yet no physiological or functional impairment for human primary cytotoxic T cells was visible, indicating that cells remain unaltered overall, despite the mechanical and physical forces during FACS.

3.3. New technological sorting approaches

As already mentioned, FACS can only be used for applications fitting to its technical requirements. With a 70 µm nozzle, the frequency for droplet generation is around 100.000 Hz, generating the same number of droplets (10^5) per second, which is the upper limitation of events per second (eps) that potentially can be sorted. Another limitation in sorting concerning electronics and hardware is the digital pulse the instrument is able to process. The best sorters on the market work with a 32-bit system, which enables processing of up to 200.000 eps. Another limit is the time the sorter needs to discriminate between events, this is given by the passage time of a particle through the laser beam. Normally the laser beam is focused to a diameter of around 100µm when hitting the cells. While this time is also dependent on the cell size, normally a passage of a blood cell takes 1-4 µsec, which limits the single cell resolution of a FACS instrument also to around 1.000.000 - 250.000 eps (instrument dependent). Above this value so called swarm effects occur and single cell resolution is lost.

Under perfect conditions FACS is suitable to sort purities of above 99%, with sample flow rates at 1/5th of the frequency used for droplet generation (approx. 20.000 EPS with 100.000 Hz). Yet this purity is influenced by the sorting mode, where purity and yield function like a pair of scales. These two “physical quantities” of sorting are counterparts, as one impedes the other. Three different types of sorting modes exist: “single”, “purify” and “enrich”. With “single” mode the scale leans towards high purity, yet reducing the yield. The “purify” mode keeps the scale pans in balance, with a light discount for both scales. The last mode, “enrich”, finally bends the scale towards yield, indicating that this mode is best suited to prevent the loss of events. Even though this sorting mode is not focusing on high purities, it is still limited on one hand by the upper limits of droplet generation, and on the other by data processing speed and single cell resolution.

For this reason due to time concerns, FACS is by far not the best method of choice to purify out of large cell numbers. Because of this, we started to improve a method already published[92]. This method of fluorescence triggering so far had few applications in the fields of cytometry; however, we show some promising new applications. So far, trigger on a fluorescence channel has already been used for the detection of small particles, such as bacteria or extracellular vesicles[93,94], as they are difficult to characterize by scatter properties as reported [95].

3.3.1. *Speed Enrichment*

For rare event sorting with frequencies lower than 1:10.000 out of a high cell count sample, conventional sorting reaches its limits, considering the capacity of sorters but

also personnel in facilities. For example, when sorting $1x10^9$ cells, a cell number easily reached in Ficoll-purified buffy coats, it takes around 9 h with conventional sorter settings to process. To overcome all these time and instrument limitations in one step, we first apply a sorting in form of a pre-enrichment. To achieve this, the event detection by the instrument is altered. The event detection, which is an electrical pulse in a PMT, can be adjusted to any channel on modern FACS instruments. Further on, the so-called “trigger” determines in which channel the initial signal is measured. By default and historically evolved, the trigger is on forward scatter (Fig. 20 A), a measurement for cell size. We in contrast set the signal detection on a fluorescence parameter (Fig. 20 C). The same way as with FSC triggering, additional information for other channels can be measured to the initial signal. PMTs are constantly generating signals, either by electronic noise or light pollution; therefore a certain signal strength threshold is set, for signal generation. This threshold barrier is freely adjustable. For conventional cell sorting this threshold is used for FSC signals, to exclude noise or protein aggregates, cell debris or other small structures (Fig 20 A, red and dotted lines).

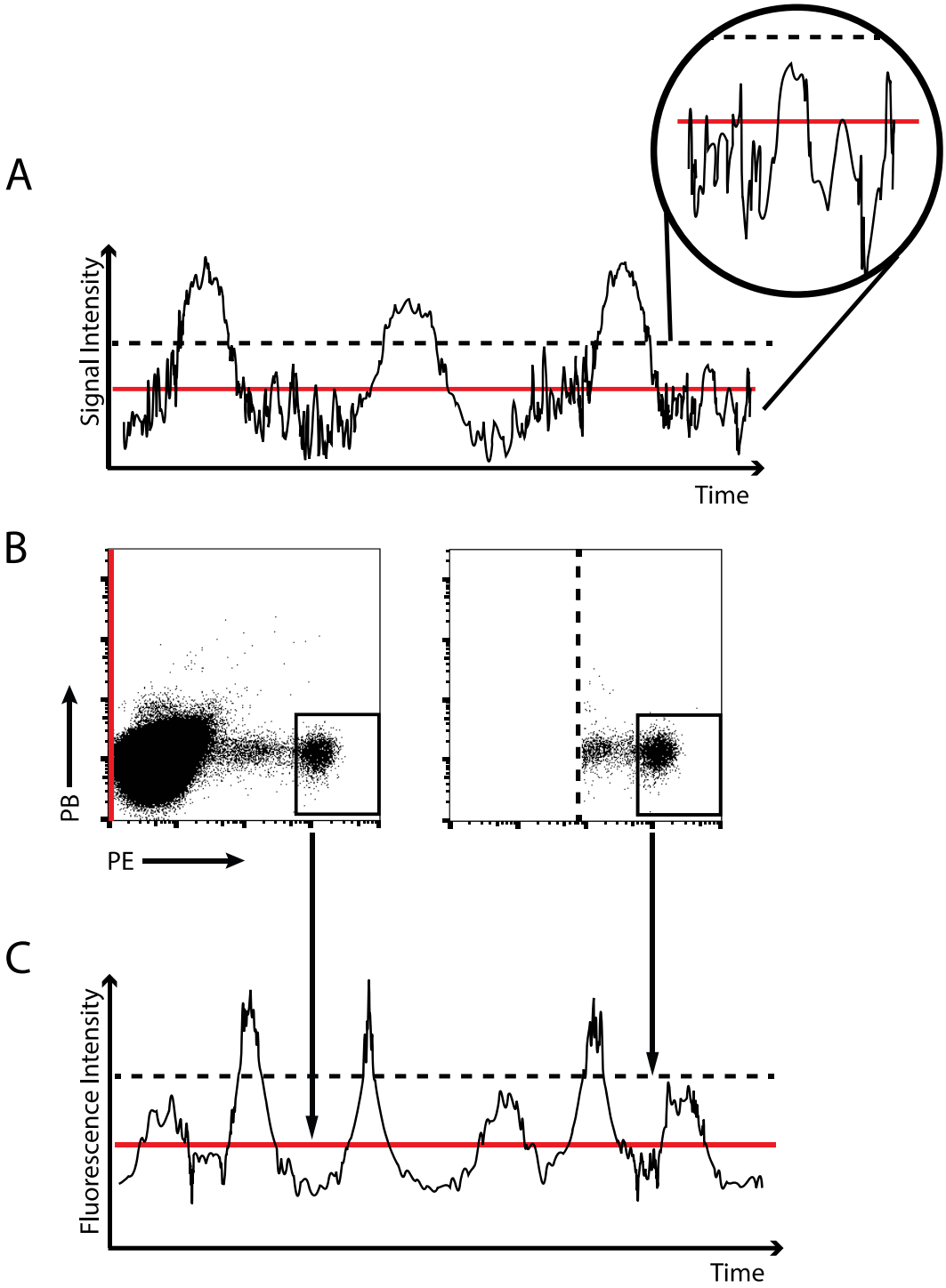

Figure 20: Schematic drawing of the electronic conversion from light signals at detectors.
The signal detection in the triggered channel proceeds over time by recognizing certain signal intensities. Horizontal lines (dotted and red) indicate a different threshold setting for the triggered channel. If the signal intensity exceeds the threshold settings, all signal information (also for all other active channels) is saved. All signals below the threshold value are not processed by computer electronics. (A) The signal detection in a FSC channel is shown with the signal pattern from electronic noise and debris magnified. (B) Dotplots of fluorescence channels with the trigger for event detection on PE. Different threshold values for the PE channel visualize the increasing threshold value. (C) The signal detection for a fluorescence channel is displayed. Due to logarithmic scaling, the background noise is reduced. Lower peaks visualize the signal intensity from an unstained population; higher peaks are produced by fluorochromes bound to cellular structures.

In contrast, when the trigger is set to a fluorescence channel, particles are detected due to their intrinsic fluorescence and no longer by their size. Additionally added antibodies, which are conjugated to fluorochromes detected in this channel, can be used to discriminate target populations from intrinsic fluorescence (Fig. 20 B). By increasing the threshold for the triggered fluorescence channel (Fig. 20 B second plot), the instrument recognizes, processes and displays only the events stained for a specific marker. As indicated in the last graphic (Fig. 20 C), fluorescence triggering also generates noise signals of interfering laser light and electronics when the threshold value is to low (noise below red line). By using a fluorescently stained marker, thus obtaining information about cell properties, the threshold can be set to eliminate unlabeled intrinsic fluorescence events (increasing threshold from red to dotted line). That allows FACS to purify one specific marker, similar to MACS positive enrichment. But in contrast with the exception that additional phenotype marker staining can be added but only to the initial target cell population. This way sorting criteria for other fluorescence channels or size and granularity can be added in a gating strategy und single cell resolution is still possible for the target population.

3.3.2. Properties of *Speed Enrichment* and scientific benefits

In conventional cell sorting, with the trigger on forward scatter (FSC), every particle is detected by a morphological parameter as an event. Thus the total number of processed cells directly correlates with the duration of the enrichment process, which proves difficult during high throughput analysis and sorting. For detection and isolation of rare particles or cell populations with frequencies lower than $1{:}10^4$, large amounts of material are required to obtain sufficient numbers of target cells for further experimentation. In contrast by fluorescence triggering, the event rate can drop drastically, especially when it is applied on a small population size or rare events and the overall sample flow rate can be increased. For most applications during *Speed Enrichment* a pressure difference between sheath and sample pressure of 2 psi, which equals a 3 µl/sec or 10.8 ml/h sample flow rate, was adjusted. Flow rates of 10^6 particles per second were determined when sorting out of whole blood, while the majority of these particles were not detected. Thereby 10 particles were confined in a droplet generated at the end of the sheath stream (Supp. Fig. 8). Due to the impurities in the droplets, this method is a pre-enrichment only. The benefit of increased sample flow rate is best seen by comparing sorting times in relation to the sample cell number (Suppl. Fig. 9). In order to obtain the high purities normally expected from FACS sorting, a second sort on FSC triggering is

needed, but subsequent purity sorts are drastically shorter due to the previous enrichment.
So far, the method of fluorescence triggered sorting is rarely applied in the field of flow cytometry, therefore we tested this method and its limitations and we directly compared MACS and SE as enrichment methods for rare event analysis.

3.3.3. *Speed Enrichment* for rare event enrichment and the comparison to MACS

First we evaluated *Speed Enrichment* and its limitations by spiking PE-stained CD8 cells into unstained PBMCs with different low starting frequencies, comparable to the demands of rare event analysis. For this 10.000 to 1.000 PE positive cells were sorted into 1ml sample material containing $1x10^8$ to $1x10^9$ PBMCs (Fig. 21 A). This way target cell frequencies of $1:10^4$, 10^5 and 10^6 were generated. These samples were enriched with a PE-trigger and gated in pseudocolor plots (Fig. 21 A). Subsequent FACS analysis (Fig. 21 A) yielded enrichments of 10.8% from a starting frequency of 0.01%, increasing the target cell population a 1.000-fold. Enrichment for lower cell frequencies even yielded better enrichment factors of 6.000-fold ($1:10^5$), and 3.000-fold ($1:10^6$). The lowest starting frequency of one cell in a million (0.0001%) resulted in a purity of 0.37%, which was then sufficient for conventional single cell sorting afterwards. This sample had a lower enrichment factor, as well as a drop in purity. Because of a denser starting material (10^9 compared to 10^8 cells in 1 ml starting sample).
To address the concerns for a loss of target cells during these two sorting processes, we tested the SE method compared to the gold standard in cell enrichment MACS, in a parallel experimental setup. Here a total of 200 CD8-PE positive cells additionally also labeled with anti-PE_MicroBeads were spiked into freshly isolated PBMCs. This resulted in a target cell frequency of 0.000275% for the starting samples (Fig. 21 B). The experimental design was in favor of MACS, as PE_MicroBead-labeled cells were already used for spiking. Four samples each were prepared equally and enriched either by MACS (in parallel) or SE (subsequently). Both enrichments took around 1h. Scaling up this experiment with respect to sample numbers would increase the processing time for SE, yet only slightly for MACS. The re-analyzed FACS plots showed similar purities with both methods for enriched material (Fig. 21 B). Keeping in mind that multiple events will be confined in one drop, SE is expected to be only a pre-enrichment, while positive enrichment by MACS, like in this case, is meant to be a cell purification step already. The recovery rate of 200 spiked-in cells, graphically displayed in percent, showed a p-value between both enrichment methods of p=0.045 (Fig. 21 C) in favor for SE. Overall numbers calculated with SEM yielded a recovery rate for MACS with 117± 5,00 cells and

for SE with 137±13,01 cells. The starting frequency of $2.75x10^{-4}$ could be enriched in both methods comparable by an average factor of a thousand-fold, which is sufficient for subsequent purity sorting. MACS and FACS performed comparably concerning the final purity after enrichment with p=0.2261 (Fig. 21 D).

Overall the SE method showed no drawbacks in yield and purity in comparison to the gold standard MACS. With a 68% recovery rate after SE, this method is well-suited for low target cell counts. However, this accounts only when no staining or washing is needed after the FACS enrichment for the subsequent purity sort.

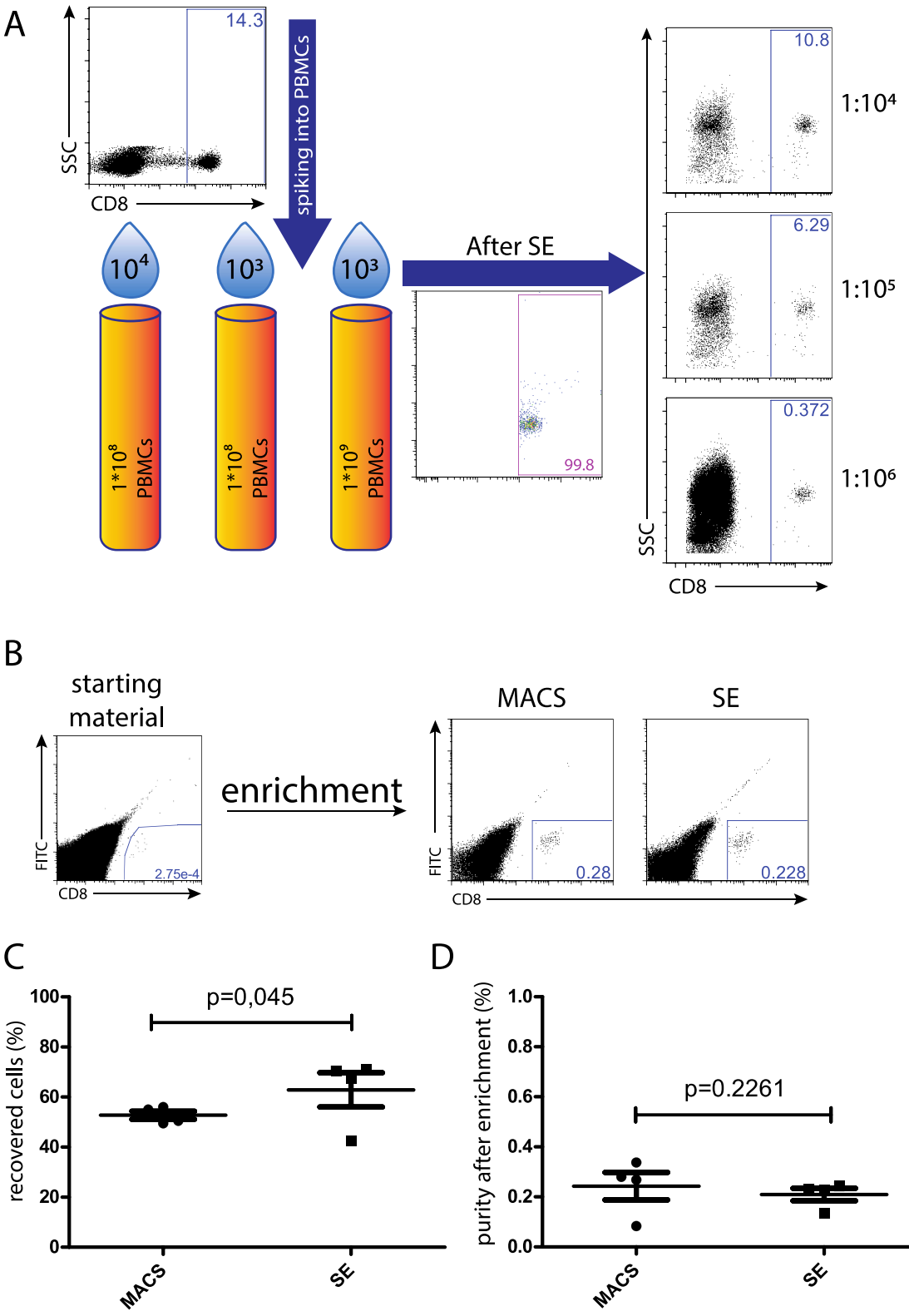

Figure 21: Potency of *Speed Enrichment* for rare events cell sorting.
(A) Spiking-in experiment for rare event enrichment. CD8 PE-stained cells were sorted into unstained PBMCs (cell counts differ) at low frequencies between $1:10^4$ to $1:10^6$ and subsequently speed enriched with a PE trigger. FACS plots show final purities of CD8 cells after SE between 10% and 0.3% dependent on the starting frequency. (B) FACS plots of spiked-in CD8 PE cells into unstained PBMCs with a frequency of 0.000275% were enriched either by MACS or SE to 0.2%. (C) Of 200 spiked-in cells, SE and MACS methods recovered between 50% to 70% of the cells, (D) and yielded, for both methods, a comparable 1000-fold enrichment to a final purity of around 0.2%.

With a better understanding for yield and recovery rate in *Speed Enrichment* we had a look concerning sort times in a cell density related manner, as differences in the flow rate between the enrichment of 10^8 and 10^9 cells in 1 ml sample material were visible. In FACS sorting experiments, the sample pressure in relation to the system pressure defines the flow rate (Suppl. Fig. 10). However this seemed true only to a certain cell density.

Flow rates in classic flow cytometry can be defined in two ways, by volume flow or particle flow in a certain time frame. For FSC triggering, the events per second (EPS) detected are often called the flow rate. But the EPS rate is strongly correlated with the threshold value set, especially by fluorescence triggering. To illustrate that, the threshold values for the PE channel were increased in steps of 0.01 (Fig. 22 A), which led to a decrease of the overall detected EPS rate by constant sample flow (differential pressure). In parallel this increased, as desired in *Speed Enrichment*, the target population frequency (Fig. 22 B). By adjusting the threshold value in fluorescence triggering the particle-based flow rate is uncoupled from the volume flow rate. For evaluating flow rates that are now unrelated to EPS, a monitoring system using the detection of TrueCount beads (TC Beads) was established. TC Beads, which were added to the sample in a known concentration of 50.000 TC beads/ml, re-establish a coupling of sample volume flow to EPS in fluorescence triggering (Fig. 22 C). TC Beads were separated via a second fluorophore from target cell populations.

In line with that TC Beads (50.000) were added to different samples with cell densities varying from $1.5x10^8$ to $5.9x10^8$ per ml. These samples contained a PE-labeled target cell population in a constant frequency of 0.0005%, adjusted to sample densities. Through this, two parameters can be determined: first, the acquired sample volume over time (volume flow rate) by TC Beads and the cell number passing the point of interrogation for the target cell frequency (a function of an EPS based flow rate). The volume flow rate, by a constant differential pressure, goes down with increasing cell densities in the sample material (Fig. 22 C, TrueCount Beads). Yet the detected events for the target population stays constant due to the overall higher total numbers of PE-labeled cells in denser sample material during the time frame (Fig. 22 C, PE target population). This experiment visualizes a limitation of *Speed Enrichment*, since denser sample material does not enable faster acquisition due to higher viscosity. In contrast, by the same EPS sort rate for the target cell population, lower cell densities yield a purer enrichment. Thus using hPBMCs, with a cell concentration higher than $2x10^8$ cells/ml, as a starting material does not enable shorter sorting times, as the optimal sample density for *Speed Enrichment* is around $1.5x10^8$ cells/ml. Achievable sorting times of *Speed Enrichment* can be calculated by the TC Bead count with up to 110 µl/min, or with

approximately $2x10^8$ cells/min, which lead to the calculation of sorting times compared to conventional cell sorting (Suppl. Fig. 8).

In another case of enrichment out of whole blood we measured event rates of up to $6x10^7$ events per minute. These high event rates were possible as blood is of low viscosity in relation to its particle compounds. Dependent on the sample material, *Speed Enrichment* can be used to enrich target cell populations at 300.000 – 1.000.000 EPS, with flow rates of about 100 to 300 µl/min.

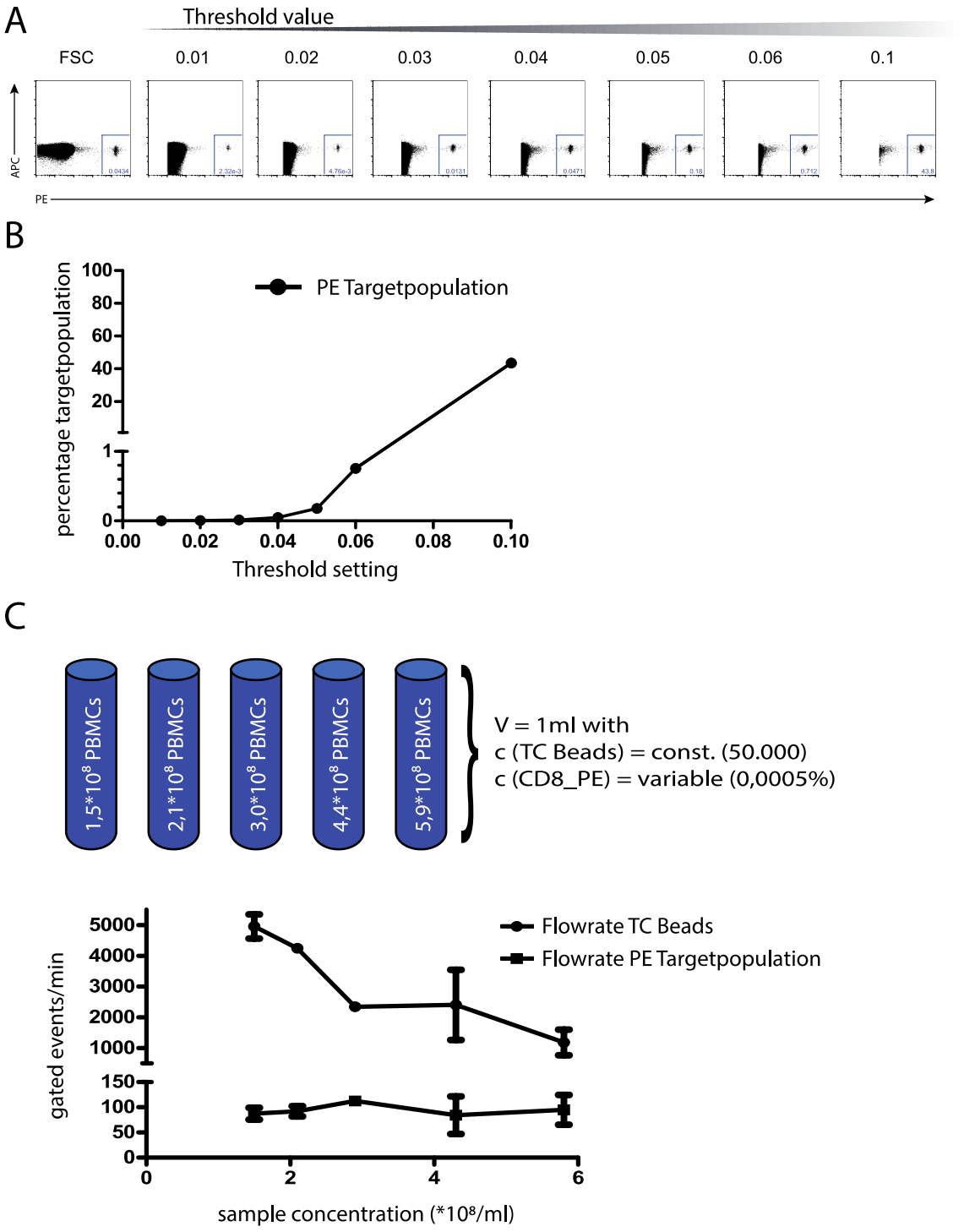

Figure 22: Potential and limitation of *Speed Enrichment*.
(A) Dotplots for conventional triggering (FSC) and fluorescence triggering on PE with increasing thresholds for the PE channel. (B) Increase of detected target cell percentage in relation to intrinsic fluorescence by increasing threshold values. (C) Volume and EPS flow rates in *Speed Enrichment* are dependent of the viscosity of the starting material. TC Beads measure acquired sample volume in a one-minute time frame. PE-labeled target cell count with a constant concentration (0.0005%) correlates directly with acquired sample particles at the point of interrogation.

After proof of concept for the enrichment of rare populations by fluorescence triggered *Speed Enrichment* and the evaluation for best sample density conditions, practical applications for this method, which previously were not achievable with conventional FACS sorting, were evaluated.

3.3.4. Applications for *Speed Enrichment*

Speed Enrichment has advantages over conventional sorting only for target cell population counts lower than 1%, as otherwise the enrichment factor is not high enough to decrease sorting times accordingly. Previous experiments showed best enrichment factors for frequencies of $1:10^4$ up to $1:10^6$. We used *Speed Enrichment* therefore as an application for the enrichment of pDCs (plasmacytoid dendritic cells) and NK cells (natural killer cells) in murine settings in which target cell numbers were low and efficient recovery was necessary. Cell populations like pDCs and NK cells already count as rare event sorting in classical FACS. But we have been facing problems in which much lower frequencies had to be enriched. Hereafter we highlight an application in a human setting, where high recovery rates of very low sample frequencies combined with the need of large sample amount throughput were needed. This application of *Speed Enrichment* for antigen specific T cells was needed as MACS is not working properly for multimer stained cells, especially compared to a flow cytometric approach (Suppl. Fig 12).

3.3.4.1. Enrichment of antigen-specific Cytotoxic T cells from naïve donor repertoire

Cytotoxic T cells are crucial in adaptive immune responses against virus and intracellular bacterial infections, as well as guardians against abnormal cells in transition to early stages of cancer. Those CD8 positive cytotoxic T cells recognize peptide antigens presented by surface-expressed major histocompatibility complex I (MHC I) molecules via their T cell receptor (TCR). T cell specificity is generated randomly, but by transition through the thymus, reactivity to autologous proteins is prevented. This way T cell reactivity is mainly directed against viral proteins and autologous proteins altered in their primary structure due to mutagenesis. Specific killing can be induced in these cytotoxic T cells with the aid of certain co-stimulatory signals when antigen presented by MHC I on other cells is recognized. Due to these properties, cytotoxic T cells hold a great potential for adoptive T cell therapy, especially in immunocompromised or cancer patients. The number of antigen-specific T cells can be very high in individuals who have already encountered a specific pathogen due to clonal expansion, but in the naïve compartment, these frequencies are relatively low. The somatic TCR recombination theoretically allows 10^{12} to 10^{15} different clonotypes. After thymic depletion and due to

limited niche resources an estimated 1:10^6 to 10^7 TCR clonotypes exist in about 4x10^{10} total CD8 T cells[96], which gives an adult human on the order of 4.000 to 40.000 CD8 T cells per clone. However, it is already known that these numbers drastically vary depending on the antigen peptide, with a frequency for many antigens of lower than 1:10^6. Isolating those cells from the naïve repertoire using conventional FACS is time consuming work and hardly practicable.

To establish the *Speed Enrichment* method for cytotoxic T cell specificity, we used the membrane protein of the influenza virus (FluMP), a well-established antigen, which nearly every human encounters in life, making it ubiquitous on a population level. In detail, the epitope of choice was $FluMP_{58-66}$, a 9 amino acid long peptide of the influenza matrix protein sequence from amino acid 58 to 66. As most adults either already had influenza or were vaccinated, cells against this epitope are relatively frequent, as shown by a double multimer stain with HLA-A2 FluMP peptide-pulsed BV421 and APC pMHC (Fig. 23 A). 1x10^8 Ficolled cells from fresh donor blood were stained, showing a target FluMP frequency of 0,079% of multimer double positive $CD8^+$, $CD19^-$ living lymphocytes. A total of 4x10^4 target cells were sorted using *Speed Enrichment* with the trigger on APC. Analyzed with the same gating hierarchy, an enrichment of this multimer double positive population to 33,7% was achieved. This enrichment factor of around 420-fold proved the feasibility of this method at least for a relatively frequent antigen.

In line with these data we evaluated an enrichment of two antigens with different frequencies in the periphery: the Wilms tumors gene 1 (WT1), an overexpressed tumor antigen often involved in different cancer developments and the viral phosphoprotein pp65 cytomegalovirus (CMV infection) antigen.

To analyze WT1 specific T cells, pMHC multimers with specificity to HLA-A2 molecules loaded with the $WT1_{126-134}$ peptide were used. For *Speed Enrichment*, 4x10^8 cells were stained first with pMHC multimer conjugated to APC. Even though the frequencies of T cells recognizing the tumor antigen WT1 is very low in healthy donors, still a CD19 PE-A610 and PI positive exclusion were possible, while the trigger was set to APC during *Speed Enrichment*. After the pre-enrichment, a total number of about 1.3x10^4 sorted APC positive cells were subsequently stained with the second pMHC multimer conjugated to BV421. Following purity sort with the trigger on FSC was performed on a MoFlo™ Legacy and gates were set for lymphocytes, singlets, $CD19^-$ negative, living cells, $CD3^+$, $CD8^+$ and double multimer positive (Fig. 23 B). The cells double positive for the pMHC multimer were then gated against CD45RA and CCR7 to determine T cell subsets (Fig. 23 C). Out of the initial 4x10^8 starting cells 44 naïve T cells specific for A2-$WT1_{126-134}$ could be identified and sorted as single cells for TCR extraction (Suppl. Fig. 13 collaboration with Hanna Ulrich). Starting donor material for the tumor antigen WT1 was low, with a frequency of multimer-specific cells of 0.004 %.

The second antigen-specificity was tested with the CMV structure protein $pp65_{495\text{-}503}$ also loaded onto HLA A2. Since CMV positivity in adults is common, several HLA-$A2^+$ donors were tested for CMV-specific IgGs prior to the experiment to get CMV negative donors. The starting material was $2.5x10^8$ freshly isolated PBMCs from venous blood. The frequency for this double positive pMHC target population was 0.016%. *Speed Enrichment* with the trigger was set to the APC channel was done on a MoFlo™ XDP. Also subsequent purity sorting was done on that instrument. In total 41 A2-pp65-specific naïve T cells could be sorted for single-clone expansion (isolated TCR sequences Suppl. Fig. 13 by Hanna Ulrich). The gating included singlet $CD19^-$, PI^-, $CD8^+$ and $CD3^+$ lymphocytes. The purity single cell sorts for the two epitopes and their location for major subset discrimination with CD45RA and CCR7 are shown (Fig. 23 C).

Taken together we enriched multimer frequencies for WT1 to 3,1% and in the case of pp65 to 0,37%, giving an enrichment factor of 775-fold for WT1 and 23-fold for pp65.

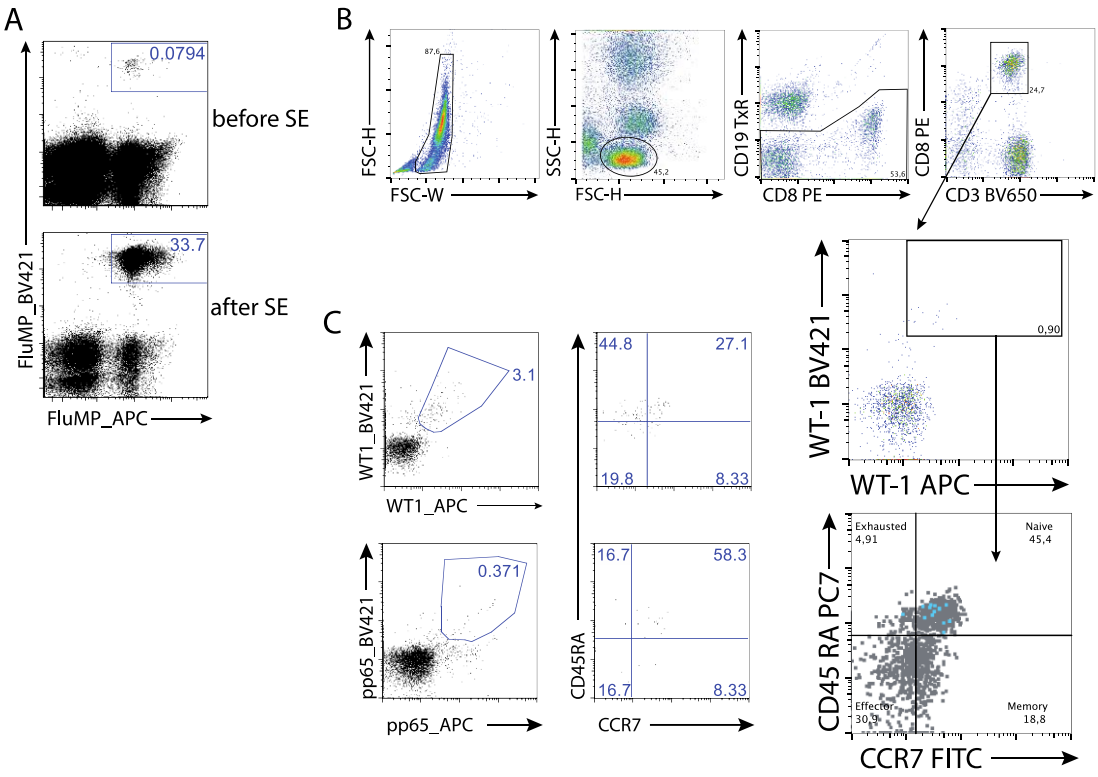

Figure 23: Isolation of antigen-specific T cells by *Speed Enrichment*.
(A) Overall double multimer staining for FluMP$_{58-66}$ of human PBMCs. Frequencies for the FluMP antigen in adult donors are relatively high due to infection and vaccination, indicated by a 0.07% frequency in starting material. Sample after *Speed Enrichment* with APC-triggered fluorescence achieved enrichment to 33.7%. (B) Gating strategy for single cell sort from naïve antigen WT-1-specific T cells of an already speed enriched sample. (C) FACS data from two different antigen specificities. Human PBMC samples post SE enrichment on APC for either WT-1$_{126-134}$ or pp65$_{495-503}$. Pre-gated on CD19-, CD3+, CD8+ single living lymphocytes, all double multimer positive naïve T cells were single cell sorted.

We showed the feasibility of this method for 3 epitopes, two of which were from naïve donors. Although TCR sequences were obtained from clonally expanded antigen positive cells, we had no data on their functionality. We therefore designed an experiment to show functional avidity of the TCRs by a multimer staining following single cell clonal expansion of antigen-specific cells. For this the MART1 antigen was chosen from which a functional TCR was already isolated for positive control. In collaboration (Manuel Effenberger and Maria Gerget) we performed *Speed Enrichment* of 1*10^8 PBMCs from buffy coat material. A total of 231 single cell clones were sorted in a following purity sort on living CD19$^-$, CD3$^+$, CD8$^{+,}$ CCR7$^+$, CD45RA$^+$ and APC and BV421 multimer double positive lymphocytes. After 11 days of clonal expansion with Expamer (antigen-unspecific CD3 conditions) stimulation, all clones were analyzed in a multiplexed staining approach (Suppl. Fig. 14 A) developed by Manuel Effenberger. Of 128 analyzed single cell progenies, 110 showed re-stainability and a functional avidity of two TCRs by the FACS-based off-rate assay[79] (Suppl. Fig. 14 B by Maria Gerget and Manuel Effenberger).

Speed Enrichment was not alone needed for the enrichment of antigen-specific T cells. We performed *Speed Enrichment* for rare sub populations in collaboration with different groups targeting different cell types of murine and human origin and demonstrated in these experiments the feasibility of *Speed Enrichment* as a cost and time saving FACS-approach for pre-enrichment.

4. Discussion

4.1. Construction of a modified cell sorter with strict temperature control assessing stable temperature sorting

To untangle the long list of sorting parameters that potentially alter cells, we made some modifications to our cell sorter. Some sorting parameters can easily be changed or controlled during sorting like pressure effects, charging, deflection and laser light irradiation, yet for one parameter especially, we had to make elaborate changes. Temperature is a crucial key parameter in cell sorting. By our modifications of the fluidics system of a MoFlo^{TM} XDP, we constructed an adjustable temperature-monitored sheath stream at stable conditions. The resultant development enabled total temperature control of the sample material throughout the sort, compared to conventional sorting, which only accounts for temperature control in the sample station or the receptacle holder. We already stated that sorting in temperature-controlled rooms is not an acceptable approach due to the fact that condensation occurs starting at 15°C, with the above-mentioned consequences for optics and electronics.

Our sorter reconstruction with complete temperature control from 4°C to 32°C proved feasible, including the implementation of a temperature monitoring system. Sorting with a fluidic system cooled down to 4°C was tested and did not show signs of a drawback in the expected counts for yield, purity and recovery. We did notice that the differences in the sheath temperature between chilled conventional sorting and a fully controlled system at 4°C needed a realignment of the sheath stream to the lasers. We hypothesize that differences of the fluids characteristics under these conditions were responsible, most likely due to viscosity.

At our institute, we generally stain cells at 4°C to avoid possible cell activation (especially for primary human cell material), as at higher temperatures activation and internalization of the dye has been reported[97]. The major issue is a balance between reduced cell alteration due to antibody activation and avoiding cell damage due to low temperature exposure. For primary cells, physiological temperature sensitivity was not detected for more than four hours, while some more sensitive cell types showed best survival and low activation for temperatures between 8°C to 12°C. All together temperature dependent activation and apoptosis varied for each cell type. With complete temperature control we could avoid cell activation processes (Ca^{2+}-Flux) induced by CD3 crosslinking compared to conventional sorting, however benefits for activation in intracellular TCR signal pathways were negligible.

We advise to validate staining intensities of antibodies for flow cytometry when working under hypothermal conditions, despite a previous titration (Suppl. Fig. 11) as MFIs can be severely affected. This effect is in line with the binding kinetics of antibodies, yet not all antibodies are affected, as shown by the example of a CD4-eF450 staining. Thus, temperature controlled but also conventional cytometry cell sorting present a balancing act between staining properties, cell fitness and activation processes cell type dependent.

Our temperature-controlled cell sorting approach could become a guideline for good manufacturing practice (GMP) as a practical use and in the future of FACS cell sorting for cell therapy, especially in combination with reversible dyes[78]. As FACS offers a benefit over other purification methods by single cell resolution and characterization with multiple marker definition; in combination with reversible dyes, the technology can also provide minimally altered and well-defined cell products. Personalized cell therapy is a growing field with different methods, like allogenic stem cell transplantation, tumor or cell therapy with antigen-specific cells, either allo- or autologous, in immunocompromised patients, which all rely on very well defined purified sample material. For this potential clinical use in particular, it was mandatory to rule out a sorter-induced influence on cell function and physiology.

4.2. Investigation of influences of current cell sorting procedures on the functionality and physiology of sorted cell types

The potential for cell alteration during cell isolation and propagation is well known. Previous work highlighted antibodies[57], temperature[58], homogenization[61] and cell preparation[62], buffer composition[53-55] and mitogens[56] as pitfalls for cell alteration. In contrast, little is known about cell alteration caused by FACS instruments[46] or the process itself. Other recent work setting out to evaluate the influence on mRNA expression due to FACS sorting[48] only proved the difficulty of analyzing sorter influences exclusively, without the effects of sample preparation. This project demonstrates the importance of using cells, which are minimally manipulated prior to sorting in order to detect any potential FACS-based influences. We addressed these problems in different ways. First, newly developed technologies were available to generate highly defined, pure, minimally manipulated cell populations by reversible staining and isolation out of fresh whole blood via Fab-TACS®, as previously shown[98]. Second, by using preferentially human primary blood cells, we reduced artifacts generated by immortalized cells or from murine organ-derived cell material. Third, with the potential to control certain sort

parameters like temperature, pressure, buffers, laser light or stream charging and deflection independently, we could evaluate these effects. Testing for these parameter, we found a FACS-induced phosphorylation of a MAPK pathway. MAPK p38 phosphorylation was affected by sorting independently of buffer composition, pressure, laser light, temperature or charging and stream deflection. Parameters like acceleration and shearing of cells are impossible to avoid, due to the concept of sorting in a pressurized fluid stream, and cannot be removed from the equation of sorting parameters. But these unavoidable FACS parameters were inducing the p38 activation in the first place. However, an evaluation of CD8 purified T cells with reversible reagents and the Fab-TACS® technology revealed no functional changes of these cells between sorted and their FACS-unsorted counterparts. FACS-sorted T cells were unaffected in their cytoskeleton coordination, migratory potential and proliferative capacity and showed nearly no changes in mRNA expression profiles, viability and effector killing function. These findings indicate that FACS-sorted cells sense some sorting parameters by their molecular signaling machinery, yet these stimuli seem insufficient to change the cellular behavior, physiology or function at least for primary human T cells isolated from blood. These findings indicate that previously performed experiments, which used the FACS technology were not biased by this method. Especially for susceptible read out systems like RNA-seq, MicroArrays or quantitative PCR following FACS sorting our data support the hypothesis of unaltered mRNA expression profiles for at least human CD8 T cells and support the hypothesis of largely unaffected single cell *in vivo* transfer experiments in animal models, at least concerning cell viability and proliferative capacity which were tested also for murine splenocytes. These data provide the basis for further evaluation and improvements of FACS-based sorting approaches, like the possibility of *Speed Enrichment* which we will discuss further on.

4.3. Development of a new technical sorting procedure to overcome FACS impairments regarding high cell count and rare event sorting (*Speed Enrichment*)

The technique of *Speed Enrichment* is a real asset for the enrichment of rare particles, e.g. cell populations, which are otherwise barely detectable. In the conventional setup, during cell isolation and propagation an event rate of only about 30,000 EPS is recommended, and even taking a lower purity of the sorted sample into account, the maximum event rate achievable is at about 200,000 EPS due to data processing, signal detection and single cell resolution. This makes sorting of high particle numbers time consuming and technically complex[99] or even impossible. With the *Speed Enrichment* setup, on the other hand, only those particles are detected which are labeled with a

certain fluorochrome and thereby have distinct fluorescence intensity. To visualize this relation, we showed that *Speed Enrichment* was capable of detecting only one cell out of a million, thus overcoming data processing issues. Hence, this method proves suitable for isolating target cells that occur in low frequencies. We showed by using this method, that cell numbers of $2x10^8$ were processed in less than 10 minutes. With the subsequent purity sort requiring much less time. Flowrates for *Speed Enrichment* are linear with increased differential pressure for fluid samples with no differences in viscosity due to high particle numbers (Suppl. Fig. 10), like blood, but with dense sample material containing more than $2x10^8$ cells/ml, Volume-flowrates decreased. Nevertheless, by processing large cell numbers, this FACS-based method can compete with the gold standard MACS, but furthermore enables a multi-colour purification. However, an advantage of MACS is the possibility to automate the process and run multiple samples at the same time (multiplexing). Experiments proved comparable yield and purity values for both technologies in rare event enrichments, despite the fact that the experimental design favored the MACS purification method.

Together with Laia Pascual Ponce, in her bachelor's thesis, pMHC-labeled antigen-specific T cells were enriched using also MACS and FACS (Suppl. Fig. 12). However these types of experiments, in the early stages of *Speed Enrichment*, differed concerning the yield and the experimental design. This was due because an older version of a cell sorter, a MoFlo™ Legacy was used. Changes in panel design and the switch to a newer version of the instrument solved these problems. We highlight that in different types of applications, a pre-enrichment step is known and beneficial e.g. for multimer-specific T cells[96,100,101] but also other cell types[101]. In the end our data showed an experimental advantage of *Speed Enrichment* over MACS concerning antigen-specific T cells isolation approaches.

With the established workflow, *Speed Enrichment* of antigen-specific T cells was tested for the Wilms tumor protein 1 (WT1) and the cytomegalovirus (CMV) structure protein pp65 from seronegative donors guaranteeing a naïve donor repertoire. The enrichment factor for pMHC-stained cells from PBMCs was around 200 to 300-fold, yielding in the case of WT1 200 and pp65 41 antigen-specific naïve T cells. These numbers are in line with previously reported data for this antigen in CMV seronegative donors[96], and fit with estimated frequencies in murine systems with 20 to 200 naïve T cells for one specific epitope[102,103].

When sorting those expected low cell numbers, one important aspect is cell loss during the FACS process. Experiments showed a recovery rate of approx. 70% for rare cell populations of a few hundred cells.

Our work on a temperature controlled FACS instruments, *Speed Enrichment* and definition of cell alterations by the sorter provides FACS technology and a foundation for approval of future FACS based individualized cell therapies.

5. Summary

The aim of this work was to investigate influences of flow cytometry cell sorting procedures on the functionality and physiology of cells. In order to accomplish this, a cell sorter with strict temperature control enabling analysis of different sorting parameters was developed. Furthermore, *Speed Enrichment*, was refined as a technical sorting procedure for the fast processing of rare event cell sorting out of high cell count sample material.

Evaluating FACS sorting induced cell alterations, we found a phosphorylation of different MAPK pathways. The sorting process alone, independent of buffer composition or sample pre-arrangements, affected mainly p38 phosphorylation. Individual effects like pressure, laser light, temperature, charging and stream deflection were not responsible for this activation. In contrast sorting associated forces like acceleration, collection tube impact and shearing were the source of this activation but were impossible to avoid and cannot be eliminated as sorting parameter due to instrument design. The pronounced p38 phosphorylation was also independent of potential endotoxin (like LPS) contaminations in the sorting systems, as controls with sorting buffer perambulated through the system were performed. Endotoxin levels were measured and sorter with and without detectable endotoxin contamination were tested for p38 phosphorylation in "mock" sorted cells. In both cases the sorter induced a pronounced p38 phosphorylation.

The evaluation of p38 activation with pure human $CD8^+$ T cells isolated by reversible staining via Fab-TACS® technology revealed no functional changes of these cells between sorted and their FACS-unsorted counterparts. FACS-sorted T cells were not or minimally affected in their viability, cytoskeleton structure, migratory potential, effector killing function, and proliferative capacity and showed only minor – if at all - changes in mRNA expression profiles.

Our data verify FACS as method for sensitive mRNA readout systems and single cell experiments, so that FACS, in retrospect, was also a good method of choice for *in vivo* generated animal data in cell transfer experiments, as unchanged cellular behavior of migration, proliferation, killing function and survival is indicated by experiments of users of our FACS facility. These data provide the basis for further evaluation of FACS-based sorting approaches for clinical applications, especially for cell therapy. These therapy approaches seem very promising in the context of minimally affected cells by reversible staining.

With our modifications of the fluidics system of a MoFlo™ XDP, we achieved an adjustable temperature-monitored sheath stream at stable conditions, allowing complete temperature control throughout the sort. In general, cells are stained at 4°C to avoid cell

activation. Therefore, the balance between reduced cell activation due to antibody activation and the occurrence of cell damage at low temperatures is a major issue. Temperature sensitivity was not detected in primary cells, while some more sensitive cell types showed better survival and low activation for temperatures between 8°C to 12°C. We show that cytometry-based cell sorting has to balance between staining properties, cell fitness and activation processes dependent on the working temperature and cell type. Our temperature-controlled cell sorting approach could become a guideline in the future for good manufacturing practice (GMP) as a practical use of FACS cell sorting in cell therapy, especially in combination with reversible reagents. However, for this type of application a major downside of FACS is the need to process large amounts of sample material.

For this we established the pre-enrichment method *Speed Enrichment* for rare event sorting with frequencies as low as 1:1.000.000 out of a high sample cell amount. Since sorting $1x10^9$ cells takes about 9h with conventional sorter settings, we first applied a FACS pre-enrichment to overcome these acquisition and data processing limitations by triggering on fluorescence. Additional sorting criteria for other fluorescence channels, as well as size and granularity, can be added in gating strategy. By fluorescence triggering, the event rate drops drastically, especially when applied on small population size or rare events. Due to the impurities in the deflected droplets, accepted and grounded by the high sample flowrate, this method is only a pre-enrichment.

With the establishment of a workflow for rare event sorting, *Speed Enrichment* of T cells specific for the epitope $WT1_{126-134}$ and the CMV epitope $pp65_{495-503}$ (both presented on HLA-A2) from seronegative donors, where the frequencies of antigen-specific T cells are extremely rare, had been performed. For both epitopes, in a subsequent FACS sort, antigen-specific T cells were single cell sorted and clonally expanded for generation of TCR sequences, demonstrating the feasibility of this sorting approach.

For MART1-specific T cells we verified the method of *Speed Enrichment* by re-staining expanded single cell clones and measuring functional avidity by K-off rate. *Speed Enrichment* reached approximately 70% recovery rate for rare cell populations of a few hundred target cells.

6. Material and Methods

6.1. Material

Chemicals/Reagents	Supplier
Acrylamide	Bio-RAD, Munich, Germany
Adefo-GV60 (western blot developer)	Adefo Chemie GmbH, Dietzenbach, Germany
Adefo-GV60 (western blot fixer)	Adefo Chemie GmbH, Dietzenbach, Germany
Ammoniumperoxodisulfate (APS)	E. Merck KGaA, Darmstadt, Germany
Biocoll Separation Solution	Biochrom AG, Berlin
Bromphenol blue	Sigma Chemie GmbH, Schnelldorf, Germany
Bovine serum albumin (BSA)	GE Healthcare Life Sciences, Freiburg, Germany
Cyto-Cal Count Tubes	ThermoScientific, Fremont CA, USA
D-Biotin	Sigma Chemie GmbH, Schnelldorf, Germany
EDTA	Roth GmbH & Co.
Ethanol 70 %, 96 % and 99,8 %	Pharmacy of the Klinikum Rechts der Isar
FACSflow	Becton Dickinson GmbH (BD), Heidelberg, Germany
FCS (Fetal Calf Serum)	PAA, Pasching, Austria
ICS-Fix/Lyse	Becton Dickinson (BD Bioscience), Franklin Lakes, USA
Ig-kappa CompBeads	Becton Dickinson GmbH, Heidelberg, Germany
Glycerin	Carl Roth GmbH & Co., Karlsruhe
Glycerol	Sigma Chemie GmbH, Schnelldorf
Glycine	Carl Roth GmbH & Co., Karlsruhe
Heparin	Liquemin® N 25 000, Roche, Basel, Switzerland
Interleukin 2	Peprotech, Hamburg, Germany
Methanol	Carl Roth GmbH & Co., Karlsruhe

NNN´,N´-Tetramethylenediamine (TEMED)	Sigma Chemie GmbH, Schnelldorf, Germany
Sodiumchlorid	Carl Roth GmbH & Co., Karlsruhe
Sodiumdodecylsulfat (SDS)	Carl Roth GmbH & Co., Karlsruhe
PBS (Phosphate Buffer Saline)	PAA, Pasching, Austria
Penicillin	GIBCO™, Invitrogen Corporation, Paisley, U.K.
polystyrene micro-particles PPS-8.0	Kisker, Steinfurt, Germany
Protease-Inhibitor Mini tablets	Roche Diagnostics GmbH, Mannheim, Germany
RPMI 1640 with L-Glutamine	GIBCO Life Technologies, Gaithersburg MD, USA
Streptavidin-APC	BioLegend®, San Diego, USA
Streptavidin-BV421	BioLegend®, San Diego, USA
Streptomycin	GIBCO™, Invitrogen Corporation, Paisley, U.K.
Tris-Hydrochloride	Carl Roth GmbH & Co., Karlsruhe
^{3}H-Thymidine	Hartmann Analytik GmbH, Braunschweig, Germany
Trypan Blue	Sigma, Taufkirchen, Germany
Tween 20	Carl Roth GmbH & Co., Karlsruhe
Western Lightning ECL detection	Perkin Elmer Inc., Waltham USA

All chemicals were of ultra-pure grade.

Instrument/Equipment/Software	Supplier
Agfa Curix 60	AGFA, Munich, Germany
Beta counter 1500TR	Former Packard Instruments Company, now ThermoFischer Scientific, Waltham, USA
Bio-Mag 10 magnetic stirrer	BCC Special Instruments, Göttingen, Germany
BioRad Experion	BIO-RAD Laboratories GmbH, Munich, Germany
Cellstar PP-tubes 15 mL	Greiner GmbH, Frickenhausen, Germany
Cellstar PP-tubes 50 mL	Greiner GmbH, Frickenhausen, Germany
Costar® 24 well Transwell® plates	Corning Incorporated, Kennebunk, USA
Cyan™ ADP Lx9 Color Analyzer	Beckman Coulter, Inc., Fullerton, USA
Electro-blot Trans-Blot SD	BIO-RAD laboratories GmbH, Munich, Germany
Electrophoresis chamber	PEQLAB Biotechnology GmbH, Erlangen, Germany,
Electrophoresis power supply EPS 600	Amersham pharmacia biotech, Freiburg, Germany
Eppendorf tubes, 0.5, 1,5, 2.0 mL (safe-lock)	Eppendorf-Netheler-Hinz GmbH, Hamburg, Germany
FACSAria™ III	Becton Dickinson (BD Bioscience), Franklin Lakes, USA
FlowJo Version 10.2	FlowJo LLC, Ashland, USA
Glass fiber filters, MLR	Perkin Elmer Inc., Waltham USA
Hera Cell 240 incubator	Thermo Electron Corp., Karlsruhe, Germany
Hera Multifuge 3SR+ centrifuge	Thermo Electron Corp., Karlsruhe, Germany
Hera Safe sterile bench	Thermo Electron Corp, Karlsruhe, Germany
IDL TRM-V wheel mixer	Kühn & Bayer, Nidderau-Heldenbergen, Germany

Affimetrix™	Life Technologies, Darmstadt, Germany
Leucosep™ Tubes	Greiner Bio-one GmbH, Frickenhausen, Germany
Metal block thermostat QBT4	CLF analytical laboratory instruments GmbH, Emersacker, Germany
Microscope, confocal, Leica DMRBE	Leica, Microsystems GmbH, Wetzlar, Germany
Microscope Axiovert 100	Carl Zeiss Jena GmbH, Jena, Germany
Micro96 Harvester	Skatron Instruments,
MoFlo™ Legacy	Beckman Coulter, Inc., Fullerton, USA
MoFlo™ XDP	Beckman Coulter, Inc., Fullerton, USA
Multical pH meter pH526	WTW, Weilheim, Germany
NanoDrop ND-1000	Nanodrop, Steinfurt, Germany
Neubauer chamber	Paul Marienfeld GmbH & Co. KG, Lauda-Königshofen, Germany
pH electrodes (BlueLine 24)	Schott Instruments, Mainz, Germany
Pipettes P10, P20, P100, P200, P1000	Gilson International B.V., Bad Camberg, Germany
Pro-Tran, nitrocellulose transfer membrane	Whatmann, Dassel, Germany
Puradisc sterile filters 0,45 µm	GE Healthcare GmbH & Co. KG, Braunschweig, Germany
OB29 radiation source (^{137}Cs) γ-ray	Buchler GmbH, Braunschweig; Germany
Sunrise™ microplate reader	Tecan Trading AG, Männedorf; Switzerland
Thermomixer compact	Eppendorf, Hamburg, Germany
ViCell™	Beckman Coulter, Inc., Fullerton, USA
Waterbath	GFL GmbH, Burgwedel, Germany
Whatman paper 3 mm	Carl Roth GmbH & Co. KG, Karlsruhe, Germany
XCELLigence®	ACEA, SanDiego, USA

Kits	Supplier
Annexin V	Molecular probes, Eugene, Oregon, USA
Flica, Cell Event Green	Molecular probes, Eugene, Oregon, USA
RNeasy	Quiagen GmbH, Hilden, Germany
Fab-TACS® Traceless Affinity Cell Selection	IBA Lifesciences, Göttingen, Germany
Pierce™ LAL Chromogenic Endotoxin Quantitation Kit	ThermoScientific, Fremont CA, USA

Antibody	Clone	Dilution	Supplier
αhCCR7-FITC	150503	1:50	R&D Systems, Inc., Minneapolis, USA
αhCD19-ECD	J3-119	1:50	Beckman Coulter, Fullerton, USA
αhCD28 purified	CD28.2		Becton Dickinson (BD Bioscience), Franklin Lakes, USA
αhCD3-BV650	OKT3	1:50	BioLegend®, San Diego, USA
αhCD3 purified	UCHT1		Becton Dickinson (BD Bioscience), Franklin Lakes, USA
αhCD45RA-PECy7	2H4	1:50	Beckman Coulter, Fullerton, USA
αhCD8-APC	B9.11	1:50	Beckman Coulter, Fullerton, USA
αhCD8-PE	3B5	1:200	Former Invitrogen now ThermoFischer Scientific, Waltham, USA
αp-p38-APC	4NIT4KK	1:20	Former eBioscience now ThermoFischer Scientific, Waltham, USA
αp-JNK-PE	Monoclonal Ab by immunization	1:50	CellSignaling, Danvers, USA
αp-Erk1/2-PerCPef710	MILAN8R	1:20	Former eBioscience now ThermoFischer Scientific, Waltham, USA
αhCD8-PB	DK25	1:20	DakoCytomation, Glostrup, Denmark
αhCD16-ECD	3G8	1:50	Beckman Coulter, Fullerton, USA
αhCD14-ECD	RMO52	1:50	Beckman Coulter, Fullerton, USA
αhCD19-ECD	UCHT1	1:50	Beckman Coulter, Fullerton, USA

αhCD4-ECD	SFCI12T4D11	1:50	Beckman Coulter, Fullerton, USA
CD8Fab	Derived from clone OKT8, with unknown point mutations	1:100	IBA Lifesciences, Göttingen, Germany
αp-p38 (wb)	Monoclonal Ab by immunization	1:1000	CellSignaling, Danvers, USA
α-p38 (wb)	Monoclonal Ab by immunization	1:1000	CellSignaling, Danvers, USA
αp-Erk5	Polyclonal Ab by immunization	1:1000	CellSignaling, Danvers, USA
αp-Erk1/2 (wb)	Monoclonal Ab by immunization	1:2000	CellSignaling, Danvers, USA
αβ-actin (wb)	Monoclonal Ab by immunization	1:1000	CellSignaling, Danvers, USA
α-GAPDH (wb)	Polyclonal	1:2000	Sigma-Aldrich Chemie GmbH, Munich, Germany
αp-eIF2 (wb)	Monoclonal Ab by immunization	1:1000	CellSignaling, Danvers, USA
αp-Zap70 (wb)	Monoclonal Ab by immunization	1:1000	CellSignaling, Danvers, USA
Mouse α-rabbitIgG-HRP	Monoclonal by IgG immunization	1:7000	CellSignaling, Danvers, USA
α -PE-MicroBeads	n.a.	1:5	Miltenyi Biotec GmbH, Bergisch Gladbach, Germany

Cell line	Origin	Reference
Jurkats ACC282	*Homo sapiens*, lymphoblast (blood, T-lymphocyte)	Weiss A et al., J. Immunol., 133: 123-128, 1984
K562	*Homo sapiens*, lymphoblast (bone marrow)	Lozzio BB, Lozzio CB.; Blood 45: 321-334, 1979
A375	*Homo sapiens*, epithelial (skin)	Giard DJ et al.; J. Natl. Cancer Inst. 51: 1417-1423, 1973
HCV-29	*Homo sapiens*, epithelial (bladder)	Hisazumi H et al.; Urological Research 5: 133-139, 1977

pMHC multimer	Peptide
HLA-A2/ hβ2m/flu MP_{58-66}	GILGFVFTL
HLA-A2/hβ2m/$pp65_{495-503}$	NLVPMVATV
HLA-A2/hβ2m/$WT_{1126-1134}$	RMFPNAPYL
HLA-A2/hβ2m/ $MART\text{-}1_{(A27L)\ 26-35}$	ELAGIGILTV

6.2. Methods

6.2.1. Cell extraction procedures and culture conditions

6.2.1.1. Isolation of human Peripheral Blood Mononuclear Cell (PBMC)

Human PBMCs were isolated by density centrifugation with Biocoll Separating Solution from fresh venous blood from healthy donors and mixed with heparin as an anticoagulant, or from buffy coat, obtained from healthy individuals during blood donation (German Heart Centre Munich) with Leucosep™ Tubes. Blood donations were obtained from voluntary donors after informed consent under regulatory conditions and in accordance with the declaration of Helsinki[104]. Ficoll was performed after the Leucosep protocol at 1000 g for 10 min at RT. After withdrawing the layer containing mono-nucleated cells, thrombocyte wash in PBS (5% BSA, 0.5 mM EDTA) at 300 g for 7 min was performed. Cells were stored until further usage in RPMI-1640 (10% FCS, PenStrep) in an incubator at 5% CO_2 and 37°C. For phospho-Immunoblot and phospho-flow analysis cell starving o.N. was done with RPMI containing 2% FCS instead. Cell counts were done manually in a Neubauer counting chamber with Trypan blue stain.

6.2.1.2. Isolation of murine splenocytes

Murine primary cells were isolated from the spleen of wild type C57BL/6 mice. Mice were sacrificed by cervical dislocation at an age ranging from 8 to 30 weeks. Spleens were

mashed by passing through a 100µm cell strainer using Klicks medium containing 44,5% DMEM and 44,5% RPMI with mercaptoethanol (0,1%), FCS (10%) and PenStrep (1%). Cells were counted with a Neubauer chamber and stained with Trypan blue for live/dead discrimination. Cells were resuspended in Ammoniumperoxodisulfate ACT (7 min at RT) for red blood cell lysis. Reaction was stopped by adding Klicks medium, cells were centrifuged 300 g, 7 min and resuspended in the appropriate cell count and buffer for subsequent experiments.

6.2.1.3. Cell culture conditions for immortalized cells

Human cell lines were cultured under 5% CO_2 at 37°C in RPMI-1640 with Glutamine (10%FCS, 50 k Units of Penicillin and 50 mg Streptomycin) in T75 tissue treated bottles, 6-well plate format and 15 cm coated dishes. Splitting was done regularly each two to three days in regard to the medium color. Before usage for phospho-Immunoblots cells, were starved o.N. with cell culture medium containing 2% FCS instead.

6.2.2. Cell purification methods

6.2.2.1. Magnetic cell separation

For magnetic cell separation (MACS), Miltenyi's Anti-PE MicroBeads were used. Before enrichment, target cells were stained for surface expression with a CD8 phycoerythrin-coupled antibody. Labeled cells after surface staining were incubated with PE MicroBeads in a concentration of 10^7 cells per 80 µl for 15 min in the dark at 4°C with 20 µl anti-PE MicroBeads. Cells were washed two times in 2 mL PBS per 10^7 cells at 300 g for 10 min. For positive selection a concentration of 10^8 cells per 500 µl was adjusted. For purification LS magnetic columns were used, enabling a purification of up to $1x10^8$ target cells in the magnetic field of a MACS holder with magnets. Columns were equilibrated in PBS before usage by passing 3 mL PBS by gravity flow through the column. After equilibration, labeled cells were added on top, washing was done by applying 3x3 mL of PBS subsequently onto the column. Elution of target cells was done with 5 mL PBS and removing the column out of the magnetic field.

6.2.2.2. Fab-TACS® Traceless Affinity Cell Selection

Fab-TACS® columns were handmade from two 20 mL tips and filled with 1 mL agarose bead-matrix, sufficient volume for purification of 10 mL human whole blood or buffy coat material. Columns were equilibrated with 10 mL FACS buffer (PBS with 0.5% (w/v) BSA and 1 mM EDTA, pH 7.4) at a flowrate of 10 ml/min. After equilibration the agarose matrix was coated two times with 30 µg CD8 Fab dissolved in 3 mL FACS at a flowrate of 1.5 ml/min. 10 mL cell material ran twice through the matrix with a flowrate of 1.5 ml/min for the first run and 2,5 ml/min for the second. Washing of the column was done four

times with 15 mL FACS buffer at a flowrate of 10 ml/min. Cells attached to the agarose matrix were dissolved by running 5 mL of FACS buffer containing 100 mM D-Biotin. The eluted fraction was subsequently washed in 50 mL FACS buffer at 300 g for 7 min. Purity, depletion and viability of sample material and purified cells were determined by CD8, CD3, CD235 and PI staining with FACS analysis.

6.2.2.3. Flow Cytometry

6.2.2.3.1. Cell sorting

For the cell sorting, the MoFlo™ legacy, MoFlo™ XDP or FACSAria III were used with a 70 µm nozzle. Samples were filtered (30 µm) with a concentration of about $1x10^7$ cells/ml. If gating strategy included live/dead discrimination, propidium iodide (Invitrogen, Darmstadt, Germany) 1 µg/ml was added right before the sort. The cells were sorted with a sample pressure of a maximum event rate of 20.000 events per second (EPS).

6.2.2.3.2. *Speed Enrichment*

For isolating cell populations with a very small frequency in human PBMCs, like antigen-specific T cells, a pre-enrichment using *Speed Enrichment* (SE) was performed on the MoFlo™ XDP with a 70 µm nozzle. The samples were filtered (30 µm) and taken up in a concentration of about $2x10^8$ cells/ml. If the gating strategy included live/dead discrimination, PI was added right before the sort. Dependent on the fluorochrome defining the cell population, the trigger was set to the respective fluorescence channel. Threshold settings were increased above the negative population displayed in FSC triggering for this fluorescence channel. Pressure difference between sheath- and sample pressure was Δ2 psi.
For the establishment of *Speed Enrichment*, polystyrene micro-particles PPS-8.0 beads and anti-rat and anti-hamster Ig-kappa CompBeads were used.

6.2.2.4. Flowrate determination and internal cell count controls

For internal controls of flowrate, Cyto-Cal Count Tubes were used, where each tube contained 50.000 beads adjusted in a dissolvable gel matrix. Beads had a diameter of around 7 µm and were distinguishable from cells by FSC/SSC gating and a high fluorescence at 488, 405 and 640 nm excitation.

6.2.2.5. Staining procedures

FACS Buffer contained PBS (with 0.5% BSA (w/v) and 1mM EDTA) sterilely filtered through 0,22 µm. All used chemicals were of ultrapure grade.

6.2.2.5.1. Staining for antigen-specific T cells

For the enrichment of multimer-specific T cells, HLA-A2 Molecules were refolded with peptide GILGFVFTL (hβ2m/flu MP_{58-66}), NLVPMVATV (hβ2m/$pp65_{495-503}$) and RMFPNAPYL ($WT1_{126-134}$) and multimerized via Streptavidin-PE, Streptavidin-BV421 or Streptavidin-APC. Multimerization was done for 45 min at 4°C in the dark with 40 µg/ml HLA molecules and 25 µg/ml Streptavidin. Finally, up to $2{,}5x10^8$ cells were stained in 600 µl for 30 min at 4°C. After staining, cells were washed in 10 mL FACS buffer two times at 300 g, 7 min at 4°C.

6.2.2.5.2. Antibody staining of cell surface markers

For optimal staining results antibody conjugates were titrated. Antibodies used are listed under materials with the titrated dilution. Staining was performed in 96-well format in 200 µl (max. $5x10^7$ cells/ml). Samples were stained in the dark for 20 min at 4°C, or as mentioned otherwise, and washed two times in 200 µl FACS buffer at 300 g, 4°C.

6.2.2.5.3. Intracellular antibody staining

When stained for intracellular phospho-proteins, first EMA staining (1:1000) was done on ice with light exposure for 20 min with FACS buffer containing NaN_3 0,06% (v/v). After washing, cell surface staining was done before fixation. Cells were then fixed by adding 2% final concentration PFA for 20 min at RT. Cells were then centrifuged and re-suspended in 20 µl FACS (NaN_3). After addition of 250 µl Methanol (99%) at 4°C and 20 min incubation, two washing steps at 300 g for 5 min 4°C were performed before intracellular staining. After an additional two washing steps cells were analyzed.

6.3. Immunochemical methods

6.3.1. Western Blotting

For cytoplasmic lysates cells were sedimented at 14.000 g for 1 min at 4°C. Lysis of cells was done by re-suspending in 50 µl of NP-40 buffer (containing 50 mM HEPES, 40 mM NaCl, 1 mM DTT, 1 mM Na_2EDTA, 1 mM EGTA, 0,5% (v/v) Nonident P-40, 10% (v/v) Glycerol, 20 mM β-Glycerolphosphat, 1 mM Na_3VO_4, 0,4 mM PMSF, 1 mM NaF, 1 tablett protease inhibitor adjusted to pH 7,6) at 4°C. Incubation on ice for 15 min followed by 10 min centrifugation of cell debris at 14.000 g at 4°C. Supernatant was stored at -20°C until usage.

Before protein electrophoresis cytoplasmic lysates were cooked at 95°C with 12 µl 4xLämmli buffer (62,5 mM Tris, 2% SDS, 50% Glycerol, 2 mM EDTA, 1% Bromphenolblue, 100 mM DTT) for 5 min. 10% SDS-Polyacrylamidgels were used for gelelectrophoresis running at 120 V for 100 min with running buffer (25 mM Tris, 3,5 mM

SDS, 200 mM Glycine) together with a protein size-ladder 10-170 kDA (10 bands) from Peqlab. After protein separation SDS gels were plotted semi-dry onto nitrocellulose at 130 mA for 100 min with transfer buffer (25 mM Tris, 15 mM Glycine, 20%(v/v) Methanol, 0,35% SDS). Membrane was blocked in PBS-T (PBS with 0,1% Tween20) containing 5% (w/v) dissolved milk powder at RT for 30 min. Membranes were subsequently washed with PBS-T and cut in size and incubated with appropriate antibodies in PBS-T with 5% BSA over night at 4°C on a shaker. After incubation membranes were washed three times in PBS-T for 10 min and incubated with a mouse-α-rabbit IgG coupled to HRP in PBS-T containing 5% milk. Detection of signals was done with WesternLightning ECL substrate.

6.3.2. Limulus Amebocyte Lysate (LAL) test

Detection of endotoxins in the sheath fluid of cell sorter systems was done by LAL test Pierce™ LAL Chromogenic Endotoxin Quantitation Kit from Thermo Scientific™ (Thermo Fisher Scientific, Waltham, MA USA) following the instructions of the distributers protocol. The concentration of the reaction product p-Nitroaniline was measured by 405nm absorbance in a Sunrise™ microplate reader (Tecan Trading AG, Switzerland) using Magellan 7 software (Tecan Trading AG, Switzerland). Absorbance values for the different samples were plotted against a standard curve generated by endotoxin levels of a known concentration (E. coli) and analyzed using Prism graph pad.

6.4. Molecular biology

6.4.1. RNA isolation

For isolation of RNA cells were Fab-TACS® purified with reversible CD8 Fab one day prior to the experiment. CD8 cells were rested o.N. at a density of $3x10^6$ cells/ml in RPMI with Glutamine (10%FCS) at 5% CO_2 and 37°C. The next day cell were resuspended in fresh pre-warmed RPMI-1640 and either mock-sorted or unsorted on a MoFlo™ XDP, and splitted for immediate (0 min) and late (240 min) time points (under cell culture conditions). At indicated time points cells were harvested by centrifugation at 14.000 g, 1 min at 4°C and RNA extracted with the RNeasy Micro Kit. For lysis cell pellets were resuspended in 350 µl Buffer RLT. 400 µl 70% ethanol was added and mixed by pipetting. Whole volume was added to a RNeasy MinElute spin column and centrifuged at 8000 g for 15 sec. Followed by washing of the spin column with 350 µl buffer RW1 at the same speed and time. DNA bound to the column matrix was digested by adding 80 µl buffer RDD (containing 10 µl DNase I) for 15 min at RT. DNase was removed by washing

the columns with 350 µl buffer RW1. Subsequent 500 µl of buffer RPE was added and spinned at 8000 g for 15 sec. Finally 500 µl of 80% ethanol was added and centrifuged for 2 min, after which the column was dried by 14.000 g for 5 min. After drying columns were immediately stored at -80°C until all time points were acquired. For eluting the mRNA columns were rewarmed to RT and centrifuged with 14 µl RNase free H_2O and stored at -80°C until MicroArray analysis. Except 1 µl of samples, which was used to determine mRNA yield via Nanodrop measurement with the absorbance from 220 to 350 nm with a peak at around 260 nm.

6.4.2. MicroArray and data analysis

At -80°C stored mRNA samples were thawed on ice. mRNA quality was determined with the friendly help of Julia Ritter with the BioRad Experion using Experion RNA Chips. RNA concentration ranged from 85 ng/µl to124 ng/µl with a ration of 28S/18S for the ribosomal RNA ranging from 1.06 to 2.58. The RQI was measured for RNA degradation. For all samples it ranged from 8.2 to 9.1 indicating good RNA quality. After quality assessment for the MicroArray, RNA were translated into DNA, fragmented and labeled and MicroArray analysis was done with the Affimetrix™ system using the Gene Chip™ Human Gene 1.0 ST. In total, 18710 MicroArray data values were gained, normalized and checked for an at least 2-fold up- or downregulation between the different conditions. Data were RMA normalized which included a log2 transformation. mRNA upregulation was determined by:

$$A - B > 1 \rightarrow \frac{2^A}{2^B} > 2$$

6.5. Assays for cell function

6.5.1. Survival and Apoptosis

Different dyes were used for determination of cellular fitness and survival. Cells were stained with trypan blue for analysis with the ViCell^{TM}. For flow cytometric assessment propidium iodide (final concentration 2,5 µg/ml), ethidium monoazide (final concentration 2 µg/ml), 7AAD, Flica-Cell event green (conjugated to FITC) and AnnexinV (conjugated to Pacific Blue) as Kits from Life Technologies were used. For life dead staining regular FACS buffer was used, except for AnnexinV were a special buffer was used. AnnexinV binding buffer (140 mM NaCl, 4 mM KCl, 0,75 mM $MgCl_2$ and 10 mM HEPES) enables binding to Phosphatidyserine PS by providing Ca^{2+} Ions.

6.5.2. Migration

Migration of cells was measured with ficolled human PBMCs. Samples were split in two (mock-sorted/unsorted) and stained with αCD4, 19, 16 and 14 on ECD. The sorted and unsorted samples were further divided into alternate CD8 staining with the fluorochromes Pacific Blue (PB) and Phycoerythrin (PE) to account for staining-induced differences in migration. For the migration assay 24-well format transwell plates with a 5 µm pore size membrane were used. A total of $2x10^5$ cells were added per well, with each $1x10^5$ cells mock-sorted and unsorted suspended in RPMI medium. A chemo taxis gradient was provided by adding RPMI (1% FCS) to the lower plate. After 4, 9 and 20 hours replicates of n=6 for each condition were measured as a percentage of migrated CD8 cells.

6.5.3. Proliferation - Mixed lymphocyte reaction

The mixed lymphocyte reaction (MLR) is based on the uptake of radioactively-labeled thymidine into the newly synthesized strands of dividing cells. Thymidine for this purpose is loaded with Tritium (^3H), which decays with a half-life of 12.32 years by emitting beta radiation.

$$T \rightarrow {}^3He + e^- + \bar{\upsilon}_e$$

A scintillation beta counter detects the emitted electrons counted by the stream of carrier gas. Proliferation assay was performed in 96well plates in 200 µl RPMI-1640 (10% FCS, 1% PenStrep, Glutamine) by adding 1 µCi 3H-thymidine per well to human PBMCs. Proliferation of $2,5x10^5$ effector cells was stimulated by adding $1x10^5$ γ-irradiated (30 Gy) stimulator cells, which were HLA-mismatched. Cells were harvested by an automated system Micro96 Harvester and transferred onto a glass fiber filter. Filters were dried overnight and analyzed the next day with a Packard beta counter. Experiments for different conditions were done in replicates of n=8.

6.5.4. Antigen-specific killing

For antigen-specific killing, TCR transgenic T cells recognizing the MART-$1_{(A27L)\ 26\text{-}35}$ epitope were kindly provided by Manuel Effenberger. TCR transgenic CD8 T cells were FACS purified based on CD8 and pMHC positivity and subsequently expanded using αCD3 αCD28 antibodies (1.0 µg/ml Okt3; 0.5 µg/ml CD28) and 50 U/ml Il2. Before the cytotoxicity assay $5x10^4$ MART-1-specific T cell clones were seeded into a 24 well CD3 and CD28 coated plate and stimulated for two days followed by a three-day resting phase. One day before the cytotoxicity assay $5x10^3$ A375 melanoma cells[105] grew confluent in 100 µl DMEM growth medium (10% FCS, 1% PenStrep, 1% sodium pyruvate) within a 96well E-plate at 37°C and 5% CO_2. The baseline growth was monitored within the xCELLigence system. For A375 cells pulsing medium was removed after 24 hours und replaced by 100 µl growth medium containing 10^{-7}M MART-1 peptide for 60 min. Subsequent, culture medium was removed and replaced with 100 µl RPMI (10% FCS, 1% PenStrep, 1% sodium pyruvate) containing MART-1 effector T cells (either mock-sorted or sort-medium exchanged) ranging in numbers from 1:1 to 8:1 E:T ratio (related to the initially seeded A375 cells). All conditions were done in duplicates in a total of n=4 experiments; while monitored impedance measurements were done for 48 hours every 15 min. Specific cell lysis was calculated from cell indices (CI):

$$specific\ lysis = \frac{nCI(A375only) - nCI(A375sample)}{nCI(A375only)}$$

7. Supplementary data

7.1. TCR signaling by CD3 activation is temperature dependent

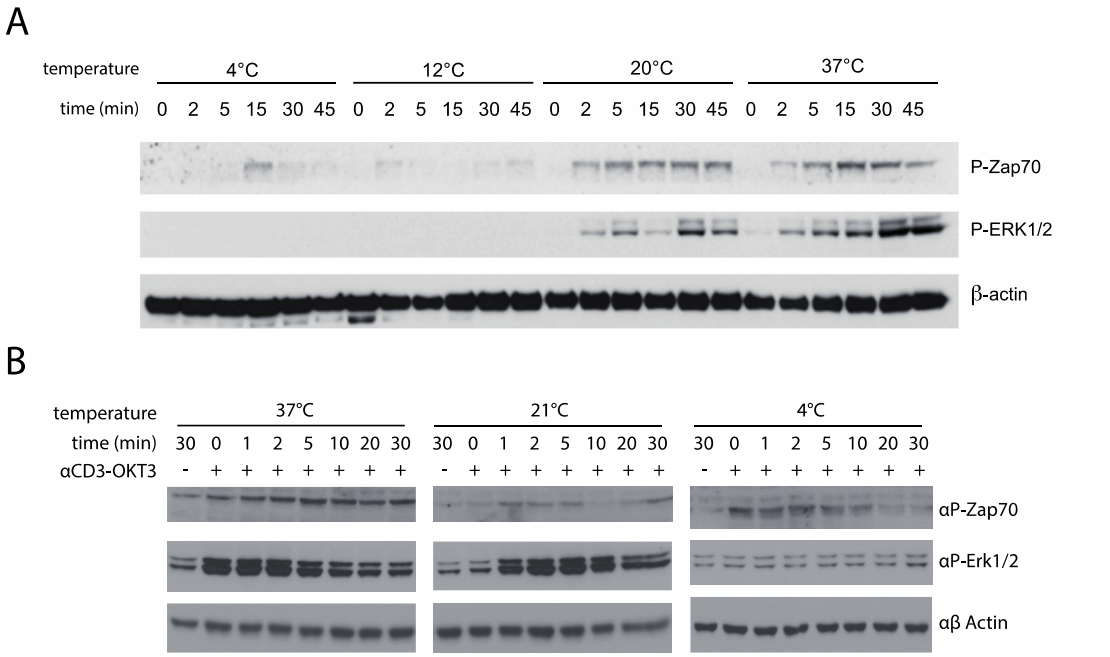

Supplementary Figure 1: Immunoblot of intracellular phospho-signaling after TCR stimulation.
(A) For human PBMCs different temperatures (37°C, 20°C, 12°C and 4°C) were adjusted in cell culture medium and Orthoclone antibody was added over a 45 min time course; aliquots were subsequently taken. Specific antibodies detected the loading control for beta-actin and the phosphorylation of Zap70 and Erk1/2 (Immunoblot kindly provided by Stefan Dreher).
(B) Orthoclone (CD3 clone Okt3) was used for TCR stimulation on Jurkat (ACC282) cells at different temperatures (37°C, 21°C and 4°C) in cell culture medium. Anti-phospho Zap70 and anti-phospho Erk1/2 antibodies were used, as loading control anti-beta actin. CD3 stimulated aliquots were lysed over a 30 min time course.

7.2. Apoptosis comparison of MACS and different FACS sorter on PBMCs

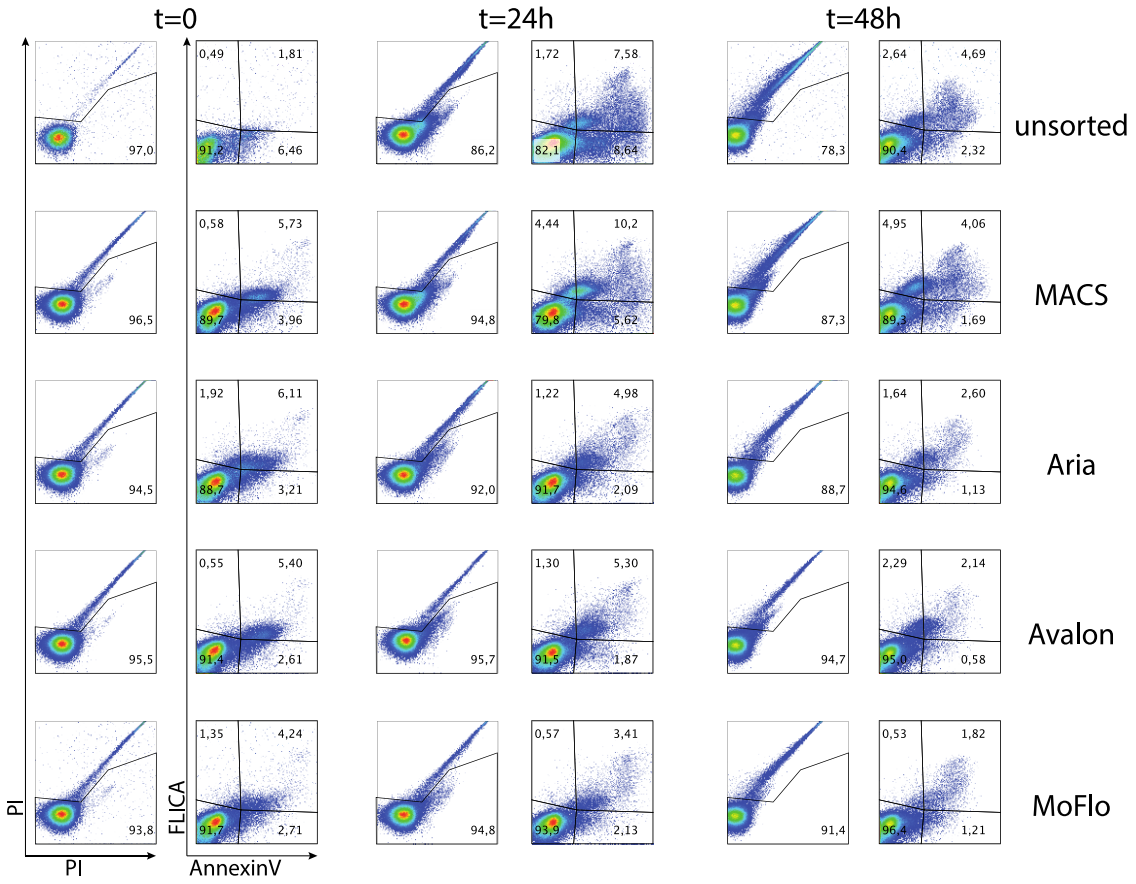

Supplementary Figure 2: Two day apoptotic marker time course with MACS and FACS sorted PBMCs.
Human PBMCs unsorted or passed either through different FACS sorter or MACS column stained with early and late apoptotic markers. In FACS sorted cells no PI exclusion previous to sorting was done to compare to MACS or unsorted cells. At indicated time points cells were stained with PI, Flica (FITC) and AnnexinV (PacificBlue) to identified cells in apoptotic progression or already dead cells, subsequent analysis was done by flow cytometry.

7.3. eIF2α stress signals

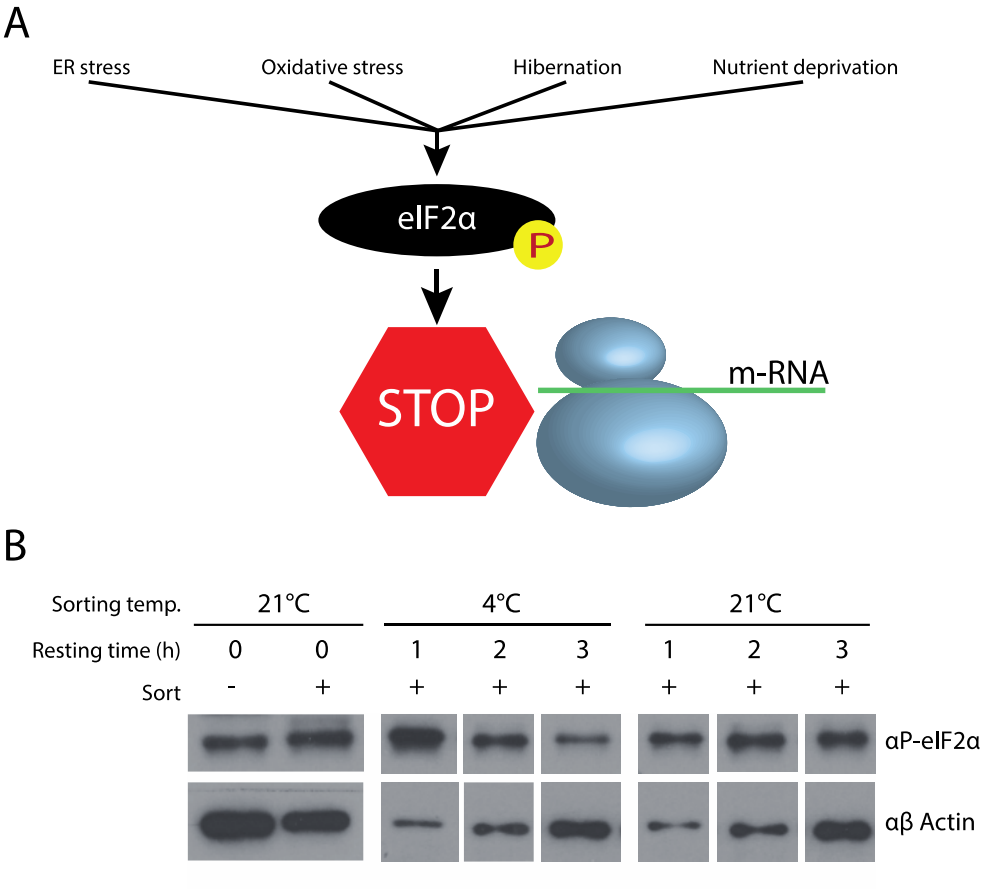

Supplementary Figure 3: FACS and temperature influence on eIF2α.
(A) Sketch of stress signals leading to stop in mRNA translation via the key mechanism of eIF2α phosphorylation. (B) Immunoblot for phosphorylated eIF2α in PBMCs. Sorting under different temperature conditions with lysis of aliquots over a resting period is shown. β-actin was used for determination of protein content.

7.4. Confocal microscopy of cell structures after sorting in adherent cell lines

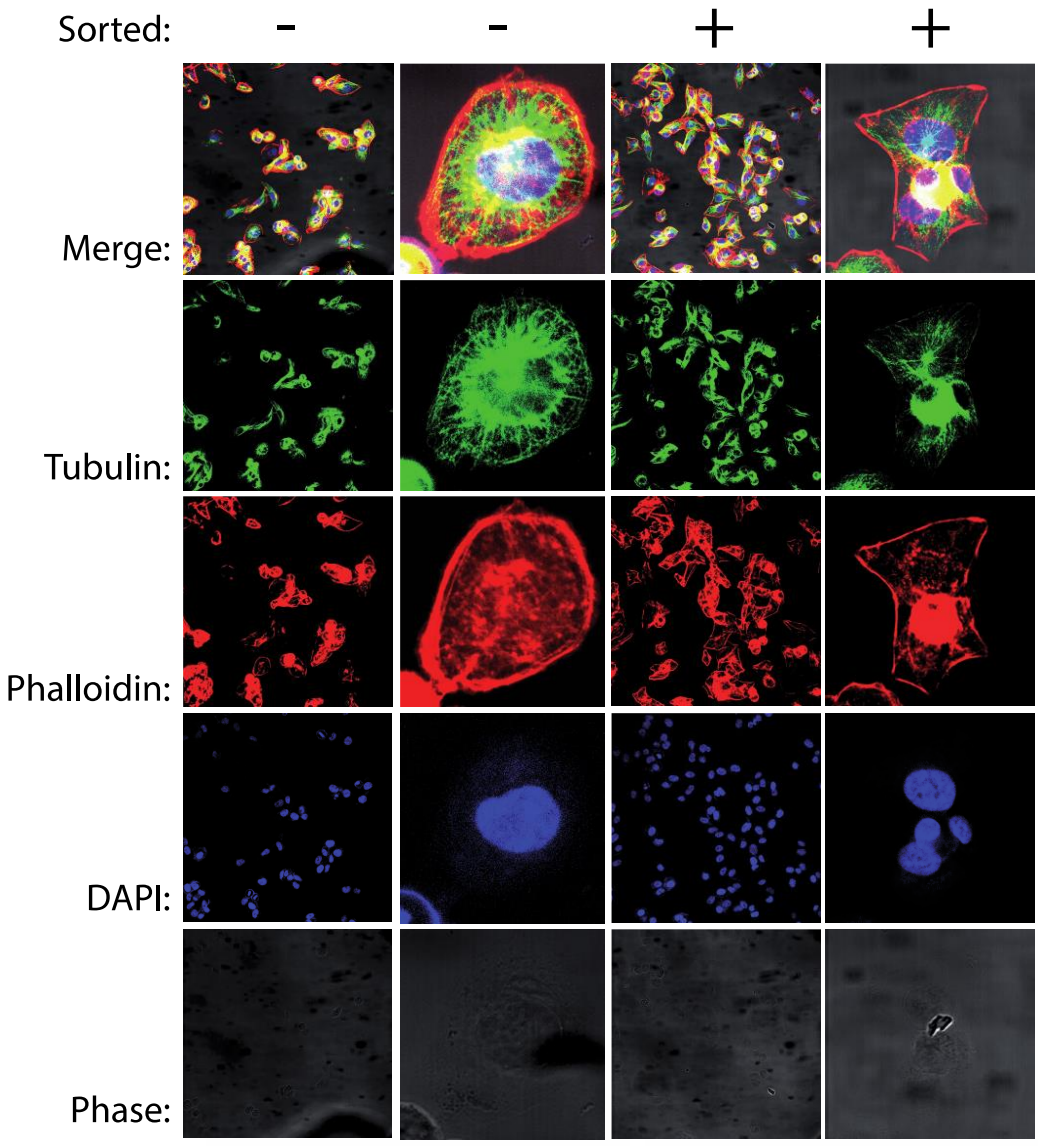

Supplementary Figure 4: Confocal microscopy of cell structure proteins of adherent cell lines. Tubulin (green), actin (red) and the cell nucleus (blue) of mock-sorted and unsorted HCV-29 cells[85] is shown. Confocal staining was done three hours after stimulus with rested adherent cells. Confocal microscopy was done in co-operation with Susi Dürr.

7.5. Confocal microscopy of cell structures after sorting in PBMCs

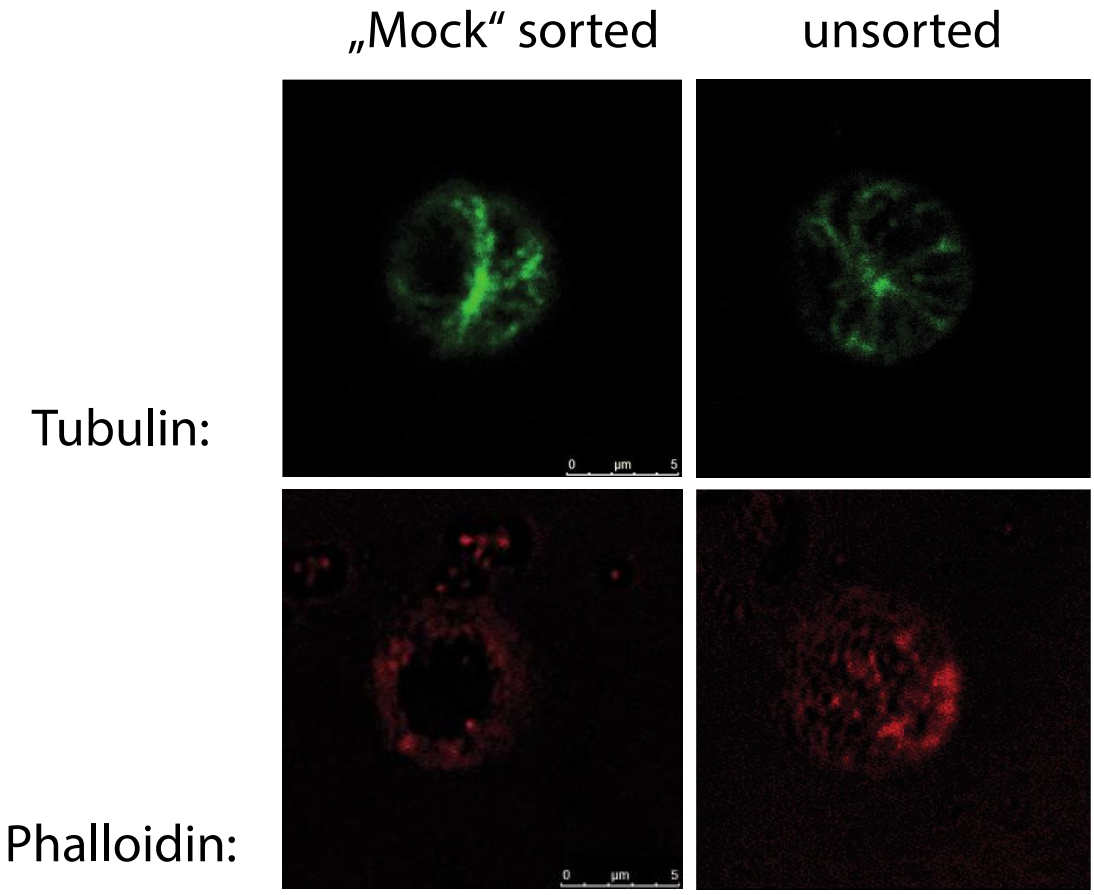

Supplementary Figure 5: Confocal microscopy of cell structure proteins of human PBMCs. Tubulin (green) and actin (red) of “mock” sorted and unsorted hPBMCs. Cells were fixed after distributer protocol on slides (ZellSafe.Basic) of the Chipcytometry platform “Zellkraftwerk”. Fluorescence staining was done immediate after flow cytometry cell sorting.

7.6. MicroArray of Tip-purified FACS-sorted CD8 cells

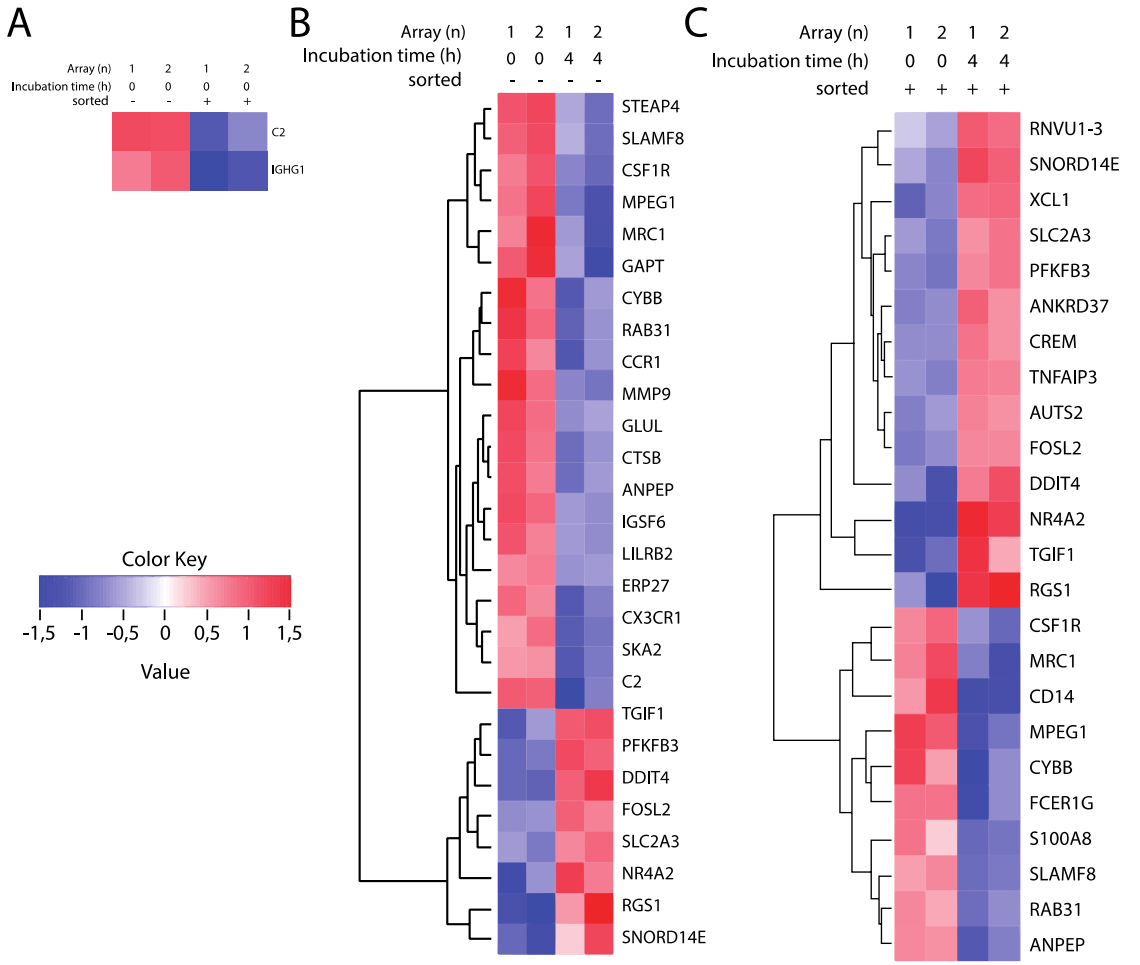

Supplementary Figure 6: Heatmap of mRNA from Fab-TACS®-purified human CD8 cells unsorted and “mock” sorted.
Color code shows differences in the regulation of genes in two arrays (n=2). (A) Comparison of sorted and “mock”-sorted datasets immediate isolated (B) Heatmap for unsorted cells rested under cell culture conditions for 4 h resting. (C) Heatmap for mock-sorted cells rested under cell culture conditions for 4 h. Genes that were differentially expressed under both conditions were excluded for the Heatmap in Figure 23.

7.7. Mixed lymphocyte reaction of human PBMCs

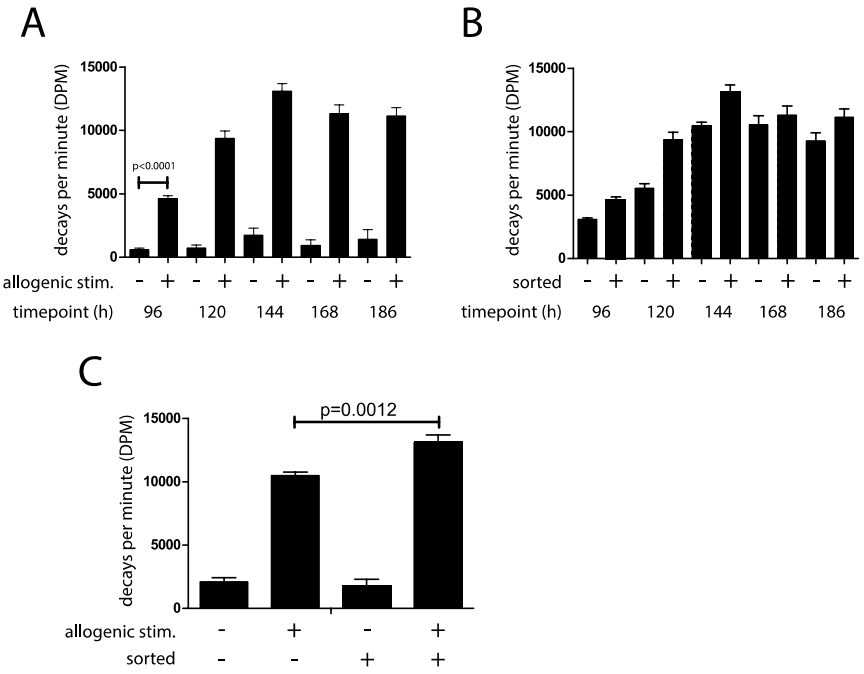

Supplementary Figure 7: Proliferation of human PBMCs a mixed lymphocyte reaction (MLR). (A) Thymidine uptake of T cells in a time course after or without allogeneic stimulation show their proliferative behavior due to this stimulation. (B) Comparison of the proliferative capacity of sorted and unsorted PBMCs in a time course MLR for longer time points. (C) Highlighted time point 144h hours after allogeneic stimulation showed the highest overall cell division rate.

7.8. Schematic draft of the signal processing in *Speed Enrichment*

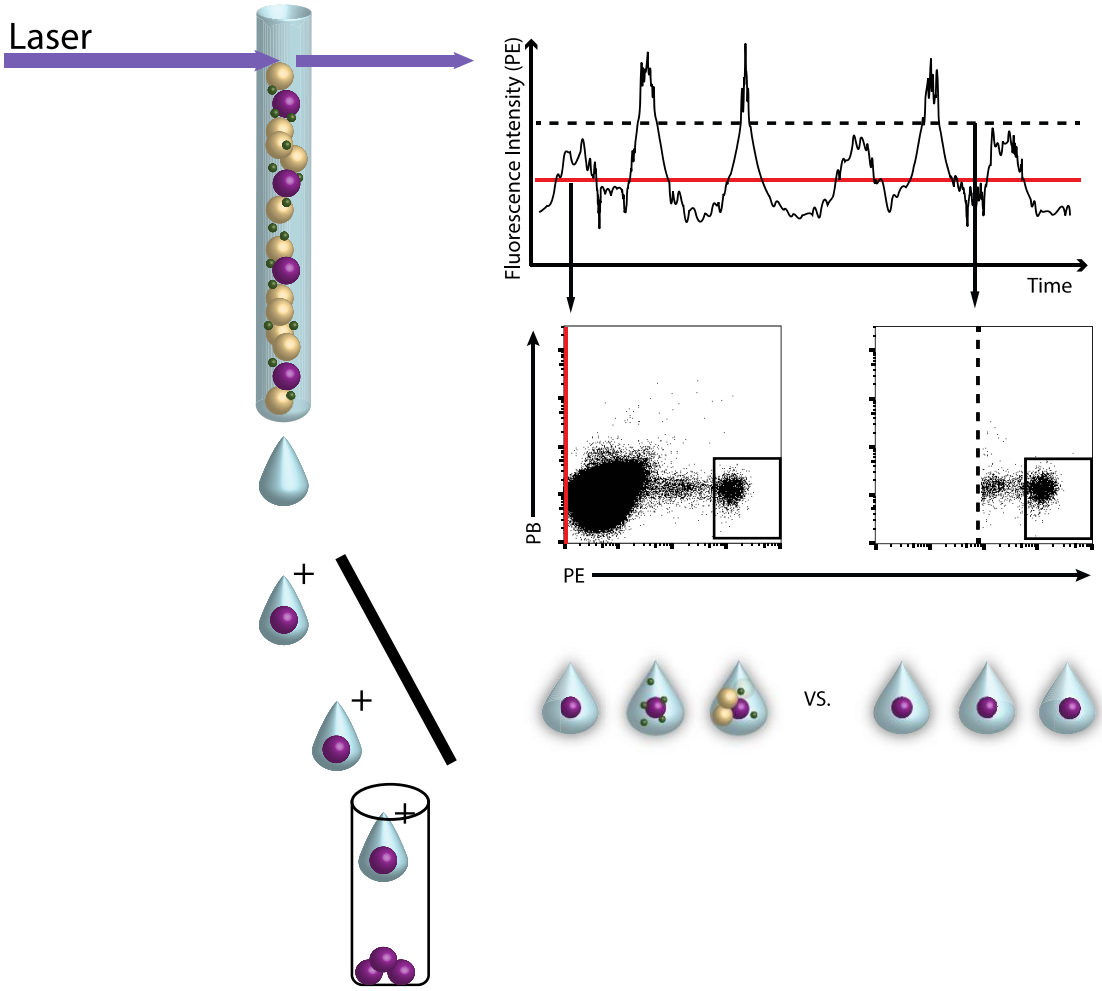

Supplementary Figure 8: Schematic draft of event detection for fluorescence triggering and *Speed Enrichment* sorting.
Laser light exciting fluorophores generates particle fluorescence signals and become digitalized for example the fluorescence channel (PE). Fluorescence intensity is directly dependent of fluorochrome labeling however cells show also florescence by their intrinsic fluorescence. Signals are displayed and analyzed when they exceed a freely adjustable threshold line (indicated by dotted and red line). Analyzed data for the PE channel with different threshold settings for detection of intrinsic fluorescence (left dotplot) or SE settings (right dotplot) are visualized by computer electronics and software. Below the information of containing particles within a deflected droplet is visualized for conventional sorting vs SE.

7.9. Table of sorting times for different cell numbers

Cell number	Conventional	SE
$1x10^6$ cells	33 sec	3 sec
$1x10^7$ cells	5,5 min	30 sec
$1x10^8$ cells	55 min	5 min
$1x10^9$ cells	9,2 h	50 min
$1x10^{10}$ cells	93 h	8 h

Supplementary Figure 9: Table of calculated sort time for human PBMCs.
Times are estimated with a flow rate of $3x10^4$ EPS for conventional and $3,3x10^5$ EPS for *Speed Enrichment*.

7.10. Flowrate measurements for differential pressures of sheath to sample fluid

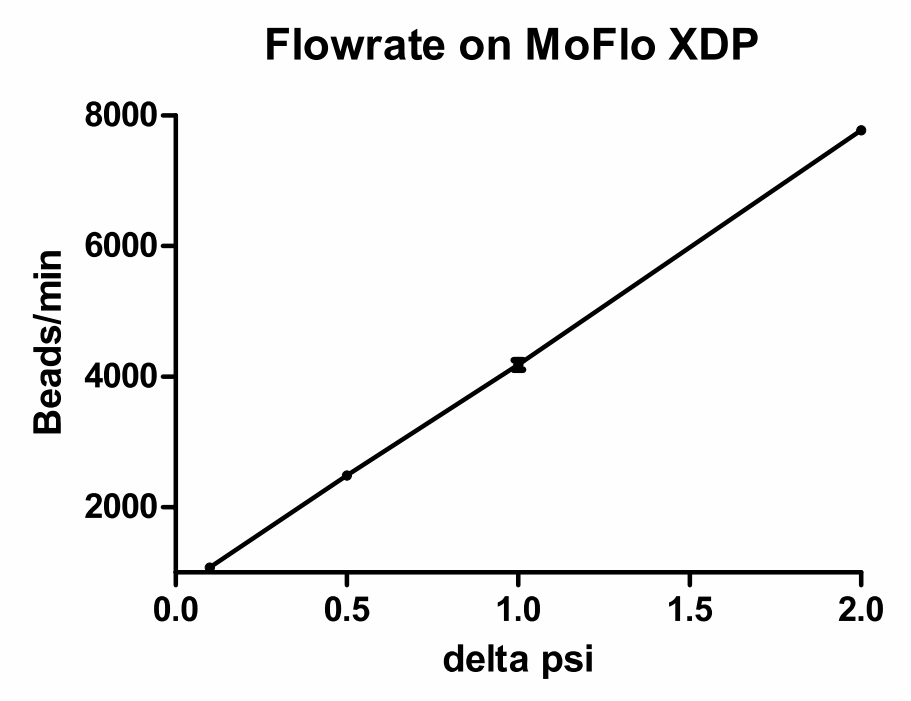

Supplementary Figure 10: Graph for evaluated sample flowrates in a MoFlo XDP.
Sample flowrates of TrueCount beads in an idealized buffer medium with optimal density. With constant densities of the sample fluid flowrate increases linearly with the differential pressure from sheath and sample fluid.

7.11. Temperature-dependent antibody staining effects

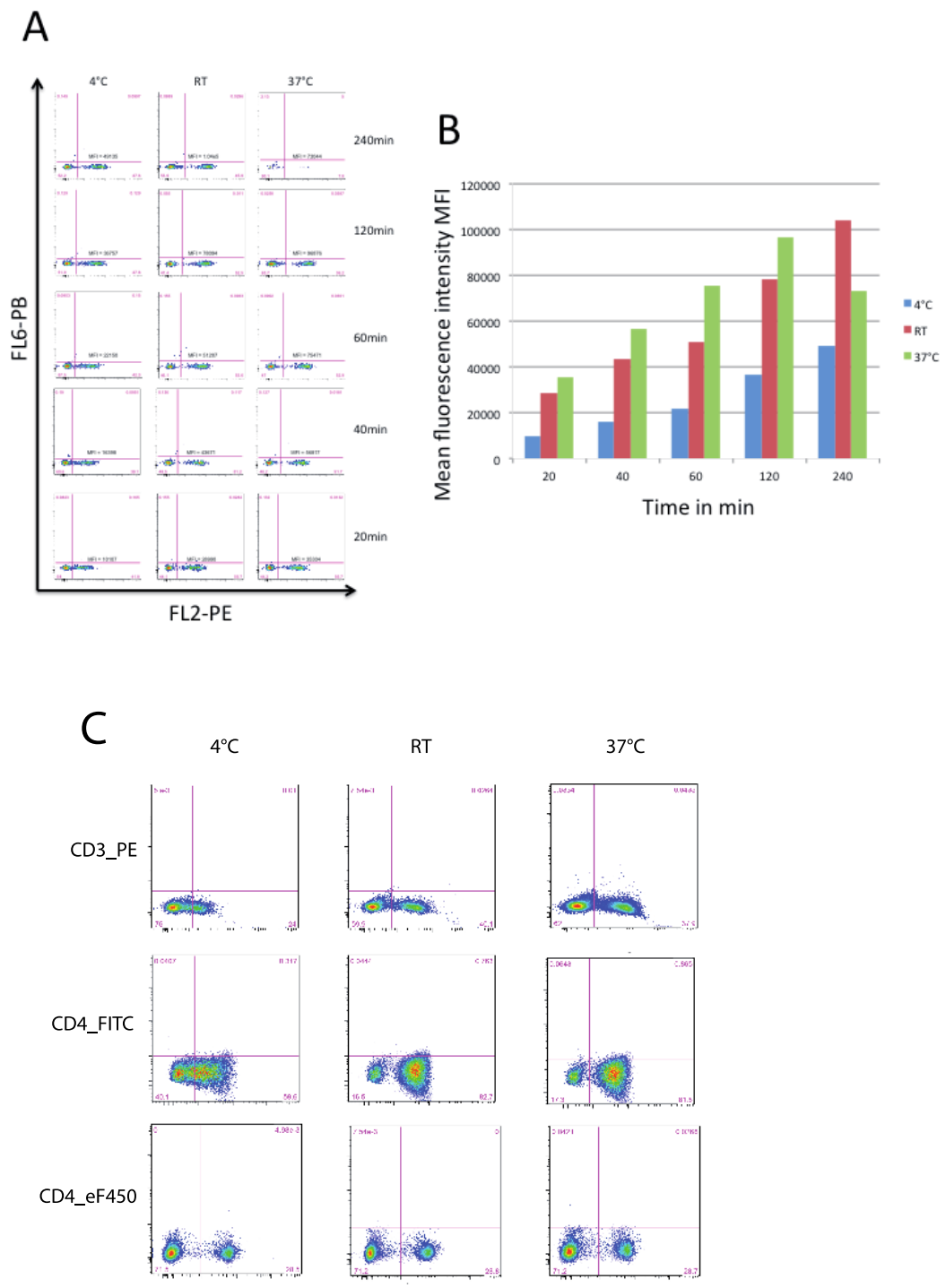

Supplementary Figure 11: Temperature influence for antibody staining (in collaboration with Barbara Teufelhardt and Hanna Ulrich).
(A) Murine splenocytes stained with CD3-PE at different temperatures 4°C, room temperature and 37°C over a time course of up to 240 min. (B) Bar graph of previous flow cytometry data calculated for the MFI values of PE positive cells. Lower initial staining values for low temperatures can be rescued with an increase of the antibody incubation time. Warmer staining temperatures increase the signal for the target cell population. (C) A temperature influence on the staining intensity is strongly antibody dependent. Murine Splenocytes were stained for 20min with different antibodies CD3-PE and CD4-FITC both stained less brightly at 4°C, yet a CD4-eF450 antibody was not influenced by the incubation temperature.

7.12. MACS vs. FACS for pMHC antigen-specific cell purification

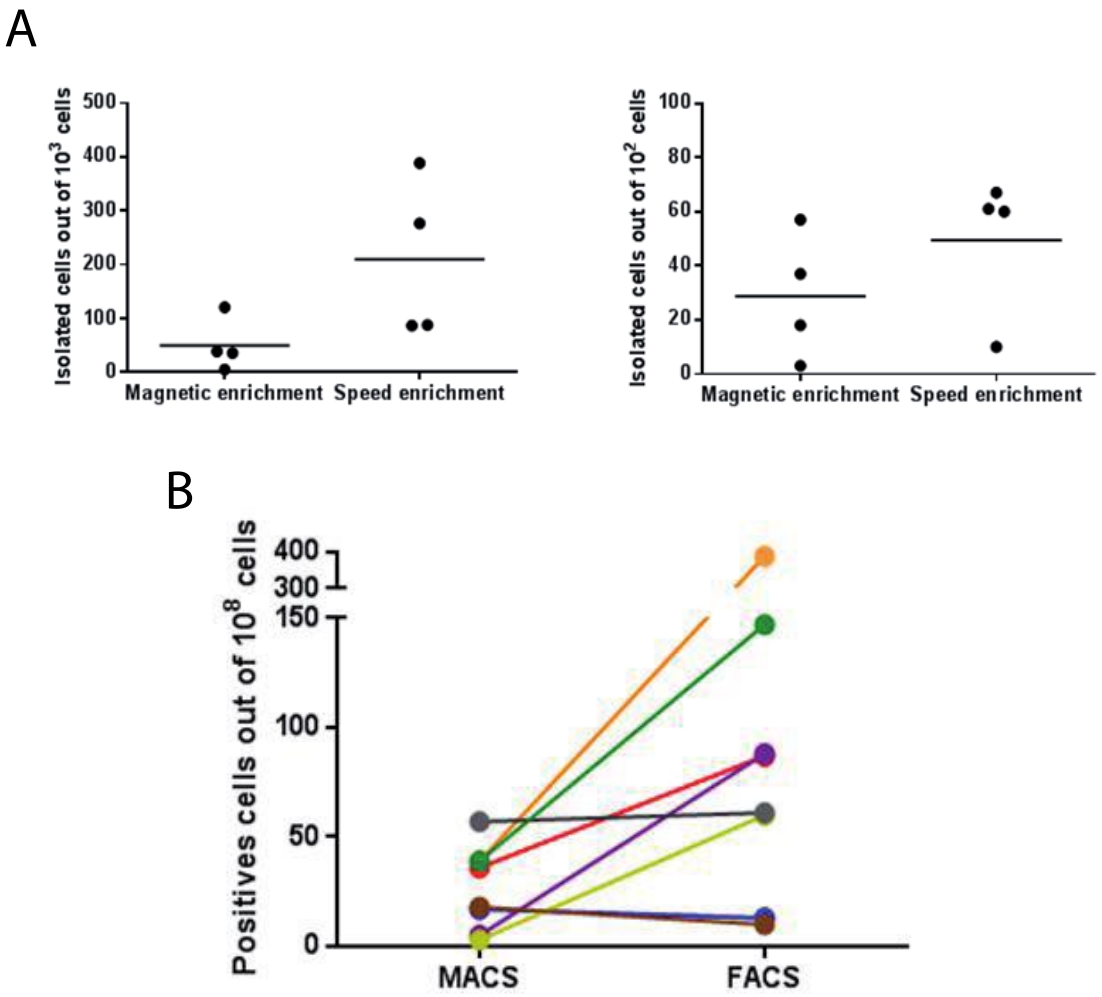

Supplementary Figure 12: *Speed Enrichment* and MACS comparison for the enrichment of antigen-specific T cells (in collaboration with Laia Pascual Ponce).
(A) 1000 or 100 target multimer-stained WT1-specific cells were spiked into 10^8 unstained cells in 4 different experiments. The two enrichment methods, MACS and SE, were in parallel compared to each other concerning cell recovery of spiked in cells. (B) Yield of WT1-specific cells from multimer stained PBMCs (total 10^8) from 8 different donors. Donor samples were split and multimer enrichment was done in parallel by SE and MACS.

7.13. Summarized V-(D)-J segment types and amino acid sequences of the CDR3 of the isolated A2-WT1-specific T cells

TCR number	V-Segment	D-Segment	J-Segment	AA sequence of CDR3 region
TCR4α	TRAV17x01		TRAJ21x01	CATEYNFNKFYF
TCR8α	TRAV17x01		TRAJ23x01	CATDARKLIF
TCR27β	TRBV5-5x01	TRBD2x01	TRBJ2-1x01	CASSLSIGGSSYYNEQFF
TCR32α	TRAV17x01		TRAJ58x01	CATDAGTSGSRLTF
TCR38β	TRBV5-1x01	TRBD1x01	TRBJ2-2x01	CASSRYGQANTGELFF
TCR40β	TRBV7-2x01	TRBD2x01	TRBJ2-1x01	CASSLKTSAGFSYNEQFF

7.14. Summarized V-(D)-J segment types and amino acid sequences of the CDR3 of the isolated A2-pp65-specific T cells.

TCR number	V-Segment	D-Segment	J-Segment	AA sequence of CDR3 region
TCR1α	TRAV29x01		TRAJ49x01	CAASSTGNQFYF
TCR1β	TRBV20-1x01 or TRBV20-1x02	TRBD2x01	TRBJ2-1x01	CSARSAGAHYNEQFF
TCR3α	TRAV24x01		TRAJ21x01	CACRLYNFNKFYF
TCR3β	TRBV4-3x01 or TRBV4-3x04	-	TRBJ1-5x01	CASSQDTSYQPQHF
TCR4α	TRAV29/x01		TRAJ52x01	CAAPNAGGTSYGKLTF
TCR4β	TRBV6-5x01	TRBD1x01	TRBJ1-2x01	CASSYSSQLSPYGYTF

Supplementary Figure 13: SE-isolated TCR sequences with *Speed Enrichment* (in collaboration with Hanna Ulrich).
Sequences of both WT1 and pp65 consisting of both alpha and beta chains of the CDR region, which is responsible for peptide binding. Abbreviations: TRAV: TCR α-chain variable region, TRBV: TCR β-chain variable region, TRBD: TCR β-chain D-Segment; TRAJ: TCR α-chain J-Segment, TRBJ: TCR β-chain J-Segment; “x” indicates allele name. AA: amino acid; CDR3: complementary determining region 3, listed in the order of VN(D)NJ.

7.15. Multiplex panel for parallel measurement of 16 single cell clones and K-off rates for functional avidity of MART1 TCRs.

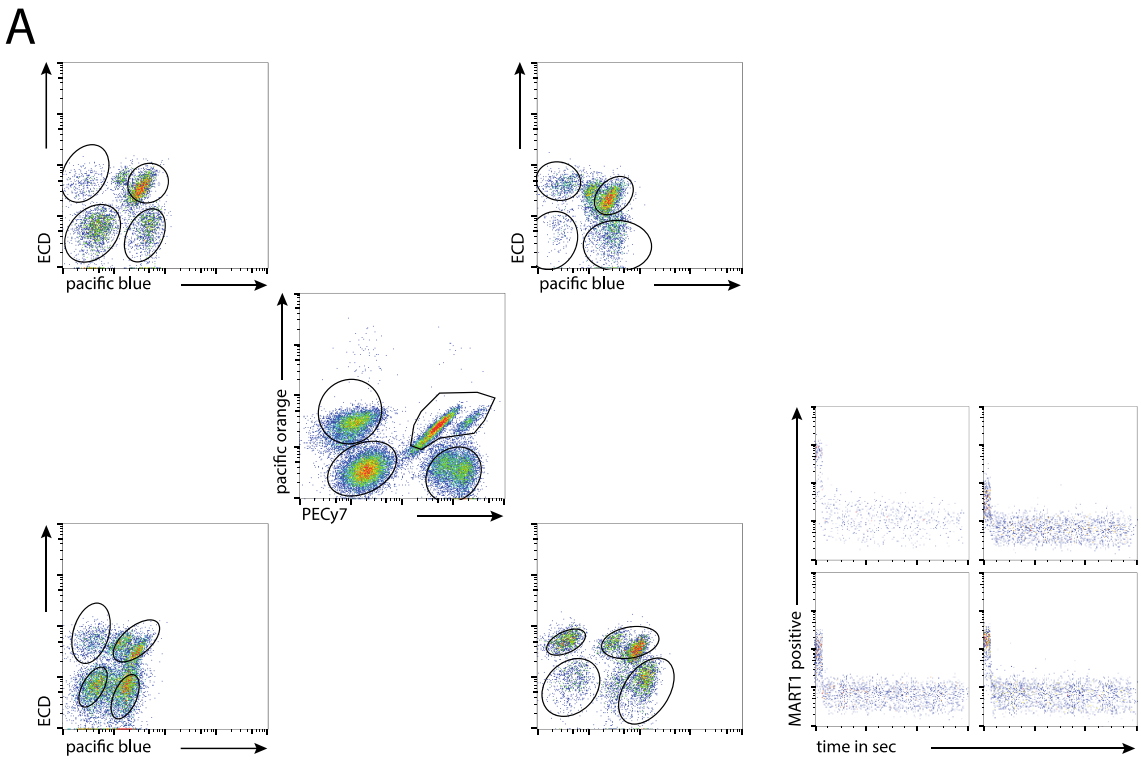

Supplementary Figure 14: Functional characterization of clonal TCRs after MART1 *Speed Enrichment*.
(A) Multiplex Panel for analysis of up to 16 different populations. CD45 staining on four different dyes ECD, Pacific Blue, Pacific Orange and PECy7 identifies 4x4 subgroups (negative, 2 single positive and double positive) each in combination.

Samples are pre-gated on living lymphocytes. APC multimer staining for MART1 proofed re-stainability and backbone dissociation after D-Biotin addition (A method established by Manuel Effenberger).
(B) Measurement of flow based K-off rates of two MART1 clones. MART1 positive clones were speed enriched and expanded and proofed after clonal expansion functional avidity in the K-off rate assay by gradual dissociation of monomerized MHC complexes. After addition of D-Biotin the APC-labeled backbone dissociates with a drop in fluorescence at the first seconds of measurement. FITC-labeled MHC-MART1 complexes remain TCR surface bound and dissociate over time, depended on their functional avidity (measurements by Maria Gerget and Manuel Effenberger).

8. Literature

1 Stemberger, C. *et al.* A single naive CD8+ T cell precursor can develop into diverse effector and memory subsets. *Immunity* **27**, 985-997, doi:10.1016/j.immuni.2007.10.012 (2007).

2 Graef, P. *et al.* Serial transfer of single-cell-derived immunocompetence reveals stemness of CD8(+) central memory T cells. *Immunity* **41**, 116-126, doi:10.1016/j.immuni.2014.05.018 (2014).

3 Stemberger, C., Neuenhahn, M., Buchholz, V. R. & Busch, D. H. Origin of CD8+ effector and memory T cell subsets. *Cellular & molecular immunology* **4**, 399-405 (2007).

4 Busch, D. H., Frassle, S. P., Sommermeyer, D., Buchholz, V. R. & Riddell, S. R. Role of memory T cell subsets for adoptive immunotherapy. *Seminars in immunology* **28**, 28-34, doi:10.1016/j.smim.2016.02.001 (2016).

5 Tomlinson, M. J., Tomlinson, S., Yang, X. B. & Kirkham, J. Cell separation: Terminology and practical considerations. *Journal of tissue engineering* **4**, 2041731412472690, doi:10.1177/2041731412472690 (2013).

6 Van Voorhis, W. C., Hair, L. S., Steinman, R. M. & Kaplan, G. Human dendritic cells. Enrichment and characterization from peripheral blood. *The Journal of experimental medicine* **155**, 1172-1187 (1982).

7 Soleimani, M. & Nadri, S. A protocol for isolation and culture of mesenchymal stem cells from mouse bone marrow. *Nature protocols* **4**, 102-106, doi:10.1038/nprot.2008.221 (2009).

8 Noble, P. B. & Cutts, J. H. Separation of blood leukocytes by Ficoll gradient. *The Canadian veterinary journal = La revue veterinaire canadienne* **8**, 110-111 (1967).

9 Pertoft, H., Rubin, K., Kjellen, L., Laurent, T. C. & Klingeborn, B. The viability of cells grown or centrifuged in a new density gradient medium, Percoll(TM). *Experimental cell research* **110**, 449-457 (1977).

10 De Paoli, P., Villalta, D., Battistin, S., Gasparollo, A. & Santini, G. Selective loss of OKT8 lymphocytes on density gradient centrifugation separation of blood mononuclear cells. *Journal of immunological methods* **61**, 259-260 (1983).

11 Tamul, K. R., Schmitz, J. L., Kane, K. & Folds, J. D. Comparison of the effects of Ficoll-Hypaque separation and whole blood lysis on results of immunophenotypic analysis of blood and bone marrow samples from patients with hematologic malignancies. *Clinical and diagnostic laboratory immunology* **2**, 337-342 (1995).

12 Collins, D. J., Neild, A. & Ai, Y. Highly focused high-frequency travelling surface acoustic waves (SAW) for rapid single-particle sorting. *Lab on a chip* **16**, 471-479, doi:10.1039/c5lc01335f (2016).

13 Ji, H. M. *et al.* Silicon-based microfilters for whole blood cell separation. *Biomedical microdevices* **10**, 251-257, doi:10.1007/s10544-007-9131-x (2008).

14 Shin, D. S. *et al.* Photodegradable hydrogels for capture, detection, and release of live cells. *Angew Chem Int Ed Engl* **53**, 8221-8224, doi:10.1002/anie.201404323 (2014).
15 Vykoukal, J., Vykoukal, D. M., Freyberg, S., Alt, E. U. & Gascoyne, P. R. Enrichment of putative stem cells from adipose tissue using dielectrophoretic field-flow fractionation. *Lab on a chip* **8**, 1386-1393, doi:10.1039/b717043b (2008).
16 Petersson, F., Aberg, L., Sward-Nilsson, A. M. & Laurell, T. Free flow acoustophoresis: microfluidic-based mode of particle and cell separation. *Analytical chemistry* **79**, 5117-5123, doi:10.1021/ac070444e (2007).
17 Hu, X. *et al.* Marker-specific sorting of rare cells using dielectrophoresis. *Proceedings of the National Academy of Sciences of the United States of America* **102**, 15757-15761, doi:10.1073/pnas.0507719102 (2005).
18 Jackson, C. J., Garbett, P. K., Nissen, B. & Schrieber, L. Binding of human endothelium to Ulex europaeus I-coated Dynabeads: application to the isolation of microvascular endothelium. *Journal of cell science* **96 (Pt 2)**, 257-262 (1990).
19 Hewett, P. W. & Murray, J. C. Immunomagnetic purification of human microvessel endothelial cells using Dynabeads coated with monoclonal antibodies to PECAM-1. *European journal of cell biology* **62**, 451-454 (1993).
20 Miltenyi, S., Muller, W., Weichel, W. & Radbruch, A. High gradient magnetic cell separation with MACS. *Cytometry* **11**, 231-238, doi:10.1002/cyto.990110203 (1990).
21 Radbruch, A., Mechtold, B., Thiel, A., Miltenyi, S. & Pfluger, E. High-gradient magnetic cell sorting. *Methods in cell biology* **42 Pt B**, 387-403 (1994).
22 Molday, R. S., Yen, S. P. & Rembaum, A. Application of magnetic microspheres in labelling and separation of cells. *Nature* **268**, 437-438 (1977).
23 Manyonda, I. T., Soltys, A. J. & Hay, F. C. A critical evaluation of the magnetic cell sorter and its use in the positive and negative selection of CD45RO+ cells. *Journal of immunological methods* **149**, 1-10 (1992).
24 Stanciu, L. A., Shute, J., Holgate, S. T. & Djukanovic, R. Production of IL-8 and IL-4 by positively and negatively selected CD4+ and CD8+ human T cells following a four-step cell separation method including magnetic cell sorting (MACS). *Journal of immunological methods* **189**, 107-115 (1996).
25 Sao, H. *et al.* A new marrow T cell depletion method using anti-CD6 monoclonal antibody-conjugated magnetic beads and its clinical application for prevention of acute graft-vs.-host disease in allogeneic bone marrow transplantation: results of a phase I-II trial. *International journal of hematology* **69**, 27-35 (1999).
26 Watanabe, N. *et al.* Expansion of human CMV-specific cytotoxic T lymphocytes to a clinical scale: a simple culture system using tetrameric HLA-peptide complexes. *Cytotherapy* **6**, 514-522, doi:10.1080/14653240410005005 (2004).
27 Hoffmann, P. *et al.* Isolation of CD4+CD25+ regulatory T cells for clinical trials. *Biology of blood and marrow transplantation : journal of the American Society for Blood and Marrow Transplantation* **12**, 267-274, doi:10.1016/j.bbmt.2006.01.005 (2006).
28 Sweet, R. G. High Frequency Recording with Electrostatically Deflected Ink Jets. *Rev Sci Instrum* **36**, 131-&, doi:Doi 10.1063/1.1719502 (1965).

29 Fulwyler, M. J. Electronic separation of biological cells by volume. *Science* **150**, 910-911 (1965).
30 Wolfgang, D. D. & Wolfgang, G. D. (Google Patents, 1971).
31 Hulett, H. R., Bonner, W. A., Barrett, J. & Herzenberg, L. A. Cell sorting: automated separation of mammalian cells as a function of intracellular fluorescence. *Science* **166**, 747-749 (1969).
32 Bonner, W. A., Hulett, H. R., Sweet, R. G. & Herzenberg, L. A. Fluorescence activated cell sorting. *Rev Sci Instrum* **43**, 404-409 (1972).
33 Hulett, H. R., Bonner, W. A., Sweet, R. G. & Herzenberg, L. A. Development and application of a rapid cell sorter. *Clinical chemistry* **19**, 813-816 (1973).
34 Futamura, K. *et al.* Novel full-spectral flow cytometry with multiple spectrally-adjacent fluorescent proteins and fluorochromes and visualization of in vivo cellular movement. *Cytometry. Part A : the journal of the International Society for Analytical Cytology* **87**, 830-842, doi:10.1002/cyto.a.22725 (2015).
35 Bendall, S. C., Nolan, G. P., Roederer, M. & Chattopadhyay, P. K. A deep profiler's guide to cytometry. *Trends in immunology* **33**, 323-332, doi:10.1016/j.it.2012.02.010 (2012).
36 Sack, U. *et al.* Diagnostic value of blood inflammatory markers for detection of acute appendicitis in children. *BMC surgery* **6**, 15, doi:10.1186/1471-2482-6-15 (2006).
37 Tsien, R. Y. The green fluorescent protein. *Annual review of biochemistry* **67**, 509-544, doi:10.1146/annurev.biochem.67.1.509 (1998).
38 Latt, S. A. Microfluorometric detection of deoxyribonucleic acid replication in human metaphase chromosomes. *Proceedings of the National Academy of Sciences of the United States of America* **70**, 3395-3399 (1973).
39 Fried, J., Perez, A. G. & Clarkson, B. D. Flow cytofluorometric analysis of cell cycle distributions using propidium iodide. Properties of the method and mathematical analysis of the data. *The Journal of cell biology* **71**, 172-181 (1976).
40 Krishan, A. Rapid Flow Cytofluorometric Analysis of Mammalian-Cell Cycle by Propidium Iodide Staining. *Journal of Cell Biology* **66**, 188-193, doi:Doi 10.1083/Jcb.66.1.188 (1975).
41 Oi, V. T., Glazer, A. N. & Stryer, L. Fluorescent phycobiliprotein conjugates for analyses of cells and molecules. *The Journal of cell biology* **93**, 981-986 (1982).
42 Gaudin, R. & Barteneva, N. S. Sorting of small infectious virus particles by flow virometry reveals distinct infectivity profiles. *Nature communications* **6**, 6022, doi:10.1038/ncomms7022 (2015).
43 Crosland-Taylor, P. J. A device for counting small particles suspended in a fluid through a tube. *Nature* **171**, 37-38 (1953).
44 Cossarizza, A. *et al.* Guidelines for the use of flow cytometry and cell sorting in immunological studies. *European journal of immunology* **47**, 1584-1797, doi:10.1002/eji.201646632 (2017).
45 Shapiro, H. M. *Practical flow cytometry*. 4th edn, (Wiley-Liss, 2003).
46 Varma, S., Fendyur, A., Box, A. & Voldman, J. Multiplexed Cell-Based Sensors for Assessing the Impact of Engineered Systems and Methods on Cell Health. *Analytical chemistry* **89**, 4663-4670, doi:10.1021/acs.analchem.7b00256 (2017).

47 Llufrio, E. M., Wang, L., Naser, F. J. & Patti, G. J. Sorting cells alters their redox state and cellular metabolome. *Redox biology* **16**, 381-387, doi:10.1016/j.redox.2018.03.004 (2018).
48 Richardson, G. M., Lannigan, J. & Macara, I. G. Does FACS perturb gene expression? *Cytometry. Part A : the journal of the International Society for Analytical Cytology* **87**, 166-175, doi:10.1002/cyto.a.22608 (2015).
49 Olesen, S. P., Clapham, D. E. & Davies, P. F. Haemodynamic shear stress activates a K+ current in vascular endothelial cells. *Nature* **331**, 168-170, doi:10.1038/331168a0 (1988).
50 Ge, J. *et al.* Standard fluorescent imaging of live cells is highly genotoxic. *Cytometry. Part A : the journal of the International Society for Analytical Cytology* **83**, 552-560, doi:10.1002/cyto.a.22291 (2013).
51 Catt, S. L. *et al.* Hoechst staining and exposure to UV laser during flow cytometric sorting does not affect the frequency of detected endogenous DNA nicks in abnormal and normal human spermatozoa. *Molecular human reproduction* **3**, 821-825 (1997).
52 Seidl, J., Knuechel, R. & Kunz-Schughart, L. A. Evaluation of membrane physiology following fluorescence activated or magnetic cell separation. *Cytometry* **36**, 102-111 (1999).
53 Zhou, X., Naguro, I., Ichijo, H. & Watanabe, K. Mitogen-activated protein kinases as key players in osmotic stress signaling. *Biochimica et biophysica acta* **1860**, 2037-2052, doi:10.1016/j.bbagen.2016.05.032 (2016).
54 Pasantes-Morales, H., Lezama, R. A., Ramos-Mandujano, G. & Tuz, K. L. Mechanisms of cell volume regulation in hypo-osmolality. *The American journal of medicine* **119**, S4-11, doi:10.1016/j.amjmed.2006.05.002 (2006).
55 Burg, M. B., Ferraris, J. D. & Dmitrieva, N. I. Cellular response to hyperosmotic stresses. *Physiological reviews* **87**, 1441-1474, doi:10.1152/physrev.00056.2006 (2007).
56 Wang, L., Wormstone, I. M., Reddan, J. R. & Duncan, G. Growth factor receptor signalling in human lens cells: role of the calcium store. *Experimental eye research* **80**, 885-895, doi:10.1016/j.exer.2005.01.002 (2005).
57 Goding, J. W. Biological effects of antibodies to lymphocyte surface receptors. *Springer seminars in immunopathology* **5**, 463-475 (1982).
58 Knight, J. R. *et al.* Eukaryotic elongation factor 2 kinase regulates the cold stress response by slowing translation elongation. *The Biochemical journal* **465**, 227-238, doi:10.1042/BJ20141014 (2015).
59 Roberts, J. R., Rowe, P. A. & Demaine, A. G. Activation of NF-kappaB and MAP kinase cascades by hypothermic stress in endothelial cells. *Cryobiology* **44**, 161-169 (2002).
60 Eisinger, J. & Scarlata, S. F. The lateral fluidity of erythrocyte membranes. Temperature and pressure dependence. *Biophysical chemistry* **28**, 273-281 (1987).
61 Nicolini, C., Baserga, R. & Kendall, F. DNA structure in sheared and unsheared chromatin. *Science* **192**, 796-798 (1976).
62 Kazi, M. *et al.* Inhibition of rat smooth muscle cell adhesion and proliferation by non-anticoagulant heparins. *Journal of cellular physiology* **193**, 365-372, doi:10.1002/jcp.10184 (2002).
63 Maxwell, W. M., Welch, G. R. & Johnson, L. A. Viability and membrane integrity of spermatozoa after dilution and flow cytometric sorting in the

presence or absence of seminal plasma. *Reproduction, fertility, and development* **8**, 1165-1178 (1996).
64 Donnelly, N., Gorman, A. M., Gupta, S. & Samali, A. The eIF2alpha kinases: their structures and functions. *Cellular and molecular life sciences : CMLS* **70**, 3493-3511, doi:10.1007/s00018-012-1252-6 (2013).
65 Ye, J. *et al.* The GCN2-ATF4 pathway is critical for tumour cell survival and proliferation in response to nutrient deprivation. *The EMBO journal* **29**, 2082-2096, doi:10.1038/emboj.2010.81 (2010).
66 Deval, C. *et al.* Amino acid limitation regulates the expression of genes involved in several specific biological processes through GCN2-dependent and GCN2-independent pathways. *The FEBS journal* **276**, 707-718, doi:10.1111/j.1742-4658.2008.06818.x (2009).
67 Giehl, K., Skripczynski, B., Mansard, A., Menke, A. & Gierschik, P. Growth factor-dependent activation of the Ras-Raf-MEK-MAPK pathway in the human pancreatic carcinoma cell line PANC-1 carrying activated K-ras: implications for cell proliferation and cell migration. *Oncogene* **19**, 2930-2942, doi:10.1038/sj.onc.1203612 (2000).
68 Cohen-Saidon, C., Cohen, A. A., Sigal, A., Liron, Y. & Alon, U. Dynamics and variability of ERK2 response to EGF in individual living cells. *Molecular cell* **36**, 885-893, doi:10.1016/j.molcel.2009.11.025 (2009).
69 Brandsma, A. M., Jacobino, S. R., Meyer, S., ten Broeke, T. & Leusen, J. H. Fc receptor inside-out signaling and possible impact on antibody therapy. *Immunological reviews* **268**, 74-87, doi:10.1111/imr.12332 (2015).
70 Waldmann, T. A. Anti-Tac (daclizumab, Zenapax) in the treatment of leukemia, autoimmune diseases, and in the prevention of allograft rejection: a 25-year personal odyssey. *Journal of clinical immunology* **27**, 1-18, doi:10.1007/s10875-006-9060-0 (2007).
71 Moreau, J. L. *et al.* Monoclonal antibodies identify three epitope clusters on the mouse p55 subunit of the interleukin 2 receptor: relationship to the interleukin 2-binding site. *European journal of immunology* **17**, 929-935, doi:10.1002/eji.1830170706 (1987).
72 Bradbury, A. R., Sidhu, S., Dubel, S. & McCafferty, J. Beyond natural antibodies: the power of in vitro display technologies. *Nature biotechnology* **29**, 245-254, doi:10.1038/nbt.1791 (2011).
73 Melero, I. *et al.* Monoclonal antibodies against the 4-1BB T-cell activation molecule eradicate established tumors. *Nature medicine* **3**, 682-685 (1997).
74 Dyavar Shetty, R. *et al.* PD-1 blockade during chronic SIV infection reduces hyperimmune activation and microbial translocation in rhesus macaques. *The Journal of clinical investigation* **122**, 1712-1716, doi:10.1172/JCI60612 (2012).
75 Schwab, R., Crow, M. K., Russo, C. & Weksler, M. E. Requirements for T cell activation by OKT3 monoclonal antibody: role of modulation of T3 molecules and interleukin 1. *J Immunol* **135**, 1714-1718 (1985).
76 Werlen, G., Hausmann, B. & Palmer, E. A motif in the alphabeta T-cell receptor controls positive selection by modulating ERK activity. *Nature* **406**, 422-426, doi:10.1038/35019094 (2000).
77 Werlen, G. & Palmer, E. The T-cell receptor signalosome: a dynamic structure with expanding complexity. *Current opinion in immunology* **14**, 299-305 (2002).

78 Stemberger, C. *et al.* Novel serial positive enrichment technology enables clinical multiparameter cell sorting. *PloS one* **7**, e35798, doi:10.1371/journal.pone.0035798 (2012).
79 Nauerth, M. *et al.* Flow cytometry-based TCR-ligand Koff -rate assay for fast avidity screening of even very small antigen-specific T cell populations ex vivo. *Cytometry. Part A : the journal of the International Society for Analytical Cytology* **89**, 816-825, doi:10.1002/cyto.a.22933 (2016).
80 Schmidt, T. G. & Skerra, A. The Strep-tag system for one-step purification and high-affinity detection or capturing of proteins. *Nature protocols* **2**, 1528-1535, doi:10.1038/nprot.2007.209 (2007).
81 Roobol, A., Carden, M. J., Newsam, R. J. & Smales, C. M. Biochemical insights into the mechanisms central to the response of mammalian cells to cold stress and subsequent rewarming. *The FEBS journal* **276**, 286-302, doi:10.1111/j.1742-4658.2008.06781.x (2009).
82 Corwin, W. L., Baust, J. M., Baust, J. G. & Van Buskirk, R. G. Characterization and modulation of human mesenchymal stem cell stress pathway response following hypothermic storage. *Cryobiology* **68**, 215-226, doi:10.1016/j.cryobiol.2014.01.014 (2014).
83 Saba-El-Leil, M. K., Fremin, C. & Meloche, S. Redundancy in the World of MAP Kinases: All for One. *Frontiers in cell and developmental biology* **4**, 67, doi:10.3389/fcell.2016.00067 (2016).
84 Nishimoto, S. & Nishida, E. MAPK signalling: ERK5 versus ERK1/2. *EMBO reports* **7**, 782-786, doi:10.1038/sj.embor.7400755 (2006).
85 Hisazumi, H., Andersson, L. & Collins, V. P. Fibrinolytic activity of in vitro cultivated human bladder cell lines. *Urological research* **5**, 133-139 (1977).
86 Matsushita, M., Endo, Y. & Fujita, T. Structural and functional overview of the lectin complement pathway: its molecular basis and physiological implication. *Archivum immunologiae et therapiae experimentalis* **61**, 273-283, doi:10.1007/s00005-013-0229-y (2013).
87 Sim, R. B. & Tsiftsoglou, S. A. Proteases of the complement system. *Biochemical Society transactions* **32**, 21-27, doi:10.1042/ (2004).
88 Luo, C., Chen, M., Madden, A. & Xu, H. Expression of complement components and regulators by different subtypes of bone marrow-derived macrophages. *Inflammation* **35**, 1448-1461, doi:10.1007/s10753-012-9458-1 (2012).
89 Duch, A., de Nadal, E. & Posas, F. The p38 and Hog1 SAPKs control cell cycle progression in response to environmental stresses. *FEBS letters* **586**, 2925-2931, doi:10.1016/j.febslet.2012.07.034 (2012).
90 Thornton, T. M. & Rincon, M. Non-classical p38 map kinase functions: cell cycle checkpoints and survival. *International journal of biological sciences* **5**, 44-51 (2009).
91 Coulthard, L. R., White, D. E., Jones, D. L., McDermott, M. F. & Burchill, S. A. p38(MAPK): stress responses from molecular mechanisms to therapeutics. *Trends in molecular medicine* **15**, 369-379, doi:10.1016/j.molmed.2009.06.005 (2009).
92 McCoy, J. P., Jr., Chambers, W. H., Lakomy, R., Campbell, J. A. & Stewart, C. C. Sorting minor subpopulations of cells: use of fluorescence as the triggering signal. *Cytometry* **12**, 268-274, doi:10.1002/cyto.990120310 (1991).
93 Arraud, N., Gounou, C., Turpin, D. & Brisson, A. R. Fluorescence triggering: A general strategy for enumerating and phenotyping extracellular vesicles by flow cytometry. *Cytometry. Part A : the journal of*

the International Society for Analytical Cytology **89**, 184-195, doi:10.1002/cyto.a.22669 (2016).
94 Nolan, J. P. & Duggan, E. Analysis of Individual Extracellular Vesicles by Flow Cytometry. *Methods Mol Biol* **1678**, 79-92, doi:10.1007/978-1-4939-7346-0_5 (2018).
95 Arraud, N., Gounou, C., Linares, R. & Brisson, A. R. A simple flow cytometry method improves the detection of phosphatidylserine-exposing extracellular vesicles. *Journal of thrombosis and haemostasis : JTH* **13**, 237-247, doi:10.1111/jth.12767 (2015).
96 Alanio, C., Lemaitre, F., Law, H. K., Hasan, M. & Albert, M. L. Enumeration of human antigen-specific naive CD8+ T cells reveals conserved precursor frequencies. *Blood* **115**, 3718-3725, doi:10.1182/blood-2009-10-251124 (2010).
97 Knabel, M. *et al.* Reversible MHC multimer staining for functional isolation of T-cell populations and effective adoptive transfer. *Nature medicine* **8**, 631-637, doi:10.1038/nm0602-631 (2002).
98 Pelak, O. *et al.* Lymphocyte enrichment using CD81-targeted immunoaffinity matrix. *Cytometry. Part A : the journal of the International Society for Analytical Cytology* **91**, 62-72, doi:10.1002/cyto.a.22918 (2017).
99 Piyasena, M. E. *et al.* Multinode acoustic focusing for parallel flow cytometry. *Analytical chemistry* **84**, 1831-1839, doi:10.1021/ac200963n (2012).
100 Bodinier, M. *et al.* Efficient detection and immunomagnetic sorting of specific T cells using multimers of MHC class I and peptide with reduced CD8 binding. *Nature medicine* **6**, 707-710, doi:10.1038/76292 (2000).
101 Kodituwakku, A. P., Jessup, C., Zola, H. & Roberton, D. M. Isolation of antigen-specific B cells. *Immunology and cell biology* **81**, 163-170, doi:10.1046/j.1440-1711.2003.01152.x (2003).
102 Schober, K., Buchholz, V. R. & Busch, D. H. TCR repertoire evolution during maintenance of CMV-specific T-cell populations. *Immunological reviews* **283**, 113-128, doi:10.1111/imr.12654 (2018).
103 Blattman, J. N. *et al.* Estimating the precursor frequency of naive antigen-specific CD8 T cells. *The Journal of experimental medicine* **195**, 657-664 (2002).
104 World Medical Association Declaration of Helsinki: ethical principles for medical research involving human subjects. *Jama* **310**, 2191-2194, doi:10.1001/jama.2013.281053 (2013).
105 Giard, D. J. *et al.* In vitro cultivation of human tumors: establishment of cell lines derived from a series of solid tumors. *Journal of the National Cancer Institute* **51**, 1417-1423 (1973).